UNIVERSITÀ DEGLI STUDI DI PADOVA

DIPARTIMENTO DI INGEGNERIA INDUSTRIALE

CORSO DI LAUREA MAGISTRALE IN INGEGNERIA CHIMICA E DEI PROCESSI INDUSTRIALI

Tesi di Laurea Magistrale in
Ingegneria Chimica e dei Processi Industriali

Integrated biogas and microalgae production process: techno-economic analysis by process simulation

Relatore: Prof. Alberto Bertucco
Correlatore: Ing. Elena Barbera

Laureando: ENRICO MORANDIN

ANNO ACCADEMICO 2019 - 2020

Riassunto

L'aumento dei gas serra nell'atmosfera ed il successivo cambiamento climatico hanno indotto la comunità internazionale a concentrare la sua attenzione sullo sviluppo di risorse rinnovabili. Dal 1997, l'Unione Europea ha promosso legislazioni che hanno reso più stringenti i limiti sull'emissione dei gas serra e l'utilizzo di combustibili fossili come fonte di energia. A questo scopo è importante considerare il concetto di economia circolare. Questo implica una riduzione dei rifiuti e dell'utilizzo di materie prime. Un contributo positivo viene dato dalla digestione anaerobica. Questo processo usa materiale organico per produrre biogas, che può essere usato come carburante. In questo caso la produzione di CO_2 può essere considerata neutra perché è il risultato della degradazione di materia organica che è stata precedentemente un agente fissante della CO_2. Il digestate liquido ottenuto da questo processo contiene i nutrienti necessari per la coltivazione di microalghe. La biomassa prodotta in questo modo non può essere utilizzata nel settore alimentare ma ha delle potenzialità come fertilizzante o come alimentazione per un ulteriore processo di digestione anerobica.

Lo scopo di questa tesi è di effettuare un'analisi tecno-economica di un processo di digestione anaerobica integrato con la coltivazione di microalghe. L'analisi economica è usata per verificare la profittabilità di un impianto di digestione anaerobica di piccola scala e l'effetto che la coltivazione di microalghe ha sull'economia del processo. I bilanci di massa dell'intero processo sono valutati usando il simulatore di processo Apsen Plus. La simulazione può essere quindi divisa in tre sezioni: digestione anaerobica, cogenerazione e produzione di biomassa. Il digestato liquido della digestione anaerobica e i fumi dal sistema di cogenerazione sono utilizzati per fornire i nutrienti necessari per la crescita della biomassa. Le variabili operative legate alla sezione di digestione anaerobica e cogenerazione sono state determinate in modo da riprodurre i risultati di un impianto ad Arzignano (VI), mentre la cinetica relativa alla produzione di biomassa è espressa secondo un modello validato. L'efficienza del processo è valutata per differenti valori delle variabili operative e in diversi mesi dell'anno (che corrispondo a diverse condizioni ambientali medie). Una combinazione dei risultati della simulazione e dati di letteratura sono stati utilizzati per condurre l'analisi economica. Da questa analisi risulta che un processo di digestione anaerobica in piccola scala risulta economicamente conveniente con un DPBP di 6,36 anni ed un IRR di 24,16%. L'aggiunta di un reattore raceway per la coltivazione di microalghe

non rende il processo più conveniente. La situazione potrebbe essere diversa se ci fosse una riduzione nei costi relativi alla produzione di microalghe oppure una diversa posizione dell'impianto con condizioni ambientali più favorevoli.

Abstract

The aim of this thesis is to carry out a techno-economic analysis of an anaerobic digestion process of the organic fraction of municipal solid waste integrated with cultivation of microalgae. The economic analysis is used to verify the profitability of a small-scale anaerobic digestion process and evaluate the effect that microalgae cultivation has on its economic viability. The overall plant mass balances are evaluated using the Aspen Plus process simulator. The simulation can be divided into three sections: anaerobic digestion, cogeneration and biomass production. The liquid digestate from the anaerobic digestion process and the off-gases from the cogeneration system are used to provide nutrients for the growth of the biomass. The operating variables related to the anaerobic digestion and cogeneration section are chosen is such a way to reproduce the result of a real plant in Arzignano (VI), while the biomass production kinetics follows a validated model. The process performance is evaluated using different values of some operating variables and in different months of the year (which correspond to different average environmental conditions). A combination of the simulation results and literature data is used to conduct the economic analysis. When considering only a small-scale anaerobic digestion plant, the process results profitable, with a DPBP of 6,36 years and a IRR of 24,16%. The addition of a raceway reactor for microalgae cultivation does not improve the economic performance, so a reduction of cost or a change in location in which the environmental conditions are more favourable is advised.

Table of Contents

Introduction

The increase of greenhouse gases in the atmosphere and the consequent climate change prompted the international community to focus its attention to the development of renewable resources. Since 1997, the European Union promoted a series of legislation gradually increasing the limits on greenhouse gases emission and use of energy derived from fossil fuels. To this end, the concept of circular economy is also important, which implies an overall reduction of waste and use of raw materials.

A positive contribute can be provided by anaerobic digestion. This process uses organic material to produce biogas, which can be utilized as a fuel. In this case, the CO_2 balance can be considered neutral because it is a results of the degradation of the organic matter that was previously a biological CO_2 fixing agent. The liquid digestate obtained from this process contains the nutrients required for microalgae cultivation. The biomass produced in this way cannot be used as food, but it has potential as fertilizer or as feed for a subsequent anaerobic digestion.

The aim of this thesis is to carry out a techno-economic analysis of an anaerobic digestion process fed by the organic fraction of municipal solid waste integrated with cultivation of microalgae. The liquid digestate and the off-gases from the anaerobic digestion process are used to provide nutrients for the growth of the algal biomass. The analysis is referred to a small scale plant, which has the aim to treat the organic waste directly at the waste collection centre.

This thesis is composed by four chapters. The first Chapter summarizes the current state of the art. First there is a description of the Italian and European context, focused on the legislative framework and the involvement of anaerobic digestion. Then, there is an in-depth explanation of the anaerobic digestion process as one of the most promising technologies to treat the organic fraction of municipal solid waste. Finally microalgae cultivation is described with a focus on its potential as treatment of liquid digestate and carbon dioxide removal.

The second Chapter describes in detail the Aspen Plus simulation and the models involved in it. First, there is a list of the components involved in the simulation and a description of the thermodynamic model. This is followed by the chemical reactions that are taken into account. Finally, the last paragraph includes the main features of the Aspen Plus simulation focusing on the kinetic model of the photobioreactor.

The third chapter shows the results of different scenarios in which the biomass production process is integrated with the anaerobic digestion process. The differences between each scenario are related to the different values of liquid level inside the photobioreactors, dilution ratio of the digestate and photobioreactor temperature.
The fourth chapter details an economic analysis of the anaerobic digestion process and of the microalgae-integrated process. First the methods used for this analysis are explained, which involve the use of literature data for the costs estimation. Finally there is an evaluation on the effect that the biomass production process has on the profitability of the anaerobic digestion using the main profitability indexes.

I would like to kindly acknowledge the help of Ing. Elena Barbera during all the development phases of this thesis work.

Chapter 1

State of the art

This chapter gives an overview of the context surrounding the development of this thesis. First, it summarizes the European and Italian context, focusing on the legislative and industrial framework. Secondly, there is a description of the Anaerobic Digestion (AD) process indicating its major characteristics. Finally, this chapter provides the necessary information to understand microalgae cultivation, focusing on its development in an industrial scale and its potential as liquid waste treatment and CO_2 fixation.

1.1. European Context

In recent years, EU increased biogas production, due to its potential as a renewable energy source. The interest in renewable energy sources started in 1997 with the "White Paper for a Community Strategy and Action Plan" (European Commission, 1997). More recently the EU published a series of binding legislations called the "2020 climate & energy package" to ensure that the EU meets its climate and energy targets for the year 2020 (EU, 2008). The "Renewable Energy directive" is a part of this package released in 2009, defining a series of targets (shown in Table 1.1) to promote the use of energy from renewable sources in the EU (European Commission, 2009). In the directive both European targets and national targets on the amount of energy from renewable resources are defined. Promoting renewable energy sources has a positive effect on the European economy considering that, between 1990 and 2017, EU emissions were reduced by 22% while the economy grew by 58% over the same period (European Commission, 2018). This reduction in emissions means that the EU is on track to meet its emissions reduction target for 2020. Stricter targets (shown in Table 1.1) are introduced with a new set of policies released, called the "2030 climate & energy framework" which was adopted by the European Council in October 2014 (European Council, 2014). The targets for renewables and energy efficiency were revised upwards in 2018 (European Union, 2018b, 2018a).

Table 1.1: *Comparison between European targets and policy objectives set for 2020 and 2030*

	2020	2030
Cut in GHG emissions (from 1990 levels)	20%	40%
EU energy from renewables	20%	32%
improvement in energy efficiency	20%	32.5%

As of 2017, there were 17,783 biogas plants and 540 biomethane plants in operation Europe-wide. In order to be injected into the natural gas network or used as automotive fuel, biomethane needs to comply with the EN 16723 standard "Natural gas and biomethane for use in transport and biomethane for injection in the natural gas network" (CEN/TC 408, 2016).

Figure 1.1 shows the distribution of biogas plants in each Member State. The country with the greatest increase in 2017 was Germany (+122 plants), followed by Italy (+100 plants), France (+74 plants), the UK (+55 plants) and Spain (+43 plants).

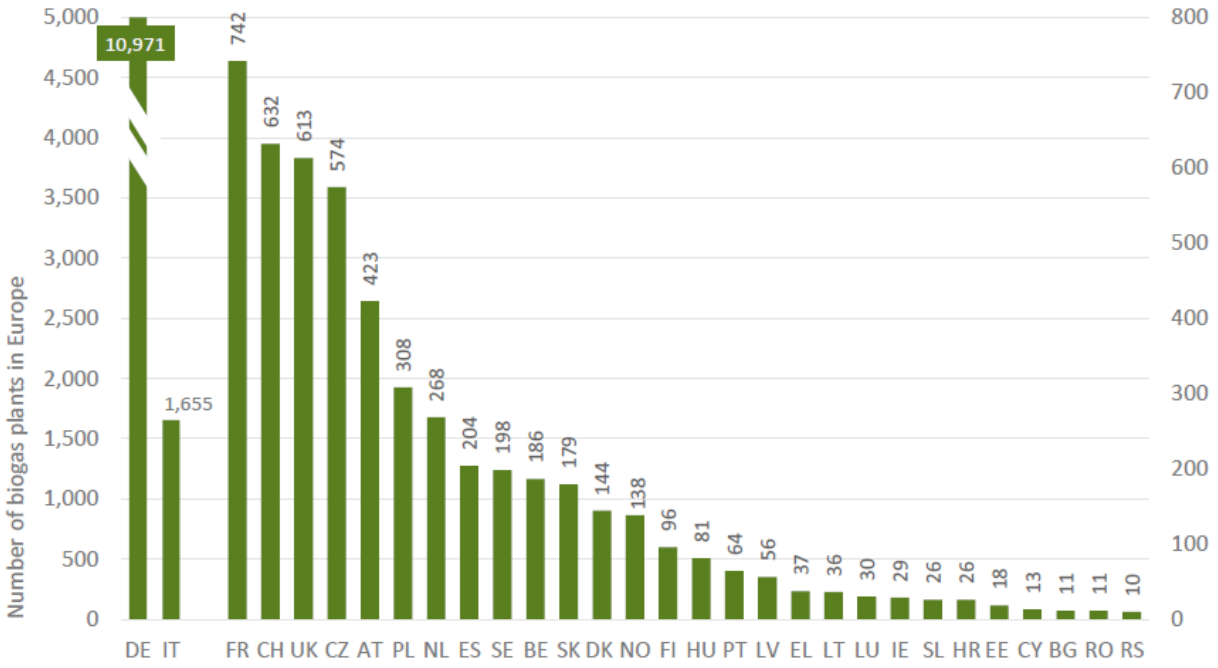

Figure 1.1: *Number of biogas plants in European countries, arranged in descending order (European Biogas Association, 2018)*

2017 saw an overall increase of 351 operational biogas plants in Europe, representing 2% growth in the number of plants relative to 2016 (European Biogas Association, 2018).

Figure 1.2 shows the relative importance of various types of feedstock used in biogas production. The "Agriculture" substrate category comprise livestock manure, farm residues, plant residues and energy crops and is the driving force of the European biogas market with a 60-70% market share. The "other" substrate category includes organic, municipal waste and organic, industrial waste from the food and beverage industry. This type of substrate is still underrepresented leaving potential for market growth in this direction (European Biogas Association, 2018).

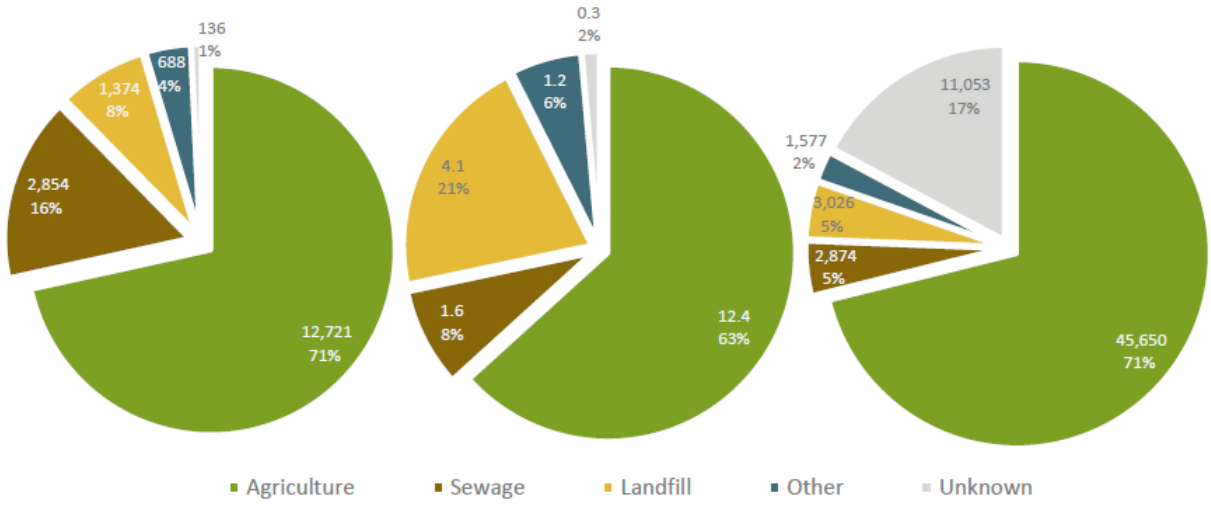

Figure 1.2: *Relative use of different feedstock types according to i) number of biogas plants, ii) Installed Electric Capacity per million head of population and iii) electricity generated from biogas production in Europe (GWh) (European Biogas Association, 2018)*

1.2. Italian Context

The "2020 climate & energy package" defines national targets as well as European targets. The Italian targets for 2020 are:

- Greenhouse Gas Emissions reduction of 13% compared to 2005 levels;
- 17% share of renewable energy;
- Energy efficiency of 158 MToe (Thousands tonnes of oil equivalent).

The "2020 climate & energy package" also asks each Member State to adopt a National Renewable Energy Action Plan (NREAP). In Italy it is represented by the "Piano d'Azione

Nazionale per le energie rinnovabili" (PAN)(EU, 2008). The PAN evaluates the amount of installed electricity capacity required to reach the targets sets by the EU for 2020. In the case of biogas, the PAN estimates that an installed electrical capacity of 1200 MWe is required (Ministero dello sviluppo Economico, 2010).

The adoption of the Biomethane Decree of 2nd March 2018 (which entered into force on March 20th) represents a key step for the development of biomethane and other advanced biofuels in the transport sector. The decree established a regulatory framework for the sector, in particular regarding advanced biomethane and plant conversion from biogas to biomethane. With the term "Advanced Biomethane" the Biomethane Decree of 2nd March 2018 defines the biofuel obtained from agricultural residues, organic waste and dedicated crops but not cultivated in naturalistic areas or in land designated to food and feed production. All these biomasses do not cause Indirect Land Use Change for their production (Ministero dello sviluppo Economico, Ministero dell'ambiente e della tutela del territorio e del mare and Ministro delle politiche agricole alimentari e forestali, 2018). It should be noted that, unlike other sectors, the evolution of biogas/biomethane production is mainly supported by the national industry with beneficial effects on stable employment growth in Italy. The biogas sector represents a production potential of renewable gas by 2030 of 10 billion Nm^3 of biomethane, of which 8 billion from agricultural matrices and 2 billion obtainable from selected organic waste, non-biogenic sources and gasification. Italy is the first European market for the use of natural gas for vehicles and has a fleet of almost 1 million natural gas vehicles (around 2.4% of the total) (CIB, 2018).

1.3. Anaerobic Digestion

1.3.1. Process overview

The AD process is defined as the biological degradation process of organic matter under anoxic conditions. Possible products include methane, carbon dioxide and other inorganic by-products (Cesaro, Belgiorno and Naddeo, 2010). This method of digestion uses wide range of bio-materials and converts a mixture of organic substrates into biogas and other valuable products (Munisamy *et al.*, 2017). These sources can be used as a single feedstock or in co-digestion.

Anaerobic co-digestion is the simultaneous AD of two or more substrates which is a promising possible option to overcome the disadvantages of mono-digestion and improve the economic viability of AD plants due to higher methane production (Hagos *et al.*, 2017). The anaerobic degradation occurs in four phases, as shown in figure 1.3:

- *Hydrolysis*: In this step insoluble complex organic matter (like carbohydrates, proteins and lipids) is broken down into their backbone constituents in order to allow their transport through microbial cell membrane (Madigan *et al.*, 2008). This is carried out by obligate anaerobes and a few facultative anaerobes (Yadvika *et al.*, 2004). Hydrolysis is recognised to be the rate-limiting step (López Torres and Espinosa Lloréns, 2008). Some industrial operations overcome this limitation by the use of chemical reagents to enhance hydrolysis. The application of chemicals to enhance the first step has been found to result in a shorter digestion time and provide a higher methane yield. (Kangle *et al.*, 2012). The hydrolysis of a complex and insoluble substrates depend on different parameters such as particle size, pH, production, diffusion and adsorption of enzymes to particles (Munisamy *et al.*, 2017). The major problem in the degradation is the lignin associated with the cellulose. In fact, lignin is one of the plants defence mechanisms against microbial attack and is practically undegradable at anaerobic conditions (Angelidaki and Batstone, 2010).
- *Acidogenic phase*: this step involves the conversion of the sugars, amino acids and fatty acids to hydrogen, acetic acid, carbon dioxide, organic acids (mainly volatile fatty acids or VFAs) and alcohols by obligate and facultative anaerobes (Kangle *et al.*, 2012).
- *Acetogenic phase*: in this step acetogens are able to convert hydrogen and carbon dioxide into acetic acid. The various organic acids are converted into acetic acid, carbon dioxide and hydrogen (Munisamy *et al.*, 2017).
- *Methanogenic phase*: in this step methane is produced from the acetic acid produced during the acetogenic phase or from the reduction of carbon dioxide using hydrogen. In general acetic acid is responsible for the production of two-thirds of the total methane (Smith and Mah, 1966; Zinder, 1993; Angelidaki and Batstone, 2010; Zou *et al.*, 2019).

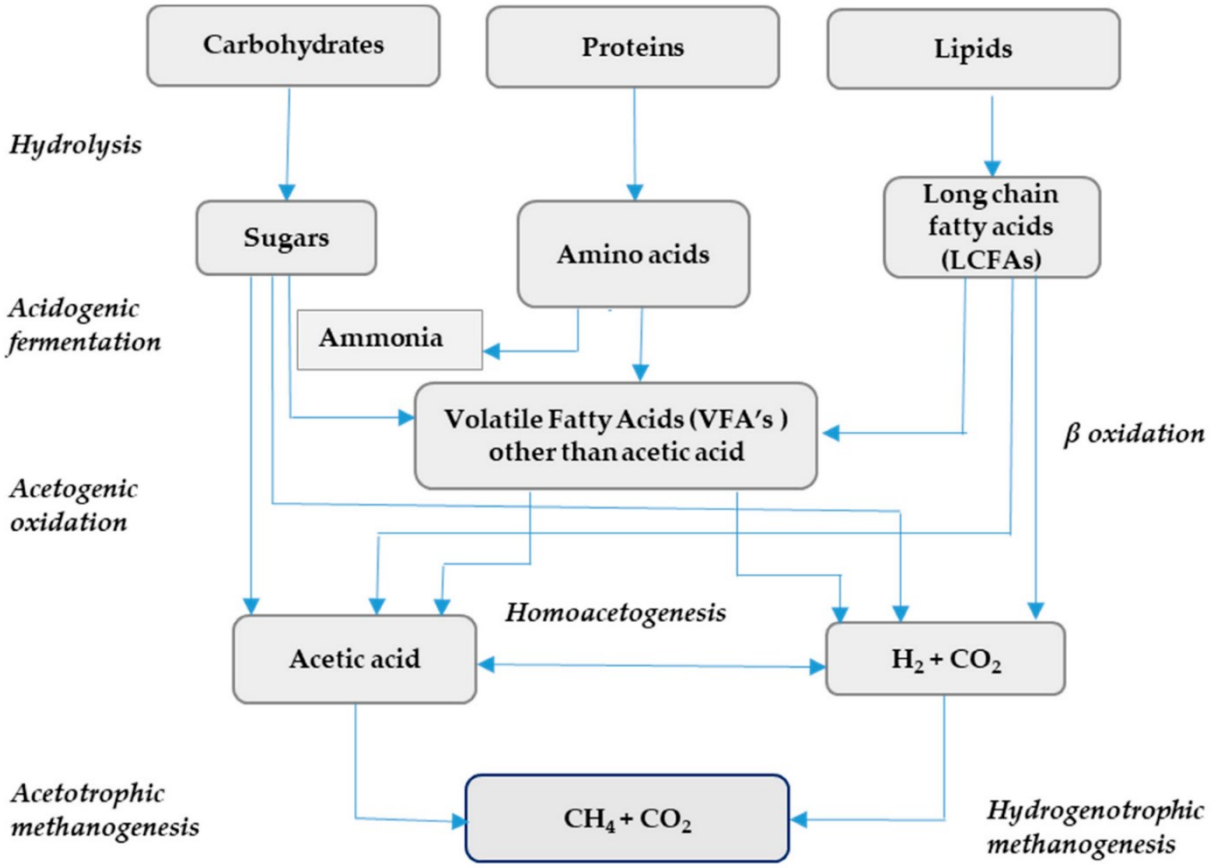

Figure 1.3: *Pathways of anaerobic digestion for biomethane production (Rabii et al., 2019).*

1.3.2.Process classification

Table 1.2 summarizes the possible classification of AD processes by means of different operative settings.

The thermophilic process is more difficult to operate and the need for heating and insulation add an extra cost to the treatment (Jansen, 1986). In general, the energy balance is better in the mesophilic range than in the thermophilic range. However the thermophilic mode of operation results in around 50% higher rate of degradation, and, particularly with fat-containing materials, a better microbial availability of the substrates and so a higher biogas yield (Deublein and Steinhauser, 2008).

Two stage systems can be a good option, because the optimal operation conditions for the different reaction stages differ. The prize for a more optimal condition for the different processes

is a more complicated construction, and normally also a more difficult process to operate (Jansen, 1986). The first stage serves as the hydrolytic-acidogenic step, while the second stage is the methanogenic step. The first stage requires a digester capable of handling high solid streams and operating at high retention times to enhance hydrolysis of the solids. The second stage can be a high-rate bio-reactor which further converts the first stage acidified effluent to biogas (Stamatelatou, Antonopoulou and Michailides, 2014).

Table 1.2: *AD technologies classification adapted from (Jansen, 1986; Riva, 2009)*

Classification parameter	Available Technology
Temperature	Psychrophilic (5-20 °C)
	Mesophilic (30-40 °C)
	Thermophilic (40-55 °C)
Quantity of process steps	One stage
	Two stages
Material flow	Batch process
	Continuous process
Water content	Dry fermentation, < 75 %
	Wet fermentation, > 90 %
	Semi-dry fermentation, >75%, <90%

Batch mode operation is more suitable for research purposes, but at full scale bio-reactors should operate on a continuous, or at least semi-continuous (fed or sequencing batch) basis (Stamatelatou, Antonopoulou and Michailides, 2014).

In function of the fraction of solids in the substrate different plant scheme are available:

- *Wet digestion.* Generally wet digestion has an amount of total solids (TS) < 10 % (Jansen, 1986). To achieve this dilution, water or recirculating part of the digester effluent is added (Vandevivere, De Baere and Verstraete, 2003; Cesaro, Belgiorno and Naddeo, 2010). In its simplicity, wet system appears attractive because of their similarity to the consolidate technology in use for the anaerobic stabilization of sewage sludge coming from wastewater treatment. Digesters of the CSTR-type (completely stirred tank reactors) are mostly used in this type of application (Lissens *et al.*, 2001; Riva, 2009). If a wet residue can be accepted as a fertilizer to be used on agricultural land, it favours a

wet process. However, if the wet digestate is believed to be wastewater, which has hence to be treated in a conventional wastewater treatment plant, the dry process is favoured, as no or almost no wet digestate is produced in this condition (Jansen, 1986);

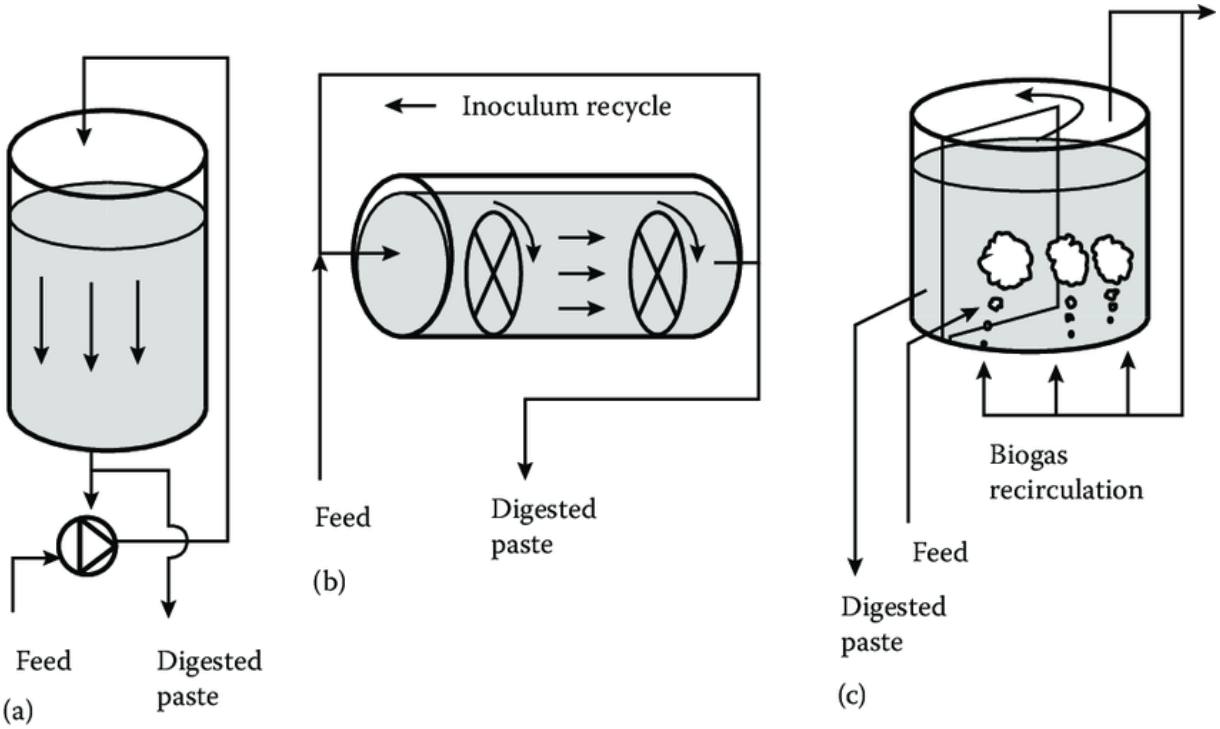

Figure 1.4: *Different digester designs used in 'dry' systems (A illustrates the Dranco design, B the Kompogas and BRV designs, and C the Valorga design)(Vandevivere, De Baere and Verstraete, 2003).*

- *Dry digestion.* Generally dry digestion is characterized by an amount of TS > 25 % (Jansen, 1986). Due to their high viscosity, the fermenting wastes move via plug flow inside the reactors. The main challenge is handling, pumping and mixing solid streams (Vandevivere, De Baere and Verstraete, 2003). At least three designs have been demonstrated effective for the adequate mixing of solid wastes at the industrial scale: Dranco, Valorga and Kompogas (Vandevivere, De Baere and Verstraete, 2003; Riva, 2009; Cesaro, Belgiorno and Naddeo, 2010). A scheme of the three reactors is shown in figure 1.4. In the Dranco process, the mixing occurs via recirculation of the wastes extracted at the bottom end, mixing with fresh wastes (one part fresh wastes for six parts digested wastes), and pumping to the top of the reactor. The Kompogas process works

similarly, except that the plug flow takes place horizontally in cylindrical reactors. The horizontal plug flow is aided by slowly-rotating impellers inside the reactors, which also serve for homogenization, degassing, and re-suspending heavier particles (Vandevivere, De Baere and Verstraete, 2003). The Valorga system is quite different in that the horizontal plug flow is circular in a cylindrical reactor and mixing occurs via biogas injection at high pressure at the bottom of the reactor every 15 minutes through a network of injectors (De Laclos, Desbois and Saint-Joly, 1997).

- *Semi-dry digestion*. This process is in between the wet and dry digestion processes. The TS is generally around 12-18 %. Mixing and pumping is easy and does not require complex pre-treatment when used for organic fraction of municipal solid waste (OFMSW). The most common reactor type used is the CSTR in both mesophilic and thermophilic regime (Riva, 2009).

1.3.3. OFMSW as possible feedstock

Biogas is produced by AD beginning from a range of feedstocks, particularly agricultural residues (e.g. manure and crop residues), energy crops, organic-rich waste waters, OFMSW and industrial organic waste (Cucchiella and D'Adamo, 2016). The definition of OFMSW varies regionally and nationally; in the United States of America, OFMSW is considered a mixture of food, garden wastes and paper. In the European Union it is considered a mixture of wastes from parks, gardens and kitchens (Campuzano and González-Martínez, 2016). Production and composition of OFMSW depend on geographic region, number of inhabitants and their social condition, predominant economic activities, regional food habits, season and recollection system (Rao and Singh, 2004; Hansen *et al.*, 2007; Heaven *et al.*, 2010; Eisted and Christensen, 2011; Campuzano and González-Martínez, 2016).

1.3.4. Pre-treatments

Several pre-treatment methods aim at increasing particle surface area or removing lignin to unpack carbohydrates from bio-fibres and contribute to an increase in the rate of hydrolysis; indirectly by making particulate more accessible for hydrolysis (Angelidaki and Batstone, 2010;

Fdez.-Güelfo *et al.*, 2011). Pre-treatment methods for lingo-cellulosic biomass can be divided into three main types: physical, chemical or physicochemical and biological.

Physical or mechanical pre-treatment refers to milling which reduces the size of the particulate matter. The specific surface area of the solids and size of pores are therefore increased, the crystallinity and degree of polymerisation of the cellulose are decreased, and enzymes can more easily access the substrate to initiate hydrolysis. Mechanical pre-treatment is always applied before any other kind of pre-treatment (Stamatelatou, Antonopoulou and Michailides, 2014). More recent studies suggest that ultrasound (US) can be effective as a pre-treatment method for OFMSW (Chen *et al.*, 2008; Cesaro and Belgiorno, 2013).

During chemical or physicochemical pre-treatment, the lingo-cellulosic biomass is exposed to chemicals (acids, alkali or solvents) at ambient or higher temperature. The main effect is to alter the lignin structure and to dissolve the hemicelluloses (Stamatelatou, Antonopoulou and Michailides, 2014). In the case of OFMSW research shows that alkali pre-treatment is effective (López Torres and Espinosa Lloréns, 2008; Li *et al.*, 2012). Another effective chemical treatment is peroxidation (Dewil *et al.*, 2007) and ozonation (Cesaro and Belgiorno, 2013).

Biological pre-treatment refers to the use of whole micro-organisms or purified enzymes to disrupt the lingo-cellulosic matrix and enhance hydrolysis. Both fungi (brown, white and soft-rot fungi) and bacteria have so far been tested for the delignification of lingo-cellulosic biomass (Stamatelatou, Antonopoulou and Michailides, 2014). In the case of OFMSW these kind of pre-treatments are generally preferred when compared to chemical pre-treatments (Fdez.-Güelfo *et al.*, 2011).

1.3.5.Process operating variables

A series of environmental factors affects the overall process performance. These factors include:

- Temperature: it has a strong influence on both physicochemical parameters and microbiological processes. The physicochemical parameters that are affected are mainly viscosity, diffusivity, equilibrium coefficients and solids availability. There are three generalized microbial operating regimes, defined by the organisms with optimal operating points in those ranges: thermophilic (40-60 °C), mesophilic (25-40 °C) and psychrophilic (0-25 °C) (Angelidaki and Batstone, 2010). Mesophilic conditions are

most commonly used even if thermophilic digestion requires lower residence time. Psychrophilic conditions are rare (Riva, 2009).

- pH: the optimal pH for this process is generally close to neutral (Yadvika *et al.*, 2004; Deublein and Steinhauser, 2008; Hilkiah Igoni *et al.*, 2008; Riva, 2009; Kangle *et al.*, 2012; Hagos *et al.*, 2017). In the biogas production process, there are multi-organism which require different optimal pH growth (Kangle *et al.*, 2012; Hagos *et al.*, 2017). In the AD process, methanogenesis microorganisms are very sensitive to pH variations and prefer a pH around 7.0. Acidogenesis microorganisms are relatively less sensitive to pH and are tolerable to the range of 4.0–8.5. However, the optimal pH for hydrolysis and acidogenesis is between 5.5 and 6.5. The optimum pH value is one main reason to separate digesters into two-phase as acidogenic phase and methanogenesis phase (Hagos *et al.*, 2017). In general the acidogenesis phase lowers the pH due to the production of VFAs, while the methanogenic phase tends to make the pH higher by consuming the VFAs. If the process is not balanced and the acidogenesis is faster than the methanogenic phase the pH decreases, lowering the efficiency of the methanogenesis (Hilkiah Igoni *et al.*, 2008; Angelidaki and Batstone, 2010; Rabii *et al.*, 2019).
- Alkalinity: Acid-neutralizing or buffering capacity of a digester is termed as alkalinity (Kangle *et al.*, 2012). It is generally expressed in equivalent concentration of calcium carbonate. Together with the production of ammonia from protein degradation it constitutes the buffering system which mitigates decrease of pH when the VFAs production is too high (Riva, 2009).
- Amount of volatile solids (VS): it is the combination of biodegradable volatile solids (BVS) and the refractory volatile solids (RVS) which is mostly lignin. BVS fractions of substrates are helpful to improve biodegradability of the waste, organic loading rate, Carbon-Nitrogen ratio, and biogas production. Waste materials containing high VS and low RVS are the most suited to AD treatment (Rabii *et al.*, 2019).
- Carbon-Nitrogen ratio (C/N ratio): it is the amount of carbon and nitrogen present in feedstock (Rabii *et al.*, 2019). A high C/N ratio is an indication of rapid consumption of nitrogen by methanogens and results in lower gas production. On the other hand, a lower C/N ratio causes ammonia accumulation and higher pH values, which are toxic to

methanogenic bacteria (Kangle *et al.*, 2012). It is generally found that during anaerobic digestion microorganisms utilize carbon 25–30 times faster than nitrogen. Consequently microbes need a 20–30:1 ratio of C to N (Yadvika *et al.*, 2004; Deublein and Steinhauser, 2008; Hilkiah Igoni *et al.*, 2008; Riva, 2009; Kangle *et al.*, 2012).

- Particle size: The size of the feedstock should not be too large, otherwise it would result in the clogging of the digester, and also it would be difficult for microbes to carry out the digestion. Smaller particles on the other hand would provide large surface area for adsorbing the substrate, that would result in increased microbial activity and hence increased gas production (Yadvika *et al.*, 2004; Deublein and Steinhauser, 2008). This is particularly useful for OFMSW due to its relatively large particle size (Hilkiah Igoni *et al.*, 2008).

1.3.6.Biogas uses and upgrade

Typical values for biogas composition are shown in table 1.3:2.

Table 1.3: *Typical biogas composition (Riva, 2009)*

Chemical species	Composition within the biogas
CH_4	50-80%
CO_2	20-50%
H_2S	<1%
H_2	traces
N_2	traces
R_2SiO	traces

In general it is more convenient to send the biogas into a cogeneration plant, even if the calorific value is lower than that of pure methane, to obtain electricity and recover heat (Riva, 2009). The biogas is generally used in-situ, since injecting it into the European methane grid requires it to be conform to the EN 16723-1:2016 (CEN/TC 408, 2016). In order to possibly achieve these specifications biogas upgrading to biomethane is required.

Conventional biogas upgrading methods can be divided into the following process types: membrane separation, scrubbing (absorption methods), pressure swing adsorption and

cryogenic separation (Niesner, Jecha and Stehlík, 2013; Muñoz *et al.*, 2015; Wilken *et al.*, 2017). Membrane separation methods are based on the principle that gases diffuse through the membranes at different speeds. A variety of polymers can be used as membranes. Scrubbing, also referred to as absorption, is based on the effect whereby gas components are soluble in different fluids to varying degrees. For example, CO_2 dissolves much better in water than CH_4. Physical scrubbing methods are based on the physical solubility of gas components in a wash solution (generally water) without chemical reaction. In physical scrubbing, it is also possible to use organic solvents instead of water to upgrade the biogas. The advantage of these solvents is the higher solubility of CO_2 and H_2S compared to water. The result is that less detergent is required and the height of the scrubber column can be reduced. Since CO_2 and H_2S are more strongly held in solution, the regeneration of the washing liquid is more complex. In chemical scrubbing, some gases (e.g. CO_2 and H_2S) react reversibly with the washing liquid. The binding agent/solution is therefore substantially stronger than in the case of physical scrubbing. Mixtures of water with the additives monoethanolamine (MEA), diethanolamine (DEA), methyldiethanolamine (MDEA) and other amine compounds are usually used as detergent. The advantages are the higher loading of the solution, higher selectivity of the gas separations, and thus a higher purity of the product gas. A lean gas treatment is therefore not necessary, but fine desulphurisation must be carried out upstream. Adsorptive methods are based on the principle that different gas components are attracted differently to specific surfaces (adsorbed) or penetrate to varying degrees into the pores of the material. Cryogenic treatment is based on the fact that, at low temperatures or high pressures, gases condense (become liquid) or sublimate (become solid). The temperatures or pressures at which this occurs can be found in a phase diagram. For example, CO_2 sublimates at -78.5°C at 1 bar while CH_4 remains gaseous. The gas components of biogas can be separated in different states of matter (Wilken *et al.*, 2017).

Innovative methods of CO_2 sequestration involving biotechnologies are being researched. These include: H_2-assisted CO_2 bioconversion, microalgae-based CO_2 fixation, enzymatic CO_2 dissolution, fermentative CO_2 reduction and in situ CO_2 desorption (Muñoz *et al.*, 2015).

1.3.7.Digestate post-treatment

Digestate is the solid-liquid suspension produced from the anaerobic digestion of organic material. In general, the anaerobic digestate is rich in nitrogen, phosphorous and potassium. After solid-liquid separation, the liquid part contains a high nitrogen percentage (TN in table 1.4) and the solid part contains is rich in phosphorous (Logan and Visvanathan, 2019).

Table 1.4: *Typical characteristics of organic fractions of municipal solid waste digestate(Peng and Pivato, 2019)*

Digestate type	pH	%TS	C/N	TN (%TS)	P_2O_5 (%TS)
Whole	8,3	0,72-51,2	1,3-29,8	1,3-12,4	0,2-0,9
Solid	8,8	7,23-27,0	12,1-20,9	1,09	1,49
Liquid	8,34-8,80	3,90	2,7	13,85	1,22

Table 1.4 shows typical values for liquid and solid digest. Often, the first step in digestate processing is to separate the solids from the liquid. To improve solid-liquid separation, flocculation or precipitation agents are commonly applied. A variety of solid-liquid separation technologies are available on the market such as decanter centrifuges, screw press separators, bow sieves, double circle bow sieves, sieve belt presses, and sieve drum presses. The decanter centrifuge and the screw press separator have gained popularity, especially among farmers who need to export their excess of nutrients to other areas. Decanter centrifuges are used in many municipal waste treatment plants in the world. Screw press separators are particularly used when the digestate is rich in fibres (Logan and Visvanathan, 2019).

Figure 1.5 shows most of the treatments used for the whole digestate and both the solid and the liquid fractions. Mainly, the solid fraction can subsequently be directly applied as fertilizer in agriculture or it can be composted or dried for intermediate storage and enhanced transportability, other than to stabilize the organic matter. Due to regulatory requirements, the liquid fraction cannot be discharged directly in to the receiving water body. There are many technologies recommended to treat the liquid fraction such as membrane technology, evaporation, stripping and biological oxidation. A part of the liquid fraction can also be added during mashing of the feedstock into the digester. Furthermore, the liquid portion can also be

used to moisturize compost heaps or as source for effective microorganism to facilitate the composting process (Logan and Visvanathan, 2019).

In order to extract nutrients from biogas digestate, microalgae cultivation in the liquid fraction is an interesting option, since nitrogen and phosphorous are readily available. In fact also the pH of the digestate is generally close to the optimal one for microalgae growth. The main inhibition effects are related to an excessive amount of nitrogen and the high turbidity of the medium (Xia and Murphy, 2016).

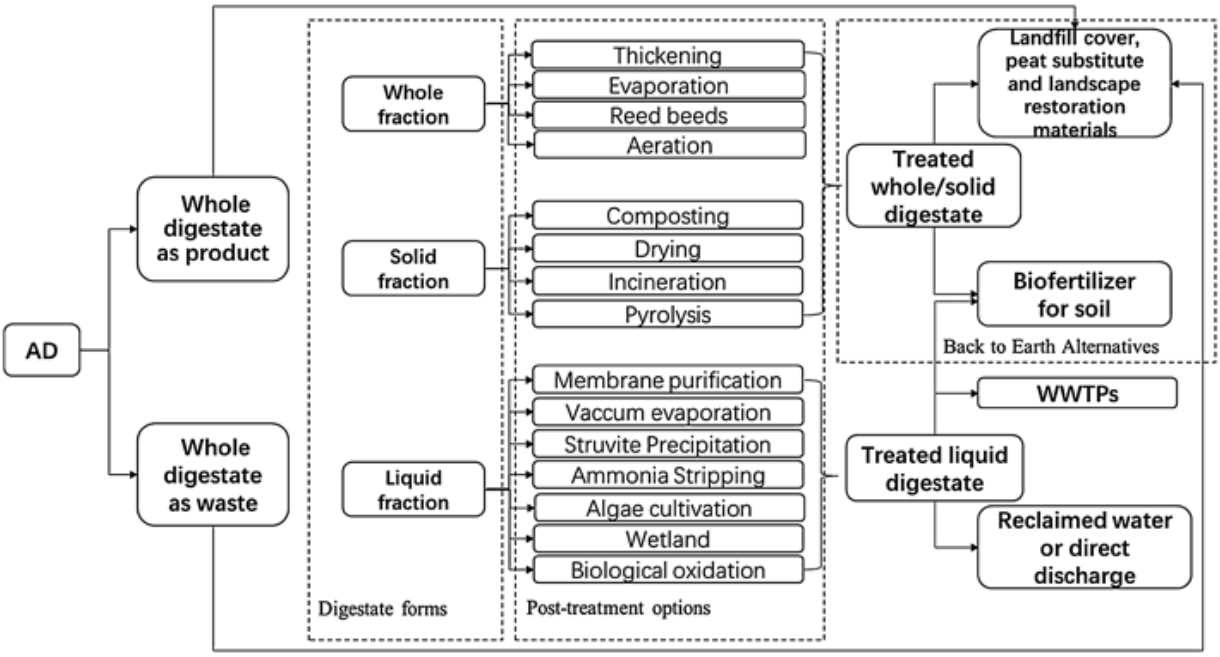

Figure 1.5: *post-treatment of digestate from Anaerobic digestion (Peng and Pivato, 2019)*

1.4. Microalgae

Algae are oxygen evolving photosynthetic microorganisms containing chlorophyll. In general they are primitive plants so they lack roots, stems and leaves, vascular tissues and a sterile covering of cells around the reproductive organ. Most of the algae are microscopic organisms known as microalgae, but some algae are quite large and known as macroalgae. Microalgae are unicellular or simple multicellular organism with size ranges from 2 to 200 μm, whereas macroalgae are completely multicellular organism, some growing to over 100 ft in length.

Microalgae are extensively studied not only due to their ubiquitous nature but also for their simple structure that allows them to grow and proliferate in a wide range of environmental conditions. For example they can survive in various aquatic environments like lacustrine, brackish, fresh water, higher saline water, hot springs, waste water maturation ponds, dams, rivers, marine and coastal areas. Their simple cellular structure provides a large surface to volume body ratio, which gives them the ability to uptake large amount of nutrients (Aishvarya *et al.*, 2015).

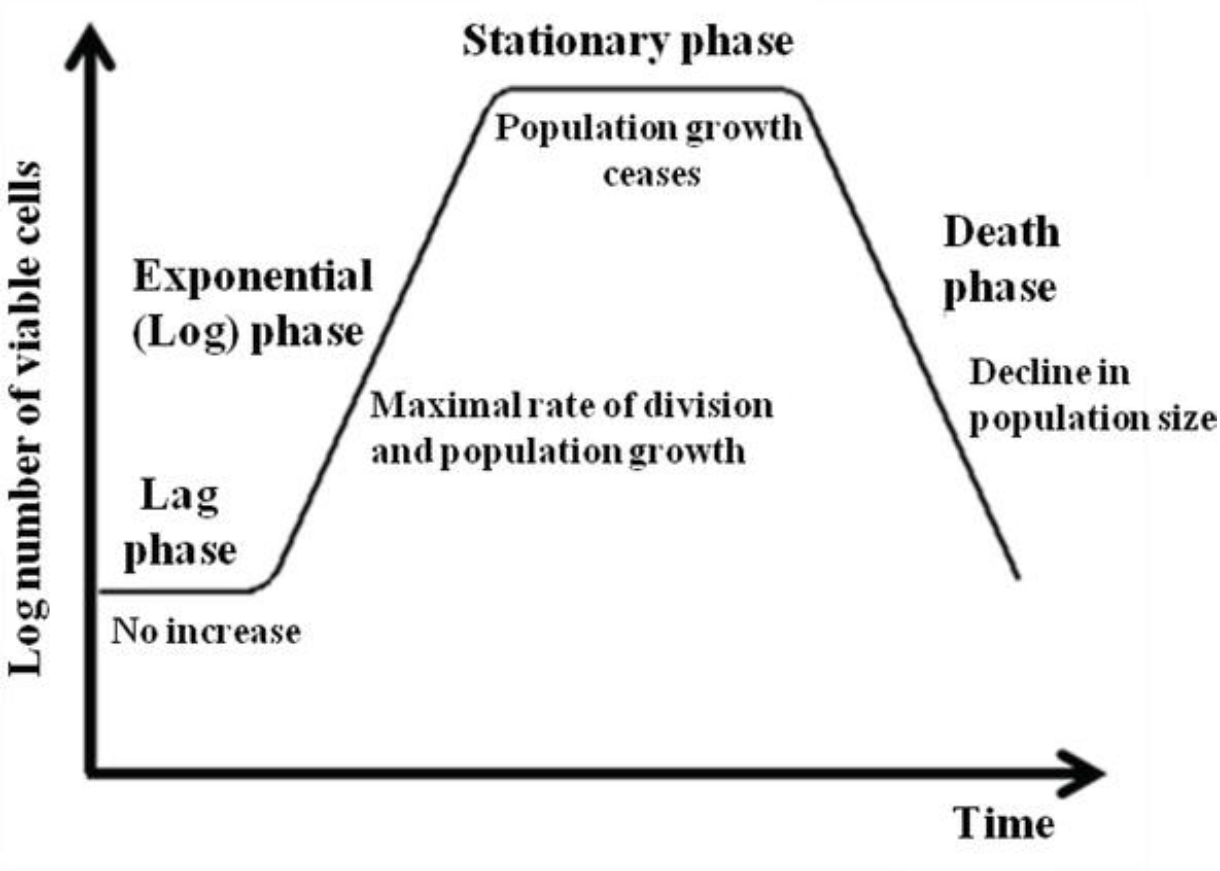

Figure 1.6: *microbial growth curve (Cruz et al., 2018)*

Microalgae growth follows the four phases showed in figure 1.6. The first phase observed under batch conditions is the lag phase, in which the growth rate is essentially zero. The lag phase is thought to be due to the physiological adaptation of the cell to the culture conditions. The second phase of growth observed in a batch system is the exponential phase. During exponential growth the rate of increase of cells in the culture is proportional to the number of cells present at any

particular time. The third phase of growth is the stationary phase. The stationary phase in a batch culture can be defined as a state of no net growth. Although there is no net growth in stationary phase, cells still grow and divide. Growth is simply balanced by an equal number of cells dying. The final phase of the growth curve is the death phase, which is characterized by a net loss of viable cells. Even in the death phase there may be individual cells that are metabolizing and dividing, but more viable cells are lost than are gained so there is a net loss of viable cells (Maier, 2009). The period of duration of each phase depends on the species and the conditions of cultivation (Cruz *et al.*, 2018).

1.4.1.Microalgae growth factors

Media used for cultivating microalgae must supply all the necessary components required for growth and maintenance of the organism. These include:

- Nutrients quantity and quality: the three most important nutrients for autotrophic growth are C, N and P, but also traces of minor nutrients are required. Phosphorous should be in phosphate form, while nitrogen is preferred in the ammonium form (Grobbelaar, 2013; Xia and Murphy, 2016);
- Light: Like plants, microalgae require light as the main source of energy to carry out fixation of CO_2 into organic matter in the process of photosynthesis. Usually the major problem in cultivating microalgae is related to the light availability, as low intensity causes photo-limitation and higher intensity causes photo-inhibition. The requirement of light varies greatly with culture growth (density) and culture system (depth) (Lavens and Sorgeloos, 1996). Generally, as microalgae grow and reproduce, biomass density increases. As a result, microalgae distant from the surface are shaded by the microalgae culture present in the upper layers, thus receiving lesser amount of light (Aishvarya *et al.*, 2015);
- Temperature: Most commonly used microalgae tolerate temperatures between 16 and 27 °C (Lavens and Sorgeloos, 1996). Temperature below the optimal temperature may not kill the microalgae but reduce the growth rate, whereas high temperature will kill most of the microalgae (Aishvarya *et al.*, 2015);

- pH: Most of the microalgae grow in the pH range of 7-9, while the optimum range is 8,2-8,7 (Lavens and Sorgeloos, 1996). As the culture grows, pH of the culture medium increases with time as a result of continuous consumption of CO_2. If the pH is not maintained within the optimum pH range, it may result in disruption of many cellular processes, leading to the inhibition of biomass growth. The pH in the growing culture can be maintained either through simple aeration or through addition of extra CO_2 (Aishvarya *et al.*, 2015);
- Salinity: The total salt concentration mostly depends on the ecological origin of the organism. Salinity changes normally affect microalgae in three ways: osmotic stress, ion stress and changes of cellular ion concentration due to the selective permeability of ion through the membrane (Lavens and Sorgeloos, 1996);
- Turbulence: Continuous mixing of the culture is essential for successful microalgal biomass production. Mixing provides appropriate distribution of nutrients, light, dissolved CO_2, O_2 elimination, maintenance of pH and temperature gradient and reduces algal sediment formation (Lavens and Sorgeloos, 1996). Further it improves the gas exchange between the culture medium and the air (Aishvarya *et al.*, 2015).

All these parameters not only affect photosynthesis and productivity of biomass but also influence the pattern, pathway and activity of cellular metabolism, and thus change in cell composition.

1.4.2. Type of Photobioreactors

The design and optimisation of photobioreactors to cultivate these microorganisms is a major step in transforming scientific findings into a marketable product (Aishvarya *et al.*, 2015). From a commercial point of view, a microalgae culture system must have as many of the following characteristics as possible: high area productivity, high volumetric productivity, inexpensiveness (both in terms of investment and maintenance costs), simple control of the culture parameters (temperature, pH, CO_2, turbulence), energy efficiency and reliability (Olaizola, 2003). The cultivation systems adopted for microalgae are traditionally either in open ponds, known as high rate ponds (HRP) or raceway ponds (RP), or in enclosed systems known as photobioreactors (PBR) (Aishvarya *et al.*, 2015). After the bioreactors, the outlet stream

needs to be processed to obtain the algae biomass. The first step is called bulk harvesting while the second step is called thickening (Aishvarya *et al.*, 2015). The main processes used for the downstream processing are summarized in table 1.5.

Table 1.5: *Methods of harvesting microalgae (Aishvarya et al., 2015)*

Stage of harvesting	Methods	Advantages	Disadvantages
Bulk harvesting	Sedimentation	Low cost, useful as first stage in separation to reduce energy input and cost	Settling rate specific to algae species; best for dense non-motile cells; can be slow
	Flotation	Uses air or gas bubbles; rapid than sedimentation	Species specific; oil-laden cells easily separated; air bubbling costs can be high
	Flocculation	Range of techniques available with low to high cost	Removal of flocculants and chemical contamination of harvested biomass
Thickening	Centrifugation	Can handle most algal cell types, efficient harvesting	High capital and operational costs
	Filtration	High concentrations can be achieved, efficient for large cells	Species dependent; clogging or fouling of filters; membrane costs can be high
	Ultrafiltration	Can handle delicate cells	High capital and operational costs

1.4.2.1. Open Ponds

These systems are generally easier and less expensive to build while also being more durable. Operation cost is also lower, since they can use natural sunlight and rainfall runoff water or sewage water. On the other hand, these system are susceptible to weather conditions, with no control of physical parameters such as water temperature, evaporation and lighting. Furthermore, biomass productivity is also limited by contamination with unwanted algal species as well as organisms that feed on algae. Consequently, this strictly limits the species of algae that can be grown in such systems, (Aishvarya *et al.*, 2015) and their applicability is mainly related to environmental applications, such as wastewater treatment.

The classical open-air cultivation systems comprise lakes and natural ponds, circular ponds, raceway ponds and inclined systems (Grobbelaar, 2013; Aishvarya *et al.*, 2015). Raceway ponds (shown in figure 1.7) are the most commonly used artificial culture system (Aishvarya *et al.*, 2015) while inclined systems are not used for commercial production of microalgae (Grobbelaar, 2013).

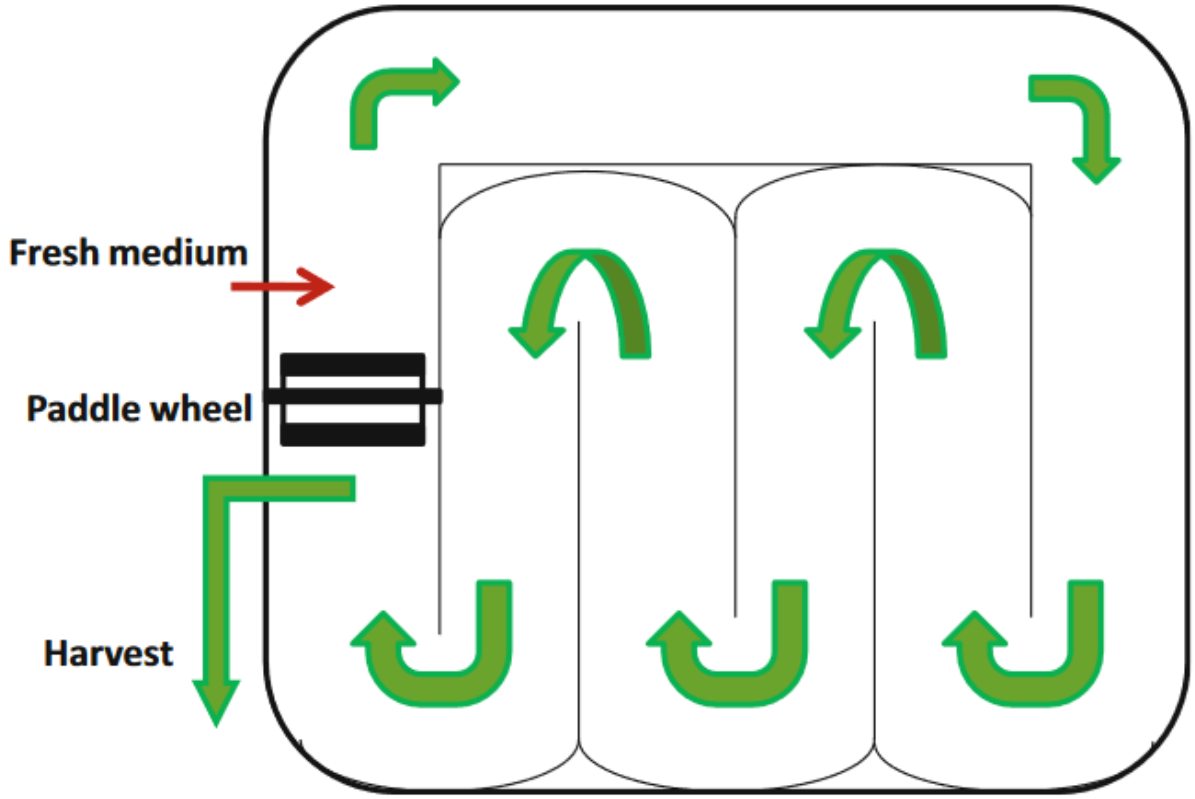

Figure 1.7: *schematic of a raceway pond (Aishvarya et al., 2015)*

1.4.2.2. Closed Systems

The main categories include: tubular (helical, manifold, serpentine and α shaped), flat plate (alveolar panels and glass plates), column (bubble columns and airlift) and stirred tank reactor. An example is shown in figure 1.8, where the PBR has an inlet for fresh feed, an outlet for recirculation or harvest and a column for gas removal and settling purpose (Aishvarya *et al.*, 2015). These systems can use both natural and artificial lighting. Closed microalgae bioreactors offer theoretical advantages in terms of avoiding contamination, yielding higher culture

densities and providing closer control over physico-chemical conditions (Greenwell *et al.*, 2010; Mata, Martins and Caetano, 2010). Even if avoiding contamination is one of the main benefits of using PBRs, full sterile conditions are achieved only when required by specific products (Grobbelaar, 2013).

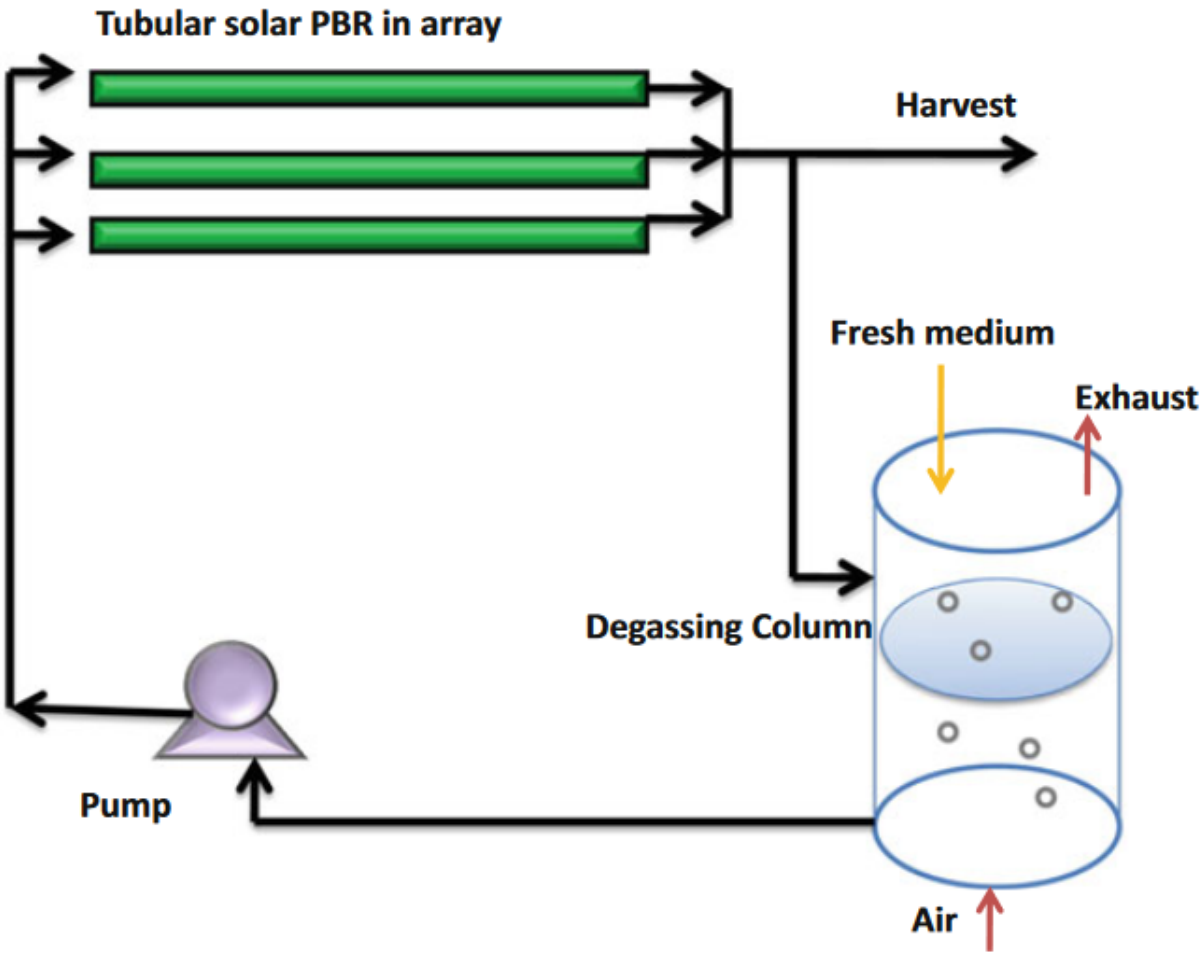

Figure 1.8*: Schematic of tubular PBR using solar light (Aishvarya et al., 2015)*

PBRs can be optimized according to the biological and physiological characteristics of the algal species being cultivated, allowing one to cultivate algal species that cannot be grown in open ponds. Their main limitations include: overheating, bio-fouling, oxygen accumulation, difficulty in scaling up, the high capital and operating costs, and cell damage by shear stress and deterioration of material used for the photobioreactor. The cost of biomass production in PBRs may be one order of magnitude higher than in ponds. The higher cell concentration and

productivity achieved in PBR may not compensate for its higher capital and operating costs (Mata, Martins and Caetano, 2010).

1.4.3. Uses of microalgae

Depending on the microalgae species both bulk commodities and high-value chemical compounds can be produced. Bulk commodities (like biofuels) are have large production scale and low value, while various high-value chemical compounds are largely used in different industrial sectors (e.g. pharmaceuticals, cosmetics, nutraceuticals, functional foods and biofuels) but have smaller production scale. Because the production of these fine chemicals and bioactive compounds normally demands the use of monocultures and controlled cultivation systems for the highest productivity and production efficiency, this has led to the development of large-scale PBRs. For example, microalgae are viewed as having a protein quality value greater than other vegetable sources, like wheat, rice, and legumes, but poorer than animal sources, for example, milk and meat. Considerable efforts have been made to promote the microalgae use in human food. However, high production costs and fear of toxicological contamination have limited algae application to expensive “healthy” foods. So far, microalgae cultures have been more successful for food source and feed additive in the commercial rearing of many aquatic animals. Although nutritional requirements for some species have been defined, no set of nutritional criteria have yet been advanced. Generally, the algae must be non-toxic, in an acceptable size for ingestion, the cell wall should be digestible, and with sufficient biochemical constituents (Mata, Martins and Caetano, 2010).

Microalgae can also be used to produce biofuels, thanks to their ability to accumulate lipids. Microalgae have several advantages like higher photosynthetic efficiency, higher growth rates and biomass production compared to other energy crops, no competition with food crops for land, less water and nutrient requirements. Algal biomass can serve as energy source in more ways than just oil. The biomass left after the extraction of oil is rich with cellular storage products. Ethanol, a valuable fuel, can be produced from the leftover biomass by fermentation. Residual biomass may be used to produce methane by anaerobic digestion, for generating the electrical power necessary for running the microalgal biomass production facility (Spolaore *et al.*, 2006). Although the microalgal biomass can be directly used to produce methane by

anaerobic digestion as the only feedstock, it cannot compete with the many other low-cost organic substrates that are available (Jankowska, Sahu and Oleskowicz-Popiel, 2017).
Microalgae cultivation can be used to remove nutrients from the liquid digestate produced during AD. This is possible because this fluid is rich in phosphorous and ammonium and its pH is generally close to the optimal one for microalgae growth. A high amount of nitrogen and high turbidity might have an inhibitory effect (Xia and Murphy, 2016). Microalgae are also able to fixate CO_2 during photosynthesis making them interesting as an innovative technology for CO_2 sequestration (Muñoz *et al.*, 2015).

1.5. Aim of the thesis

The aim of this thesis is to evaluate the performance and the economic potential of an integrated process involving anaerobic digestion of OFSMW and microalgae cultivation, by means of process simulation. For the AD and the cogeneration plant, the simulations refers to a plant scale treating 1 ton/day of OFMSW while the photo-bioreactor performances are evaluated by means of a kinetic model calibrated on previous experimental data. The techno-economic analysis is about the effect that adding microalgae cultivation has on the profitability of an AD plant at such scale, in order to check if the costs of biogas production can be reduced. Microalgae growth is used as liquid pre-treatment for the liquid digestate produced during AD as well as a method of capturing the CO_2 produced during co-generation. The liquid digestate and the off-gas provide the necessary nutrients (ammonium, phosphorous, carbon) for microalgae growth. The material balances of the entire integrated process will be evaluated using the process simulator Aspen Plus V.9, while secondary calculations will be carried out using MatLab R2018b and Excel 2016.

Chapter 2

Models and Methods

Chapter 2 describes the structure of the Aspen Plus simulation. First, the chemical species taken into consideration in the simulation are listed, followed by a description of the thermodynamic model employed. Then all the equilibrium chemical reactions that are taken into account are described. Finally, the Aspen plus simulation flowsheet is laid out, with particular focus on the unit operations involved and the main operating variables.

2.1. Components and thermodynamic model

Table 2.1 reports the components used in the Aspen simulation. Some of these components either appear in the kinetic model or in the equilibrium reactions. In the Aspen Plus simulations the components can be defined as conventional components and non-conventional components. The non-conventional components are the ones that are not included in the databases available within Aspen Plus: these are the microalgal biomass, the dry OFSMW and the bacterial sludge produced during the anaerobic digestion process. These non-conventional components are called ALGA, FORSU and FANGO in the simulation. Non-conventional components are treated as solids within the Aspen Plus simulation and are defined using the GENANAL component attributes, ENTHGEN as an enthalpy model and DNSTYGEN as a density model.Some of the components are defined as Henry Components, which means that their vapour-liquid equilibrium behaviour is calculated according to the Henry's law. One species is defined as Henry Components when it is in supercritical condition with respect to the temperature range of the process (which is higher than ambient temperature).

Table 2.2 shows the critical temperature present in the Aspen Plus database for the species that are ultimately defined as Henry Components. The critical temperature of CO_2 is higher than the typical ambient temperature. Even if this might be the case in the plant, experience shows that considering CO_2 a Henry Component gives better results with respect to solubility of CO_2 in H_2O.

Table 2.1: *chemical species involved in the Aspen Plus simulation*

Fortran Id	Chemical specie	Aspen type	Henry Component
1	CO_2	Conventional	Yes
2	CH_4	Conventional	Yes
3	H_2O	Conventional	No
4	NH_3	Conventional	No
5	NH_4^+	Conventional	No
6	OH^-	Conventional	No
7	H_3PO_4	Conventional	No
8	H_3O^+	Conventional	No
9	$H_2PO_4^-$	Conventional	No
10	HPO_4^{2-}	Conventional	No
11	PO_4^{3-}	Conventional	No
12	O_2	Conventional	Yes
13	N_2	Conventional	Yes
14	NO	Conventional	Yes
15	H_2S	Conventional	No
16	S^{2-}	Conventional	No
17	SO_2	Conventional	No
18	NH_2COO^-	Conventional	No
19	HS^-	Conventional	No
20	HCO_3^-	Conventional	No
21	HSO_3^-	Conventional	No
22	CO_3^{2-}	Conventional	No
23	SO_3^{2-}	Conventional	No
24	ALGA	Nonconventional	No
25	FORSU	Nonconventional	No
26	FANGO	Nonconventional	No

Table 2.2: *critical temperature of the Henry components defined ined in the Aspen plus simulation*

Chemical Specie	Critical Temperature (°C)
$\boldsymbol{CO_2}$	31,05
$\boldsymbol{CH_4}$	-82,55
$\boldsymbol{O_2}$	-118,55
$\boldsymbol{N_2}$	-146,95
$\boldsymbol{NO}$	-93,15

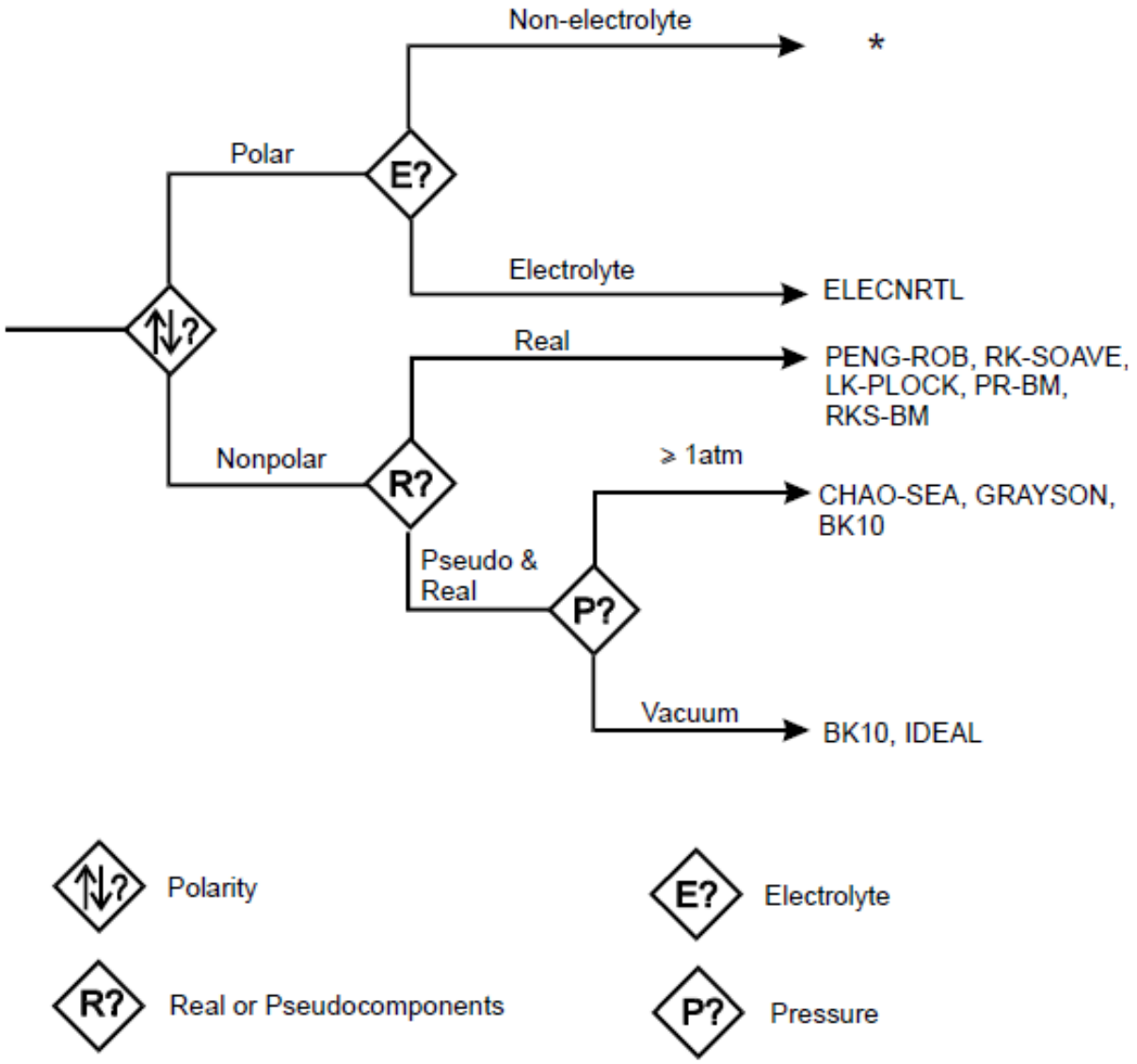

Figure 2.1: *guidelines for choosing a property method (Aspen Technology Inc, 2000). The "*" indicates other property methods present in Aspen Plus*

2.2. Chemical reactions

Once the components present in the simulation are defined, the chemical equilibrium reactions involving them are generated using the Elec Wizard tool in Aspen Plus and can be found in GLOBAL chemistry.

Table 2.3 lists the formation of ionic species and their dissociation equilibria which are considered in the Aspen Plus simulation. Besides the equilibrium reactions, other reactions are required to simulate OFMSW degradation in the anaerobic digester and microalgae growth in the raceway reactor.

Table 2.3: *equilibrium reactions considered in the Aspen plus simulation*

Id	Type	Reaction
1	Equilibrium	$H_2O + HPO_4^{2-} \leftrightarrow H_3O^+ + PO_4^{3-}$
2	Equilibrium	$H_2O + HSO_3^- \leftrightarrow H_3O^+ + SO_3^{2-}$
3	Equilibrium	$2H_2O + SO_2 \leftrightarrow H_3O^+ + HSO_3^-$
4	Equilibrium	$H_2O + H_2PO_4^- \leftrightarrow H_3O^+ + HPO_4^{2-}$
5	Equilibrium	$H_2O + H_3PO_4 \leftrightarrow H_3O^+ + H_2PO_4^-$
6	Equilibrium	$NH_3 + HCO_3^- \leftrightarrow H_2O + NH_2COO^-$
7	Equilibrium	$NH_3 + H_2O \leftrightarrow NH_4^+ + OH^-$
8	Equilibrium	$H_2O + HCO_3^- \leftrightarrow CO_3^{2-} + H_3O^+$
9	Equilibrium	$2H_2O + CO_2 \leftrightarrow H_3O^+ + HCO_3^-$
10	Equilibrium	$H_2O + HS^- \leftrightarrow H_3O^+ + S^{2-}$
11	Equilibrium	$H_2O + H_2S \leftrightarrow H_3O^+ + HS^-$
12	Equilibrium	$2H_2O \leftrightarrow H_3O^+ + OH^-$

In the anaerobic digester, the stoichiometry of the degradation reaction is calculated using a modified version of the McCarty equation (Małgorzata, 1999) to account for the production of phosphoric acid.

$$\frac{1}{2}\cdot\left(-a+\frac{d\cdot e}{2}+\left(c-y\cdot s\cdot\frac{d}{d'}\right)\cdot 3+\left(f-z\cdot s\cdot\frac{d}{d'}\right)\cdot 3+2\cdot g+x\cdot s\cdot\frac{d}{d'}\right)H_2O \quad (2.1)$$
$$+ C_nH_aO_bN_cP_fS_g$$
$$\rightarrow s\cdot\frac{d}{d'}C_vH_wO_xN_yP_z+\left(n-\frac{d\cdot e}{8}-v\cdot s\cdot\frac{d}{d'}\right)CO_2+$$
$$+\frac{d\cdot e}{8}CH_4+\left(c-y\cdot s\cdot\frac{d}{d'}\right)NH_3+\left(f-z\cdot s\cdot\frac{d}{d'}\right)H_3PO_4+gH_2S$$

In which $d=4\cdot n+a-2\cdot b-3\cdot c+5\cdot f-2\cdot g$ and $d'=4\cdot v+w-2\cdot x-3\cdot y+5\cdot z$. $C_nH_aO_bN_cP_fS_g$ is the elemental composition of OFMSW, while $C_vH_wO_xN_yP_z$ is that of the anaerobic sludge produced during the AD process. The latter comprises both the production of

bacterial biomass and the precipitation of P in the form of inorganic solids. Coefficient s is the fraction of waste converted to cells, while e is the fraction of waste converted to methane (energy). The sum of s and e must be equal to 1. The value of s is the one required to reach a biogas productivity in the simulation of 180 Nm^3, corresponding to the actual yield obtained in real plant, and it equal to 0,04.

Equation 2.1 requires to know the molar composition representing the OFSMW. This composition was obtained using an average of the mass fraction of each element from a dataset found in the literature (Hansen *et al.*, 2007), shown in table 2.4, and converting it into molar fraction through the molar weight (MW).

Table 2.4: *average mass composition of OFSMW (Hansen et al., 2007) and corresponding molar composition*

Atoms	MW (kg/kmol)	Average normalized mass fraction (%)	stoichiometric coefficient in OFMSW
C	12,0107	56,49	21,81
H	1,0079	8,362	38,47
O	14,0067	31,43	9,110
N	15,9994	3,021	1
P	30,9738	0,4554	0,0682
S	32,066	0,2332	0,0337

In the same way, an elemental composition of the sludge is also required. A typical $CHON$ elemental composition can be found in the literature (Małgorzata, 1999), while the coefficient for P was adjusted based on the experimental mass concentration of phosphorous in the liquid digestate (Renesto, 2019). The required value of the coefficient is 0,305.

Given this composition the resulting reaction is:

$$C_{21,81}H_{38,47}O_{9,110}NP_{0,0682}S_{0,0337} + 7{,}8451H_2O \rightarrow \quad (2.2)$$
$$\rightarrow \ 0{,}19468C_5H_7O_2NP_{0,305} + 8{,}2652CO_2 + 12{,}5713CH_4$$
$$+ 0{,}8053NH_3 + 0{,}00880H_3PO_4 + 0{,}0337H_2S$$

A similar methodology is used to simulate microalgae growth using a chemical reaction. The nutrients involved are C, N and P.

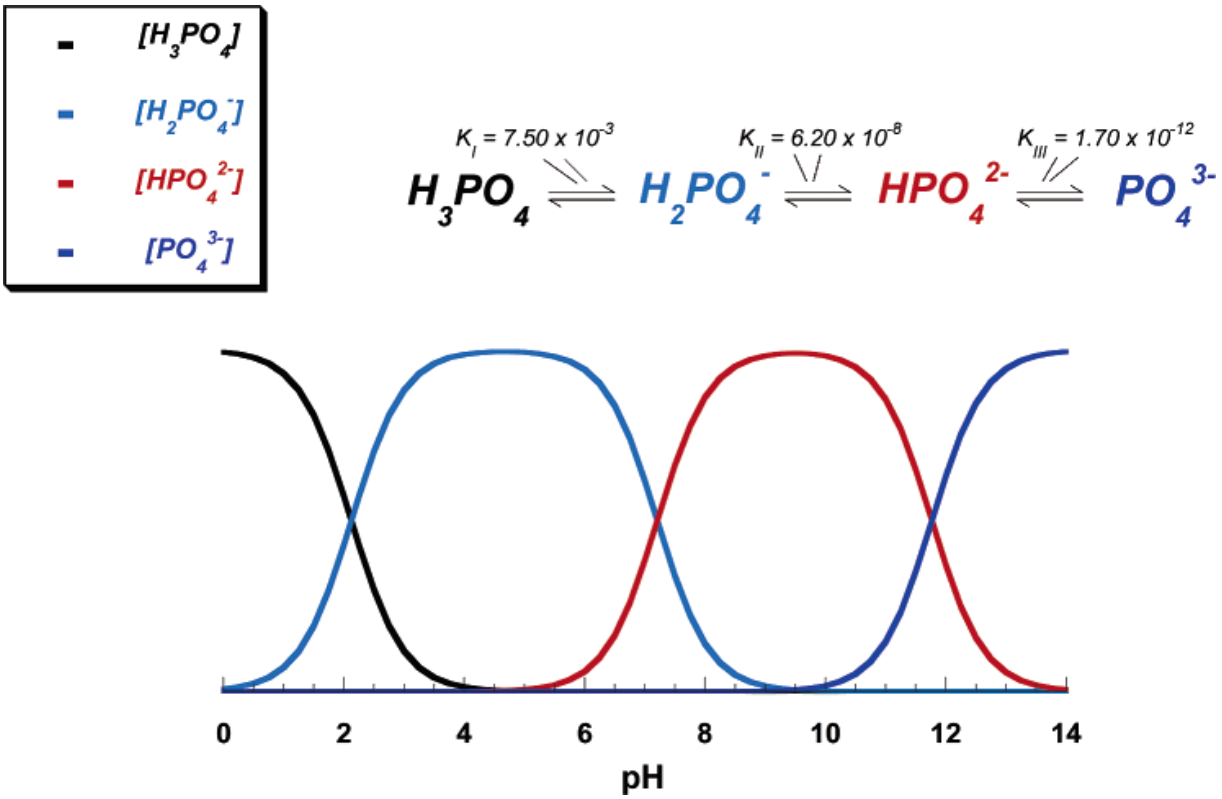

Figure 2.2: *ionic concentrations of the species in equilibrium in phosphoric acid solutions versus pH (Lynn and Bonfield, 2005)*

These nutrients are provided in the simulation in the form of CO_2, NH_4^+ and $H_2PO_4^-/HPO_4^{2-}$ respectively, since microalgae absorb nutrients in the form of ions. These particular phosphate anions are selected because they are the ones present at pH values between 7 and 9 (as shown is figure 2.2), which is the typical range for microalgae growth (Lavens and Sorgeloos, 1996). H_3O^+ is used to close the charge balances. The microorganism photosynthetic growth produces biomass and O_2. The microalgae stoichiometry is defined using composition obtained from literature data of *Chlorella vulgaris* (Musolino, 2016) and adjusting it considering the system. *Chlorella vulgaris* is one of the most common microalgae species used in wastewater treatment (Hena, Fatimah and Tabassum, 2015; Zuliani *et al.*, 2016) and it is able to grow under high ammonia concentration (Tam and Wong, 1996; Collos and Harrison, 2014). In fact, the original chemical composition is related to an uninhibited microalgae growth. This is not true for the cultivation of microalgae in the liquid digestate, since in this environment phosphorous is limiting (Renesto, 2019). Given this information, the amount of P in the microalga is modified

to a lower value found in literature (Markou, Vandamme and Muylaert, 2014). The coefficient of O is changed accordingly, so that the sum of all the fractions is equal to 1. From this data is possible to define a stoichiometry for the biomass.

Table 2.5: *mass and molar fraction from* (Musolino, 2016) *and actual*

Atoms	Original mass fraction	Original molar fraction	Modified mass fraction	Modified molar fraction
C	0,4645	0,2848	0,4645	0,2849355
H	0,0677	0,4984	0,0677	0,4948805
O	0,3803	0,1749	0,3942	0,1815273
N	0,0734	0,0386	0,0734	0,0386091
P	0,0139	0,0033	0,0002	0,0000476

The resulting reaction for biomass production is obtained by the atom and charge balances, assuming that the coefficients of $H_2PO_4^-$ and HPO_4^{2-} are identical to each other. The resulting reaction is:

$$\begin{aligned} &0{,}800157H_2O + 0{,}135501NH_4^+ + CO_2 + \\ &+ 0{,}00000835H_2PO_4^- + 0{,}0000835HPO_4^{2-} \rightarrow \\ \rightarrow\ &CH_{1{,}736816}O_{0{,}637082}N_{0{,}135501}P_{0{,}000167} + 1{,}014246O_2 + 0{,}135251H_3O^+ \end{aligned} \tag{2.3}$$

2.3. Simulation Flowsheet

The simulation was divided into three sections: the anaerobic digestion section, the cogeneration section and the biomass production section. The anaerobic digestion and cogeneration sections aim to replicate the empirical/expected data gathered from an existing AD plant fed with OFMSW, by Berica Impianti s.r.l., located in Arzignano (VI), as well as the experimental analysis of the liquid digestate (Renesto, 2019). These data are shown in table 2.6. It is assumed that the biomass production section is going to operate only during spring and summer, since the light intensity and temperature are too low at these latitudes during the rest of the year.

Table 2.6: *empirical data from the Arzignano plant and liquid digestate measurements from* (Renesto, 2019)

Characteristic	Value
Process Feed flowrate (ton/day)	1
TS% process feed	25-30%
TS% digester feed	10-12%
TS% liquid digestate	4-5%
TS% solid digestate	25-30%
Fraction of liquid digestate recycled to the digester	66,67%
Digester temperature (°C)	50
Expected Biogas Production (Nm^3/day)	180
Produced electrical power MWe (kW)	15
Produced thermal power MWt (kW)	20
Off-gas Temperature (°C)	257
liquid digestate P concentration (mg$P-PO_4$/L)	51,05
liquid digestate N concentration (mg$N-NH_3$/L)	2887

2.3.1.Anaerobic digestion section

The process flowsheet of the AD section is shown in figure 2.3. The system is fed with 1 ton/day of OFMSW through the WETFORSU stream. When it reaches the plant OFMSW is not made entirely of dry organic matter, but it is a mixture of components. As a simplification the feed is considered to be composed of water and FORSU. It is assumed that during the spring-summer season the OFMSW is richer in water since it contains a larger amount of fruits and vegetables so, given the range provided in table 2.6, the lower value is chosen. The chosen composition is shown in table 2.7.

Table 2.7: *composition of the OFSMW feed*

Component	Mass Fraction
Water	0,75
FORSU	0,25

At this point, the feed is mixed with recycled liquid digestate from stream LIQ-REC, to bring the TS% content down to 12%, since the process simulates a wet digestion system.

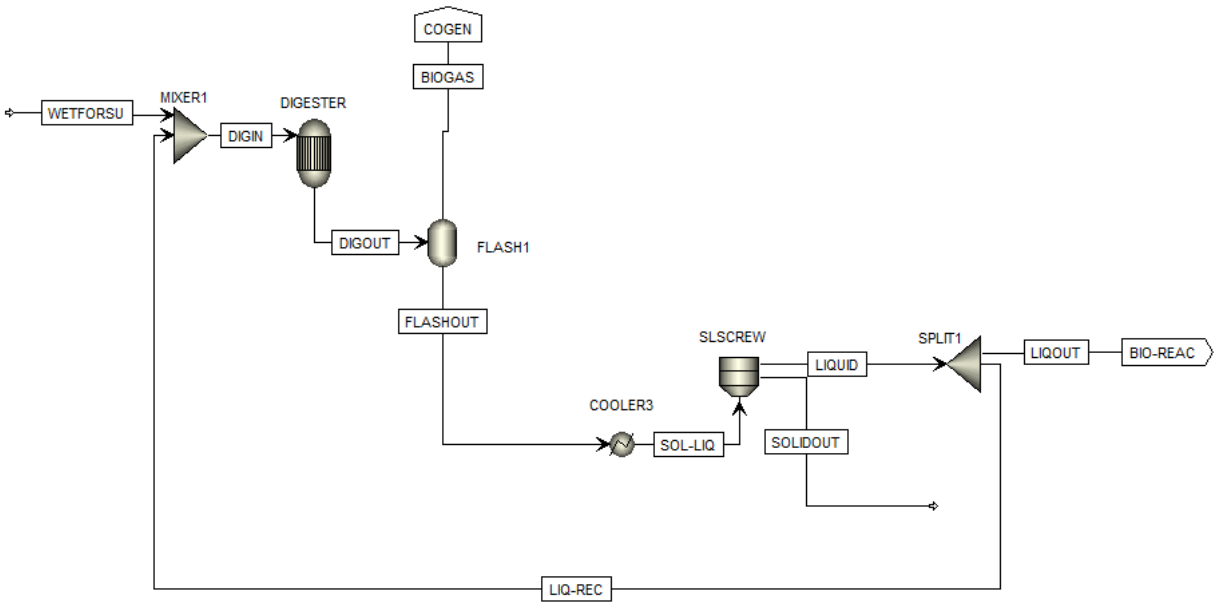

Figure 2.3: *flowsheet of the anaerobic digestion section*

The digester is represented by a RYield block. This type of reactor is a mass balance-based reactor, thus the yields for each reactant and product component, together with the reactor temperature and pressure, are the only required information. In this case the temperature is 50 °C since the process is thermophilic and the pressure is 1 atm. The yield of product (on mass basis) per kg of OFMSW fed are expressed as:

$$Y_i = F_{DW} \cdot BD \cdot \nu_{i,1} \cdot \frac{PM_i}{PM_{OFMSW}} \tag{2.4}$$

Where F_{DW} stands for dry fraction of the OFMSW, BD is the fixed degree of biodegradability of the OFMSW, $\nu_{i,1}$ is the stoichiometric coefficient of product i (from equation 2.2) and PM_i represents the molecular weight of the specific product (obtained from the Aspen Plus database and shown in table 2.8) while PM_{OFMSW} is that of the overall OFSMW. PM_{OFMSW} is calculated by multiplying the molar fraction of each element by its corresponding molecular weight (from table 2.4) and summing them up.

The organic waste is not completely degraded, so that it is characterized by its own yield, depending on biodegradability and amount of water, calculated as:

$$Y_{OFMSW} = F_{DW} * (1 - BD) \tag{2.5}$$

The water yield is calculated as the difference of all the other compounds yields from the unity:

$$Y_{water} = 1 - \sum_{1}^{n} Y_i \tag{2.6}$$

The values of dry weight fraction and biodegradable part over the total mass are fixed $F_{DW} = 0{,}12$, from table 2.6, and a value of $BD = 0{,}7$ is assessed from literature data for the organic fraction of municipal solid waste (Jeon *et al.*, 2007). The resulting yields are shown in table 2.8. After the digester, the outlet is separated into a gas stream and a solid-liquid stream using a flash unit set at the same temperature of the digester. The gas stream, containing the biogas, is sent to the cogeneration section, while the other outlet stream is sent to a solid-liquid screw press separator.

Table 2.8: *calculated component yields (mass basis) used in the RYield reactor*

Component	PM (kg/kmol)	Y
CO_2	44,0098	0,065897325
CH_4	16,0428	0,036536540
NH_3	17,0306	0,002484649
H_2S	34,0819	0,000208161
H_3PO_4	97,9952	0,000156151
FANGO	113,1143	0,003989333
FORSU	463,675	0,036
H_2O	18,0153	0,85472784

The solid-liquid separator produces two streams: a solid digestate and a liquid digestate. In order to simulate this unit, a CFuge block is selected, using the solids separator model. This model requires to define the fraction of liquid directed to the liquid outlet (LIQUD stream in figure 2.3) and the fraction of solid directed to the solid outlet (SOLIDOUT stream in figure 2.3).
These variables are adjusted to have a TS% of the solid digestate of 25% and a mass flowrate of solid digestate equal to 13% of the separator feed. The final values of the operating variables are 0,905 and 0,7 respectively. After the solid-liquid separation, 2/3 of the liquid digestate stream are sent back to the digester, to reduce the TS% of the process feed, while 1/3 of the liquid is sent to the biomass production section. This is simulated using a Split block in Aspen plus.

2.3.2. Cogeneration section

The biogas produced from the AD process is utilized in a cogeneration plant to produce both heat and energy (the flowsheet is shown in figure 2.4). Moreover, the produced CO_2 can be exploited as carbon source for microalgae, in order to minimize the production of this greenhouse gas in a sustainable way. The process has been modelled by using a RStoich reactor. This type of reactor allows to perform the simulation of a combustion process by selecting the option GENERATE COMBUSTION (considering NO as a combustion product), and defining the reaction conditions (shown in table 2.9).

Table 2.9: *Thermodynamic settings for the RStoich reactor*

Variable	UOM	Value
Pressure, P	bar	13
Duty	Cal/s	0

The flowrate of air needed to obtain a complete combustion is achieved by means of a design specification (COMBTEMP). In this design specification the air mass flow has let been varying between 1-1000 kg/h in order to reach a combustion temperature of 1100 °C. The high temperature inhibits the formation of NO_x. The air flowrate required to meet the specification resulted equal to 158 kg/h.

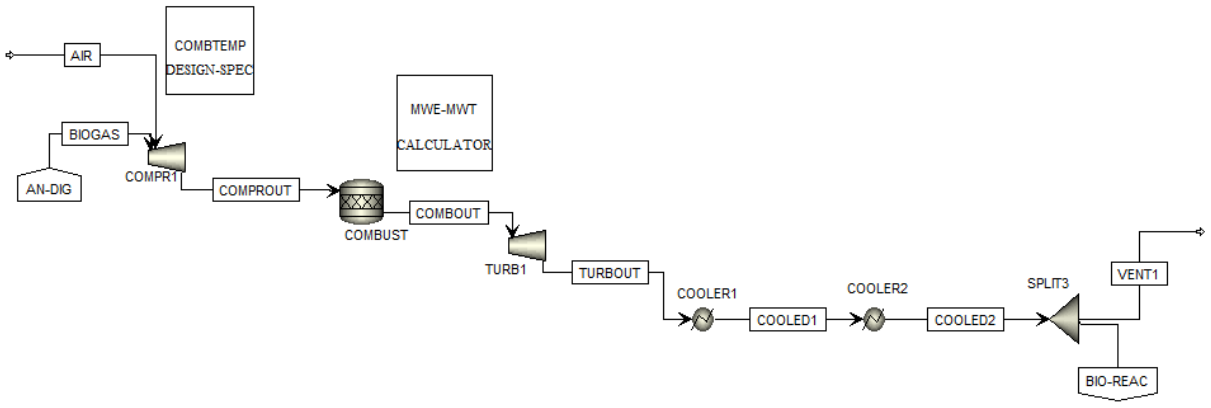

Figure 2.4: *flowsheet of the cogeneration section*

The pressure in the reactor is reached by mixing together the biogas stream with air in a compressor working isoentropically with an efficiency of $\eta_e = 0{,}835$. The off-gases are then expanded back to 1 atm using a turbine working isoentropically with an efficiency of $\eta_e = 0{,}857$ (Renesto, 2019). The gases are then cooled down to 257°C first and then to 40°C, by means of two heat exchangers. The net electrical power produced by the cogeneration system is calculated as difference between the power produced by the turbine and the power consumed by the compressor. The overall thermal power is the sum of the heat recovered from the two heat exchangers. Lastly, a split block determines the fraction of off-gases to be directed towards the biomass production section, and the fraction that is released to the atmosphere.
The flowrate is decided by another design specification (FEEDTEMP). This design specification changes the split ratio so that the photobioreactor feed temperature is 30°C, which is a suitable operating temperature for the microalgae.

2.3.3.Biomass production section

The whole biomass production process flowsheet is shown in figure 2.5. The SPLIT2 split unit regulates how much of the liquid digestate is going to be treated by the photobioreactor and how much is going to other kinds of treatment. The chosen amount of liquid digestate is diluted using a pure water stream (it should be noted that in real practice the dilution is supposed to be made using any kind of waste stream, provided it is clear) to reduce its turbidity. The amount of water to be added is decided by a design specification (DILRATIO), which fixes the dilution ratio to 1:5 or 1:10. The resulting stream is mixed with the off-gases coming from the cogeneration section and sent to the photobioreactor. It is assumed that the photobioreactor is a raceway with a surface of 100 m^2. Since the size of the photobioreactor is fixed, modifying the split ratio of SPLIT2 changes the overall hydraulic residence time. This type of photobioreactor can be considered similar to a CSTR, so in the Aspen Plus simulation the rCSTR unit is used. This unit operation requires temperature, pressure and overall reactor volume to be specified. Temperature and pressure are the same of the reactor feed. The overall volume is the sum of the liquid volume and the vapour volume. However, only the liquid volume needs to be considered in relation to the raceway surface. A design specification (SURFACE) is then set to change the

overall volume of the reactor so that the liquid reactor volume (calculated by Aspen Plus) divided by the liquid level is equal to 100 m^2.

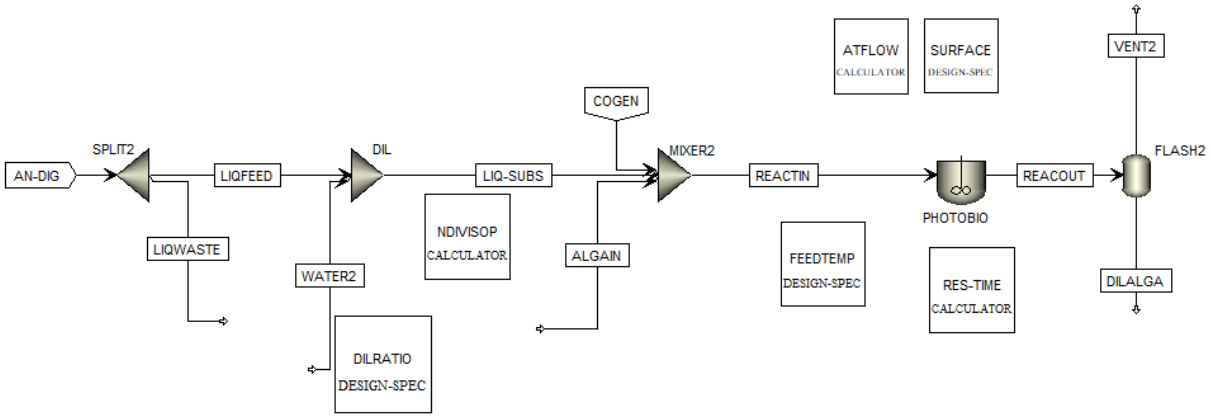

Figure 2.5: *flowsheet of the microalgae cultivation section*

After the raceway, the vapour phase and the liquid phase are separated using a flash unit set at the same temperature of the reactor outlet. The resulting product is sent to further processing to increase the biomass concentration, while the gases are released to the atmosphere.

2.4. Photobioreactor kinetics

In order for the rCSTR unit to work, it is necessary to define a reaction set. The reaction set is not defined as a stoichiometry but as a Fortran77 subroutine. The subroutine is reported in its entirety in Appendix A. This subroutine calculates the production/consumption rates of each component present in the simulation. For conventional and solid components the rate is expressed as kmol/s while for non-conventional components the rate is in kg/s.

2.4.1.Liquid concentration calculations

The calculation of the production/consumption rates requires the concentration of all the components in the liquid phase. In the subroutine, all the variables of the problem are first declared and all the Aspen COMMON blocks are included, so that the program user can retrieve from the Aspen Plus units the required information. First the total molar flowrates of the conventional and solid components in the liquid phase is calculated as:

$$n_{liq} = n_{tot,C} \cdot (1 - v_{frac}) \quad (2.7)$$

In which n_{liq} (kmol/s) is the molar flowrate in the liquid phase, $n_{tot,C}$ (kmol/s) is the molar flowrate in both phases and v_{frac} is the molar vapour fraction in the reactor/stage. The last two variables are retrieved by the Aspen simulation through the Fortran77 subroutine. This is used to calculate the volumetric flowrate of the liquid phase $\dot{V}_{liq}$ (m^3/s) using the molar volume of the liquid mixture $stwork_{vl}$ (m^3/kmol), retrieved from Aspen Plus, according to the following equation:

$$\dot{V}_{liq} = n_{liq} \cdot stwork_{vl} \quad (2.8)$$

The volumetric flowrate is then exploited to calculate the hydraulic residence time τ_{CSTR}:

$$\tau_{CSTR} = \frac{VLIQ}{\dot{V}_{liq}} \quad (2.9)$$

In this equation, $VLIQ$ (m^3) is the reactor volume (fixed by the Aspen Plus design specification) and $\dot{V}_{liq}$ is the liquid volumetric flowrate. The mass flowrates m_i (kg/s) of all the conventional components involved are therefore calculated as a function of the total molar flowrate n_{liq}, the corresponding molecular weight PM_i and the molar fraction X_i of each compounds (eq. 2.10). These last two variables are retrieved from the Aspen Plus simulation.

$$m_i = n_{liq} \cdot PM_i \cdot X_i \quad (2.10)$$

The non-conventional components mass flowrate can be directly retrieved from the Aspen Plus simulation. With these flowrates it is possible to calculate the concentration of each component c_i (kg/m^3) as the mass flowrates m_i over the volumetric flowrate $\dot{V}_{liq}$.

2.4.2.Biomass production rate

After the calculation of the concentrations is complete, it is possible to calculate the biomass production rate r using the following kinetic model:

$$r = \mu_{max} \cdot c_{alga} \cdot f(T) \cdot f(c_N) \cdot f(c_P) \cdot f(c_C) \cdot f(I_{av}) - \mu_e \cdot c_{alga} \quad (2.11)$$

In this equation, μ_{max} is maximum specific growth rate and it is equal to 2,63 1/d (Ortega, 2019), μ_e is the respiration rate, which is assumed to be equal to 0,2 l/d, and c_{alga} is the biomass concentration. A number of dimensionless factors affect the microalgae growth kinetics as

shown in equation 2.11. The first factor is related to the temperature of the reactor *T*, and it is calculated according to the cardinal model, as proposed by (Ras, Steyer and Bernard, 2013).

$$f(T) = \frac{(T - T_{max})(T - T_{min})^2}{(T_{opt} - T_{min})\left[(T_{opt} - T_{min})(T - T_{opt}) - (T_{opt} - T_{max})(T_{opt} + T_{min} - 2T)\right]} \quad (2.12)$$

Parameter T_{min} is the hypothetical temperature below which the growth rate is assumed to be zero growth, T_{max} is the temperature above which there is no growth, T_{opt} is the temperature at which the growth rate is maximal. Their values are 11,7°C, 43,65°C and 31,2°C, respectively, for the microalgal species considered, and were measured experimentally using the same procedure of (Sforza *et al.*, 2019).

Additionally, there is a series of factors related to the nutrients. These are generally calculated in terms of the concentration of the atoms involved (C, N and P), following the Monod kinetics. Instead, in this specific fortran77 subroutine it is considered to be more practical to convert these factors in terms of the molecules involved (CO_2, NH_4^+ and $H_2PO_4^-/HPO_4^{2-}$).

$$f(N) = \frac{c_N}{K_N + c_N} = \frac{c_{NH_4^+}}{K_{NH_4^+} + c_{NH_4^+}} \quad (2.13)$$

$$f(P) = \frac{c_P}{K_P + c_P} = \frac{c_{H_2PO_4^-} + c_{HPO_4^{2-}}}{K_{H_2PO_4^-/HPO_4^{2-}} + c_{H_2PO_4^-} + c_{HPO_4^{2-}}} \quad (2.14)$$

$$f(C) = \frac{c_C}{K_C + c_C} = \frac{c_{CO_2}}{K_{CO_2} + c_{CO_2}} \quad (2.15)$$

Accordingly, also the half-saturation constants (K_N, K_P and K_C) are referred to the corresponding species:

$$K_{CO_2} = K_C \cdot \frac{PM_{CO_2}}{PM_C} \quad (2.16)$$

$$K_{NH_3} = K_N \cdot \frac{PM_{NH_4^+}}{PM_N} \quad (2.17)$$

$$K_{H_2PO_4^-/HPO_4^{2-}} = K_P \cdot \frac{m_{H_2PO_4^-} + m_{HPO_4^{2-}}}{n_{liq} \cdot \left(X_{H_2PO_4^-} + X_{HPO_4^{2-}}\right)} \quad (2.18)$$

$$PM_P$$

The values of K_N, K_P and K_C are equal to 14 mg_N/l, 1,8 mg_P/l and 1,3 mg_C/l respectively (Sforza *et al.*, 2019). Another important factor is related to the light intensity (considering only

the photosynthetically active radiation (PAR) range) which is described by the Haldane kinetic model.

$$f(I_{av}) = \frac{I_{av}}{K_L + I_{av} + \frac{{I_{av}}^2}{K_I}} \tag{2.19}$$

K_L and K_I are equal to $125\ \mu mol/m^2/s$ and $1570\,\mu mol/m^2/s$ respectively (adapted from (Sforza *et al.*, 2019)). I_{av} $(\mu mol/m^2/s)$ is the average light intensity along the reactor height, and it is approximated as an integral average of the Lambert-Beer law:

$$I_{av} = \int_0^H I_0\, e^{-(K_{alga}\cdot C_{alga}+K_d)\cdot z} dz = I_0 \frac{1 - e^{-(K_{alga}\cdot C_{alga}+K_d)\cdot H}}{\left(K_{alga}\cdot C_{alga} + K_d\right)\cdot H} \tag{2.20}$$

In equation 2.19, I_0 is the light intensity at the raceway surface, H is the level of the liquid in the reactor, K_{alga} is the light absorption coefficient of the microalgae while K_d is a parameter that takes into account the light absorption of the liquid digestate. In this simulation, the liquid level H was set to either 5 cm or 7,5 cm. K_{alga} is equal to $0{,}08\ m^2/g$ (Ortega, 2019), while K_d needs to be measured or calculated, and depends on the liquid digestate dilution. The procedure followed to evaluate K_d is described in the next paragraph.

The consumption/production rate are hence calculated according to equation 2.21 if it is referred to a conventional or solid component, and to equation 2.22 if it is referred to the biomass.

$$R_{i,conv} = \frac{\nu_{i,2}}{PM_{alga}} \cdot r \cdot VLIQ \tag{2.21}$$

$$R_{alga} = \nu_{i,2} \cdot r \cdot VLIQ \tag{2.22}$$

$\nu_{i,2}$ is the stoichiometric coefficient from equation 2.2. It is assumed to be zero for components that are not involved in the reaction. The molecular weight of the biomass, PM_{alga}, is calculated by multiplying the molar fraction of each element by its corresponding molecular weight and summing them all up.

2.4.3. K_d Evaluation

As previously mentioned, the value of the absorption coefficient of the liquid digestate was measured experimentally in the lab. The experimental setup to measure K_d consisted in a

transparent flat-plate reactor (optical path 4,2 cm), placed in front of a LED lamp. The experiments consisted in measuring the light intensity at the front and at the back of the reactor (average of three measurements), filled with liquid digestate, diluted with distilled water (the dilution ratio was 1:10). The measurement was carried out using a photo-radiometer delta ohm HD 2102.1. A 1:5 dilution ratio was not feasible because, at such optical depth, the shading effect was too large, making it difficult for the instrument to measure a reliable light intensity at the back of the reactor. The results of the experimental runs are shown in table 2.9.

Table 2.9: *experimental run results. I_0 is the light intensity at the front of the reactor while I_a, I_b, I_c are measured at the back*

Experimental Run	UOM	1	2	3	4
$\mathbf{I_0}$	$\mu mol/m^2/s$	2320	1245	793	216
$\mathbf{I_a}$	$\mu mol/m^2/s$	9,87	6,45	4,1	1,32
$\mathbf{I_b}$	$\mu mol/m^2/s$	11,51	6,55	3,86	1,09
$\mathbf{I_c}$	$\mu mol/m^2/s$	10,97	6,22	3,84	1,36

Starting from the value of incident light intensity at the front of the reactor, it is possible to calculate the light intensity at the back of the reactor using the Lambert-Beer equation (equation 2.19, where $c_{alga} = 0$).

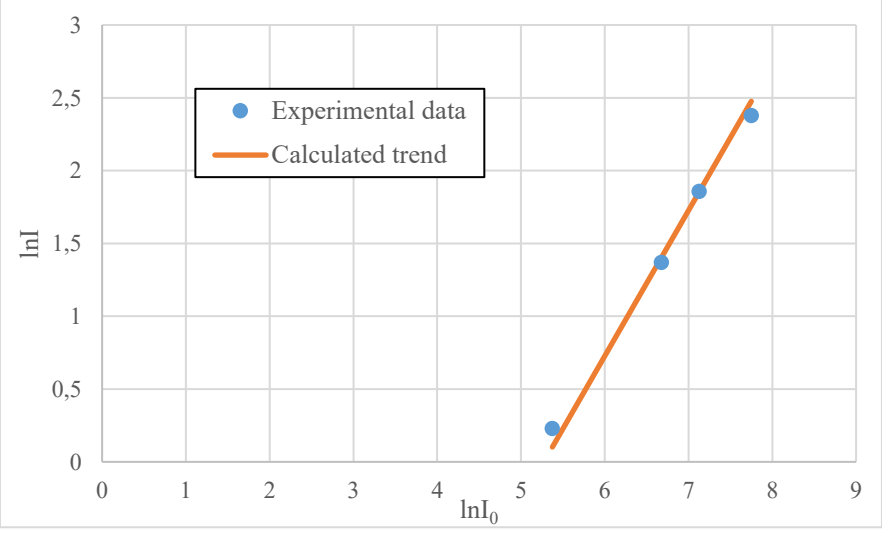

Figure 2.6: *comparison between the experimental data (blue dot) and the calculated trend (orange line) using* $\boldsymbol{K_d}$ *equal to* 126 1/m

K_d was hence changed following the GRG nonlinear solving method in Excel in order to minimize the sum of the squared errors between the natural logarithm of the calculated light intensity and natural logarithm of the average between I_a, I_b and I_c (i.e., the experimental measurements). The resulting K_d is equal to 126 1/m. Figure 2.6 shows the comparison between the trend obtained with the calculated K_d and the experimental data.

To obtain the value of K_d at a dilution ratio of 1:5, a Matlab r2018b script was used (appendix B). A simplified version of the kinetic model in equation 2.10 was implemented alongside the mass balance equation of a CSTR reactor at constant density:

$$0 = \frac{c_{out} - c_{in}}{\tau_{CSTR}} - r \cdot c_{out} \tag{2.23}$$

c_{out} and c_{in} are the mass concentration of N, P and biomass at the reactor outlet and inlet. τ_{CSTR} is hydraulic residence time. The script uses the function Lsqnonlin to close the material balance, and find the outlet concentrations. The required guess are 0,51 g/l of N, 0,012 g/l of P and 3 g/l of biomass. The simplified model assumes a value of $f(c_C)$ equal to 0,92, which is reasonable considering that the reactor operates at excess CO_2 conditions. K_d is used as tunable parameter in this model, which was applied to validate the experimental results obtained from (Renesto, 2019). The simulation assumes that the reactor temperature is the average one of the available data points, which is 25°C. The data used in the Matlab simulation are listed in table 2.10.

Table 2.10: *relevant data points from (Renesto, 2019)*

Data	UOM	Value		
Optical path	cm	4		
Surface light intensity I_0	$\mu mol/m^2/s$	559		
liquid digestate P concentration $c_{in,N}$	mg$P-PO_4$/L	11,08		
liquid digestate N concentration $c_{in,P}$	mg$N-NH_3$/L	508,3		
hydraulic residence time θ	days	5,5	6,5	9
Volumetric Productivity	g/l/d	0,123	0,156	0,213

The Matlab script uses the fminsearch function to reduce the norm of the relative error between the experimental volumetric productivity and the calculated one at the given residence times.

The volumetric productivity is calculated as the outlet concentration over the residence time. Figure 2.7 shows the results of the fitting. The resulting value of K_d is 315 1/m.

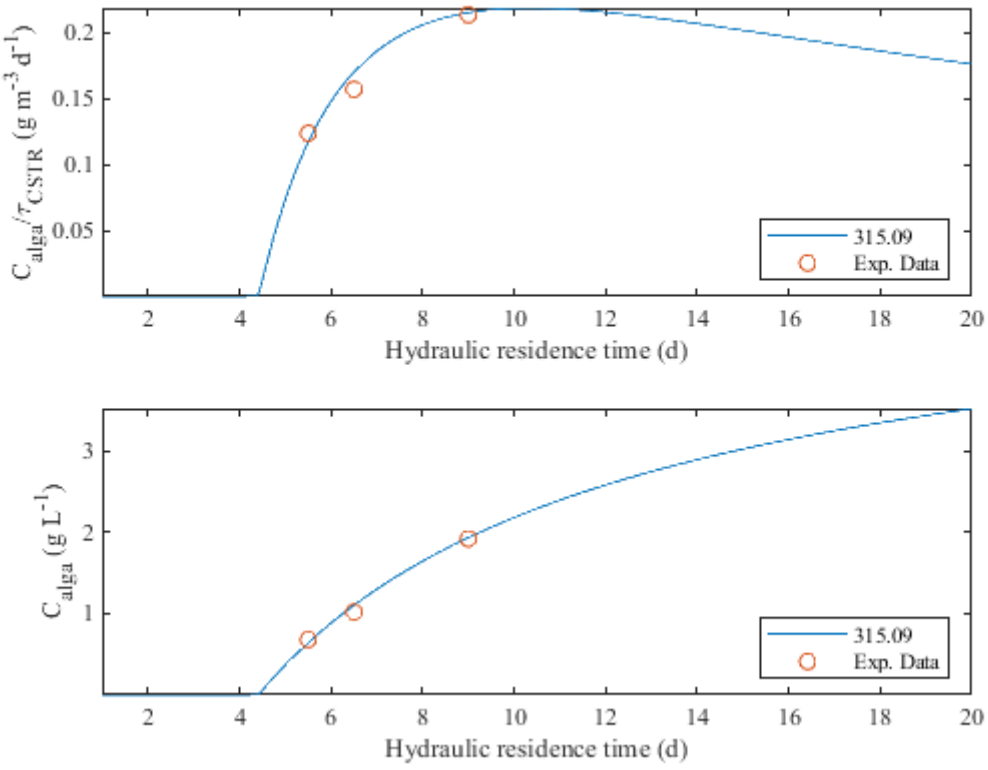

Figure 2.7: *fitting of the experimental data (orange circles) using the K_d parameter (blue line) in Matlab*

The Lambert-Beer law indicates that the absorptivity of the digestate is directly proportional to its concertation. Therefore the expected value of K_d is 252 1/m, which is twice the value of K_d at a dilution ratio of 1:10. This deviation from the Lambert-Beer law is likely caused by the limitation of the model which does not consider scattering. This is likely to occur due to the high turbidity of the medium (Metha, 2012).

The calculated concentrations fit well the experimental ones especially close to a hydraulic residence time equal to 9 days. At 6,5 days the Matlab simulation slightly overestimates the experimental data, while at 5,5 day there is a minor underestimation. This might be causes by the fact that each experimental point was measured at a different temperature, while for practical reasons the Matlab calculation are all conducted at 25°C.

Chapter 3

Simulation Results

In this chapter, the results of the Aspen Plus simulations are proposed and discussed. First the results of the anaerobic digestion section and the cogeneration section are compared with the available data. Then, the biomass growth performance in the month of July, taken as a reference, is presented, considering different values of liquid level of the raceway and dilution ratios of the photobioreactor feed. Lastly, the optimal operating variables are investigated and applied to different months of the year (May, July and September) to assess the process performances at different environmental conditions.

3.1. Anaerobic digestion section

The overall anaerobic digestion section produces three outlet streams: the biogas, the liquid digestate and the solid digestate. These are shown in figure 2.3 as the BIOGAS stream, the LIQUIDOU stream and the SOLIDOUT stream, and their weight fraction with respect to the process feed WETFORSU is shown in percentage in table 3.1.

Table 3.1: *Product percentages of the entire anaerobic digestion section outlet with respect to the process inlet*

Product stream	%kg/kg$_{processfeed}$
BIOGAS	22,5
SOLIDOUT	22,8
LIQUIDOU	54,7

These percentages do not find correspondence with literature data. In fact, differently from other processes, part of the liquid digestate is here recirculated to reduce the %TS in the feed. Since commonly anaerobic digestion plants do not involve digestate recirculation, for comparison table 3.2 shows the yields obtained with respect to the sub-section between the digester feed (DIGIN) and the final splitter (SPLIT1). With reference to figure 2.3, these are the flowrates of the BIOGAS stream, the LIQUID stream and the SOLIDOUT stream divided by the digester

feed DIGIN. These yields are similar to the value that can be retrieved from literature data (MØller, Christensen and Jansen, 2010; Duan *et al.*, 2018).

Table 3.2: *Product yields of the entire digester outlet with respect to the digester feed*

Product stream	$\%kg/kg_{digesterfeed}$
BIOGAS	10,8
SOLIDOUT	10,8
LIQUID	78,4

The composition of the nutrients in the liquid digestate is shown in table 3.3. The phosphorous concentration is similar to the experimental value of the liquid digestate indicated in table 2.6, while the nitrogen concentration is lower (experimental value = 2887 mg N/L). However, it should be remembered that the N composition in the digestate varies depending on several factors, including the feed composition, and the value obtained from the simulation is realistic. The TS content is slightly lower than the value found in the plant. This is probably due to the fact that the simulation treats the formation of solids in a simplified manner, in particular regarding orthophosphate precipitation. The pH is coherent with previous experimental digestate measurements (Renesto, 2019).

Table 3.3: *main characteristics of stream LIQUIDOU*

characteristic	value
liquid digestate P concentration (mg$P-PO_4$/L)	57,95
liquid digestate N concentration (mg$N-NH_3$/L)	1701
%TS	1,53
pH	7,65

The solid digestate has a %TS equal to 25,69% which is coherent with the given plant data. The liquid fraction of the stream has the same composition of the liquid digestate. The composition of the biogas produced is shown in table 3.4. The composition of CO_2 and CH_4 are comparable to the values show in table 1.3 (Riva, 2009). The overall biogas flowrate is 179 Nm^3/day, which is close to the productivity expected from the plant in Arzignano and other literature data (Kangle *et al.*, 2012).

Table 3.4: *molar composition of stream BIOGAS*

Specie	Molar fractions (%)
CO_2	33,28
CH_4	54,22
H_2O	12,28
NH_3	0,1846
H_2S	0,03540

3.2. Cogeneration section

The combined heat and power cogeneration process produces energy by burning the methane contained in the biogas. Before reaching the RStoich reactor, the biogas is mixed with air and compressed. The reactor outlet flux is thus enriched in CO_2 mainly, and other components such as NO and SO_2. The complete composition of the inlet and the outlet streams of the RStoich reactor is shown in table 3.5. With reference to figure 2.4, these are the COMPROUT stream and the COMBOUT stream respectively.

Table 3.5: *molar composition of stream COMPROUT and COMBOUT*

Specie	Molar fractions inlet (%)	Molar fractions outlet (%)
CO_2	1,8776	4,9366
CH_4	3,0591	0
H_2O	0,6926	6,8282
NH_3	0,0104	0
O_2	19,8153	13,6809
N_2	74,5431	74,5419
NO	0	0,0104
H_2S	0,002	0
SO_2	0	0,002

The system is able to achieve complete combustion of the methane, sensibly increasing the amount of steam in the outlet stream. This steam is then going to condense into the liquid

digestate. The condensed steam contribution to the overall liquid flowrate is negligible compared to the high amount of liquid digestate. The combustion also removes completely the NH_3 and H_2S contained in the biogas stream, converting them into NO and SO_2. Table 3.6 summarizes the electrical and thermal energy produced in the cogeneration system.

Table 3.6: *electrical and thermal power involved with the unit operations in the cogeneration section*

Unit Operation	Simulation name	UOM	Power Produced/Consumed
Compressor (consumed)	COMPR1	kWe	18,21
Turbine (produced)	TURB1	kWe	30,68
Heat exchanger 1	COOLER1	kWt	16,24
Heat exchanger 2	COOLER2	kWt	10,84
Total electrical power (produced) MWe	-	kWe	12,47
Total thermal power (produced) MWt	-	kWt	27,08

The amount of electrical energy produced is slightly lower than the one expected by the installed generator (15 kW), while the overall thermal power produced is slightly higher than the declared one (20 kW). However, the results are comparable with the nominal data of the plant. Differently from the electrical power, the thermal power is not planned to be sold, but to be used within the plant. From the Aspen Plus simulation shows that the digester only consumes 2,13 kW to move the digester feed from 24°C to 50°C. Therefore 20 kW of thermal power are assumed to be enough to heat up the digester, with some residual heat to be possibly used in the photobioreactor.

3.3. Biomass production section

The production of algal biomass occurs by suppling to the PBR both the nutrients contained in the liquid digestate and the CO_2 available in the off-gases from the cogeneration plant. The simulation of the biomass production section is computed at different values of two operating variables: the liquid level of the culture in the photobioreactor, and the digestate dilution ratio.

The system is first simulated using the average temperature and irradiation data in the month of July in Arzignano (VI), retrieved from the PVGIS database (European Commission and Hub, 2016). PVGIS Solar Irradiation Data is an online available database of typical day evolution of irradiation on a given surface for any location and time of the year. The month of July is taken as a reference as the one representative of the summer season, where microalgal growth conditions are most favourable at these latitudes. Then, the performance of the process is evaluated at different months of the year in which the environmental conditions are assumed to still be favourable for microalgae production: May, July and September. During the winter time, instead, the low light availability and temperature conditions make it difficult for microalgae to survive in a complex medium such as the digestate. The temperature and the irradiation data (reported as PAR) for each month is shown in table 3.7.

Table 3.7: *average temperature and light intensity data at different months in Arzignano* (European Commission and Hub, 2016)

	UOM	May	July	September
Surface light intensity I_0	$\mu mol/m^2/s$	509	592	360
Temperature T	°C	17	24	19

3.3.1. Growth factor optimization

In these simulations the effect of operating variables (liquid level and digestate dilution) on the photobioreactor performances is assessed, with reference to the month of July. In particular, the liquid level is either 5 cm or 7,5 cm, while the dilution ratio is either 1:5 or 1:10. For each configuration a sensitivity analysis is conducted by changing the split ratio of SPLIT2 (first split unit in figure 2.5). Varying the split ratio changes the amount of liquid digestate which is going to be treated by the raceway. Since the reactor has a fixed surface (and therefore a constant liquid volume), the variation in the flowrate is reflected into a change in the hydraulic residence time. It is thus possible to obtain a profile of the volumetric productivity of the biomass (which, for a CSTR configuration, is calculated as the ratio of the biomass concentration in the liquid stream exiting the PBR over the residence time).

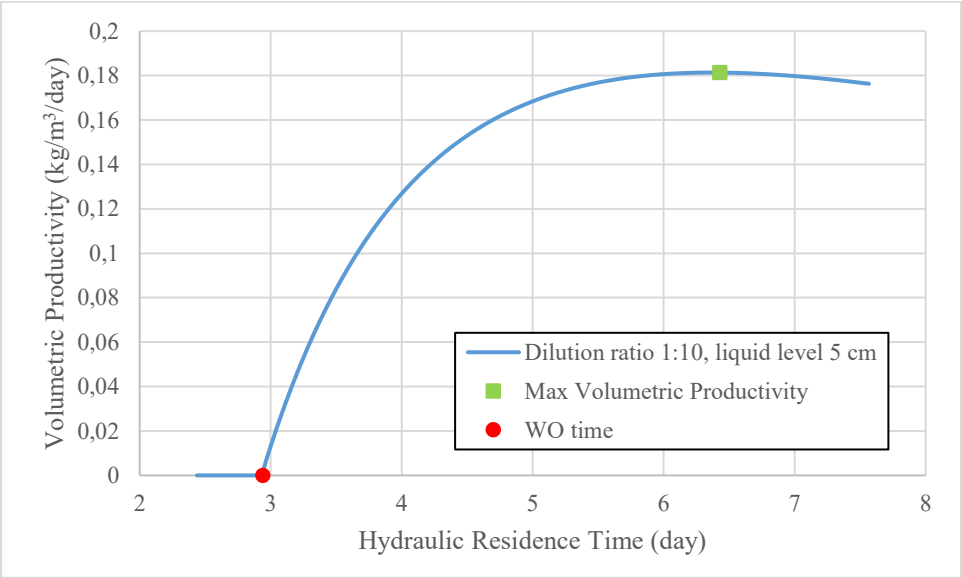

Figure 3.1: *Profile of the volumetric productivity (kg/m^3/day) versus the hydraulic residence time (day) (blue line). In the figure are also indicated the highest value of the volumetric productivity (green square) and the Wash-Out time (red circle)*

Figure 3.1 shows an example of the profile obtained for a dilution ratio of 1:10 and a liquid level of 5 cm. From this plot is it possible to identify the optimal hydraulic residence time (τ_{opt}, which corresponds to the highest productivity) and the wash-out hydraulic residence time (τ_{WO}, which corresponds to the point in which the productivity profile has the highest positive slope). Table 3.8 shows τ_{opt} and τ_{WO} for each studied combination of liquid level and dilution ratio. In each configuration the values of CO_2, P and N conversion are evaluated at the optimal hydraulic residence time together with the concentration of biomass, the volumetric productivity and the mass fraction (in percentage) of liquid digestate actually treated. The first simulation is carried out with a dilution ratio of 1:5 and a liquid level of 7,5 cm. The dilution 1:5 corresponds to the one used in the previous experimental investigation involving this liquid digestate (Renesto, 2019). This case presents some convergence problems due to the low production of biomass. In this situation both τ_{opt} and τ_{WO} are quite large (28,7 and 26 days respectively), which would be quite unfeasible in real practice operation. Moreover, even at the optimal hydraulic residence time, even though the percentage of liquid digestate treated is relatively high (with respect to the other cases) the conversion of nutrients as well as the volumetric productivity and the biomass concentration are almost null.

Table 3.8: *results of the Aspen Plus simulation at different values of dilution ratio and reactor liquid level for the month of July (I_0 = 592 µmol/m2/s, T = 24°C)*

Configuration Id		**1**	**2**	**3**
Liquid level	cm	7,5	7,5	5
Dilution ratio	-	1:5	1:10	1:10
Optimal residence time τ_{opt}	day	28,73	9,640	6,428
Wash-out time τ_{WO}	day	26,053	4,448	2,940
% CO_2 Conversion X_{CO_2}	-	3,18E-05	0,3105	0,4587
% P Conversion X_P	-	6,29E-04	3,120	4,615
% N Conversion X_N	-	4,92E-03	29,19	43,18
Biomass concentration c_{alga}	kg/m^3	0,000197	0,7877	1,166
Volumetric Productivity	kg/m^3/d	6,86E-06	0,0817	0,1813
% digestate	-	16,54	13,96	13,96

The difference between previous experimental data (Renesto, 2019) and the values of conversion calculated by the Aspen Plus simulations is possibly due to the fact that the laboratory-scale set-up used a reactor with a shorter optical path (4 cm instead of 7.5) and a higher surface light intensity.

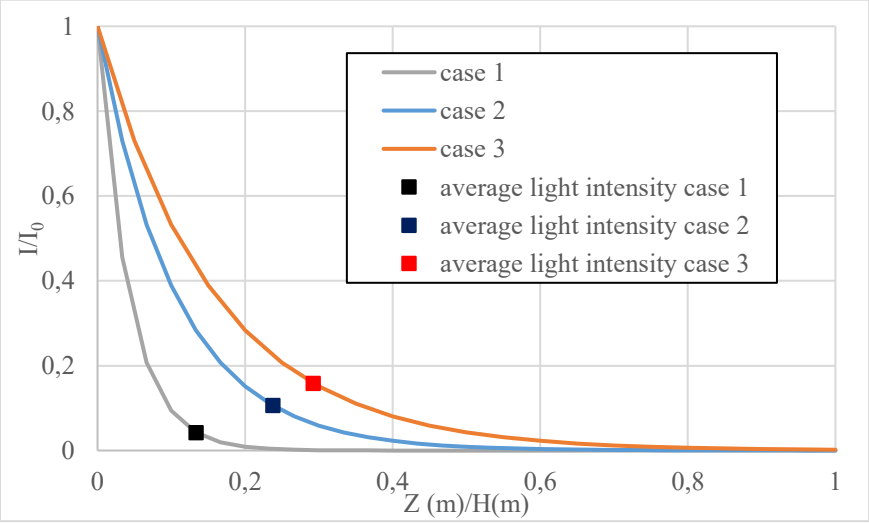

Figure 3.2: *profile of the normalized light intensity along the normalized reactor depth for three different combination of operating variables*

These poor performances can be better understood by analysing the light profile inside the photobioreactor. As it can be seen in Figure 3.2, the light intensity is entirely absorbed by the digestate within the first 1,5 cm of reactor depth, so that the value of average light intensity is reduced to 25,05 µmol/m^2/s only due to the digestate turbidity.

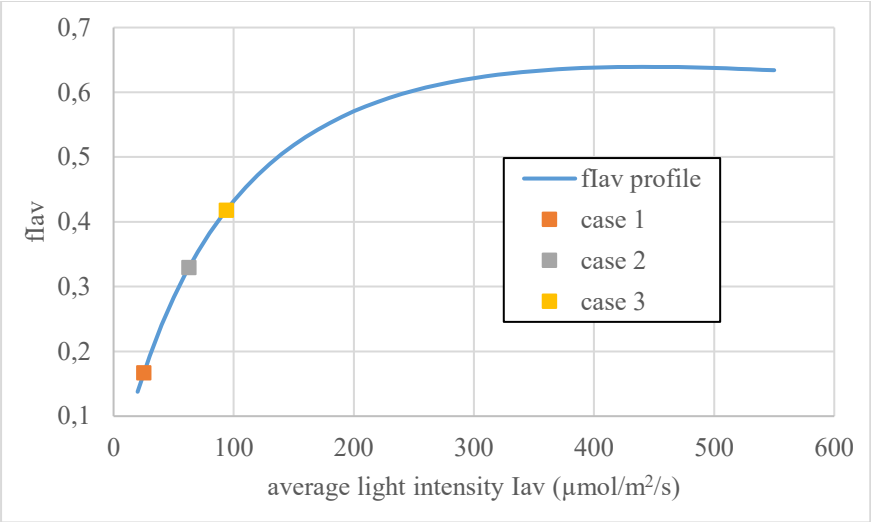

Figure 3.3: *profile of the Haldane kinetic model versus the average light intensity for three different configuration of operating variables*

In fact, by looking at the trend of the light kinetic factor of equation 2.19, which is displayed in Figure 3.3, it can be noticed that the available light intensity is strongly limiting for microalgae growth. Increasing the dilution ratio of the liquid digestate reduces the shading effect, as confirmed by the reduction in the value of K_d. For a dilution of 1:10, in fact, the light profile improves, as shown in the previous figure 3.2, with the average value increasing to 62,64 µmol/m^2/s. This is caused by the fact that the value of K_d is reduced from 315 1/m to 126 1/m. The increase in the light penetration thanks to the higher dilution is reflected in the dramatic decrease of both τ_{opt} and τ_{WO}. Due to this decrease in the hydraulic residence time, even if the dilution ratio is larger, the percentage of liquid digestate that can be treated at τ_{opt} does not decrease much. The conversion of nutrients increases a lot with respect to the previous configuration, but the conversion of CO_2 and P remain low. In this context, the concentration of biomass is close to 0,80 g/l. To possibly further improve the performances, in the next

configuration the liquid level maintained in the reactor is reduced to 5 cm, which is the minimum in this type of photobioreactors. Decreasing the liquid level increases the average light intensity in the reactor. In this way it is possible to make the process more efficient since having a photobioreactor with a longer optical path is going to add an amount of liquid digestate in which microalgae growth is hindered due to the low amount of light. This has the effect of further decreasing τ_{opt} and τ_{WO} by about 30% with respect to the second configuration, with the optimal value at about 6 days. Decreasing the liquid level does not seem to have a sensible effect on the percentage of liquid digestate treated at the optimal hydraulic residence time. The conversion of nutrients increase by 50% with respect to the second configuration, while the concentration of biomass increases up to 1,18 g/l. The overall biomass production is hence equal to 0,9067 kg/d.

3.3.2. Process effectiveness in different time periods

If the same operating variables (5 cm of culture depth and 1:10 dilution ratio) are kept at different months of the year (May and Spetember in this case), the corresponding washout times reach unreasonably high values, which is mainly due to the low temperature and surface light intensity.

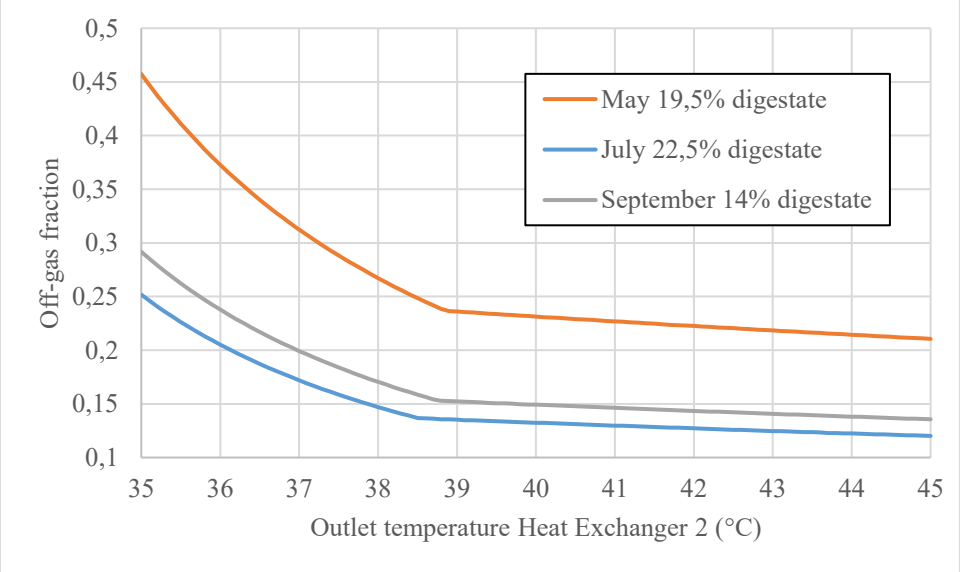

Figure 3.4: *profile of the off-gas fraction with respect to the outlet temperature of heat exchanger COOLER2 in different months (liquid digestate flowrate correspond to the highest volumetric productivity)*

To improve the performance of the photobioreactor in these conditions, it is possible to exploit the heat from the the offgases, instead of cooling them down to ambient temperature. Instead, they can be kept at 40°C and partially diverted to the liquid digestate in order to increase the temperature of the medium in the photobioreactor to 30°C. This temperature is close to the optimal temperature for microalgae growth T_{opt} (as reported in paragraph §2.4.2). The temperature of 40°C is chosen by looking at how the fraction of off-gas required to increase the liquid digestate temperature changes with respect to the outlet temperature of the second heat exchanger (COOLER2 in figure 2.4). From figure 3.4 it can be noticed that during all three months the temperature of the heat exchanger outlet has a bigger effect when changed from 35 °C to 40°C. After 40°C the relation between temperature and offgas fraction is almost linear. Since the CO_2 is in excess, using only a fraction of the offgases does not hinder the amount of it provided to the liquid digestate considerably.

Table 3.9: *results of the Aspen Plus simulation at different months of the year*

	UOM	May	July	September
Optimal residence time τ_{opt}	day	5,157	4,513	7,201
Wash-out time τ_{WO}	day	2,184	1,933	3,008
% CO_2 Conversion X_{CO_2}	-	0,7325	0,9109	0,4064
% P Conversion X_P	-	5,318	5,753	4,110
% N Conversion X_N	-	49,75	53,82	38,44
Biomass concentration c_{alga}	kg/m^3	1,512	1,651	1,171
Biomass flowrate	kg/hr	0,06107	0,07623	0,03388
Volumetric Productivity	kg/m^3/day	0,2931	0,366	0,1626
% liquid digestate	-	19,5	22,5	14
% offgas	-	24,44	13,25	14,92

Table 3.9 summarizes the simulation results. The increase of temperature has a positive effect on all the major process variables. In particular, the optimal hydraulic residence time is always lower than 9 days. Since all the cases are conducted at the same temperature, the main factor is the surface light intensity.

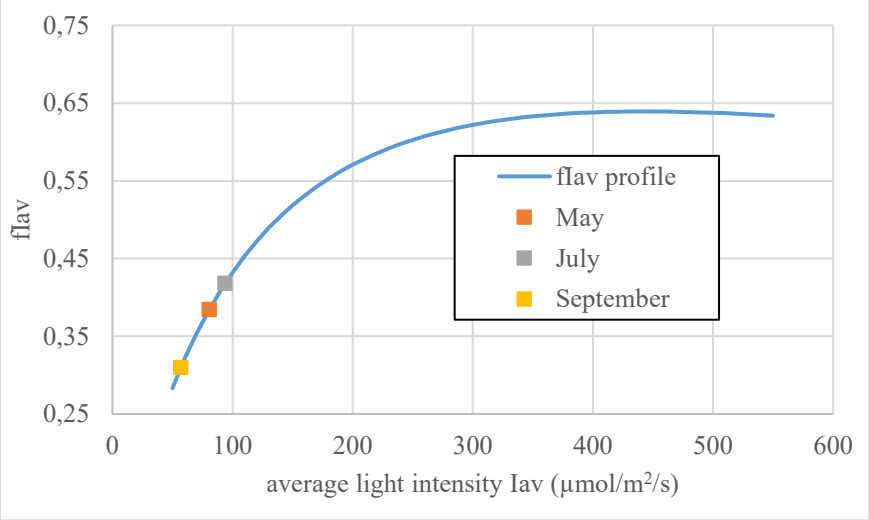

Figure 3.4: *profile of the Haldane kinetic model versus the average light intensity for three different months*

From figure 3.4 is easy to notice that the best performance is achieved in July, which has the higher average light intensity, while the worst month is September. Figure 3.5 shows that the majority of the light intensity is lost in the first 2 cm of the reactor depth in all three months of the year. The main difference in the overall performance is then caused by the surface light intensity.

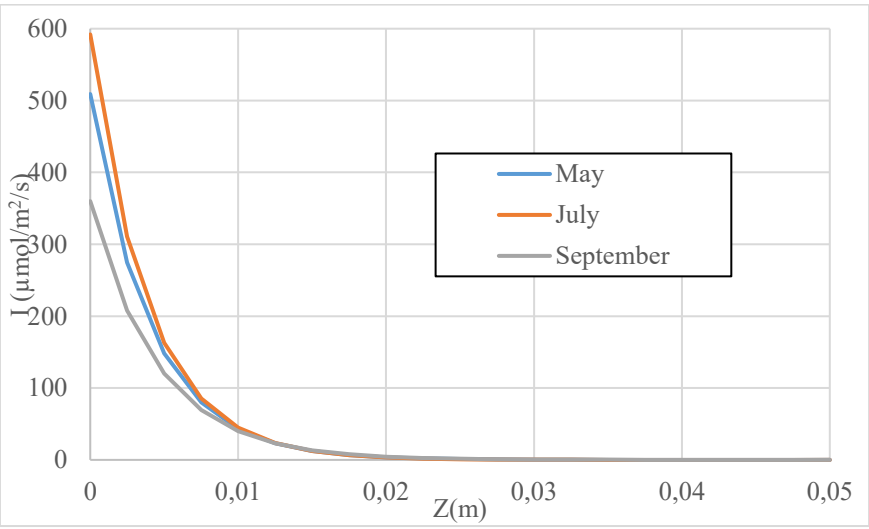

Figure 3.5: *profile of the light intensity along the reactor depth for three different months*

In all the time periods the concentration of biomass is larger than 1 g/l. This means that, thanks to the heat integration, the biomass growth could be extended further than the months considered

here (e.g. late October). The percentage of off-gas required to raise the temperature of the digestate to 30°C is 25% during the month of May. In this situation the amount of heat required to change the temperature of the digestate from 17°C to 30°C is 0,60 kW. Therefore, it is possible to use the hot water generated from the cogeneration section to heat up the photobioreactor. In general the fraction of offgases to send to the photobioreactor might be underestimated, because the simulation does not consider the heat dispersion to the environment from the raceway reactor.

Chapter 4

Economic Analysis

This chapter includes the results of the profitability analysis and the methodology used to achieve them.

These include the assessment of capital and production costs as well as the revenues using both literature data and the simulation results of Chapter 3. In order to assess the influence that the microalgae production facility has on the economic viability a small scale anaerobic digestion process, the analysis is carried out for the anaerobic digestion plant alone and for the microalgae-integrated process.

4.1. Methods

To conduct the economic analysis two main information are required: the total capital investment (TCI) and the cost of manufacturing (COM_d).

4.1.1. Total capital investment

The total capital investment (TCI) or capital cost is the money required to purchase and install the plant and its accessories and to provide the expenses needed to start the process operations.

$$TCI = FCI + WC + StC \tag{4.1}$$

As indicated by equation 4.1 the total capital investment is comprised by three factors: the fixed capital investment (FCI), the working capital (WC) and the start-up costs (StC).

FCI is the money required to pay for the processing equipment and the auxiliary units, acquiring and preparing land, civil structures, facilities, and control systems. The money invested into fixed capital cannot be readily converted into cash.

$$FCI = ISBL + OSBL + IC \tag{4.2}$$

The main components of the FCI are the inside battery limits ($ISBL$) plant investments, the outside battery limits ($OSBL$) plant investments and the indirect cost (IC).

The $ISBL$ and $OSBL$ are the direct cost. The $ISBL$ mainly include plant equipment, while $OSBL$ is related to the auxiliary buildings like offices and laboratories.

The IC can include expenses related to engineering, supervision and construction, contractors' fees and contingencies.

The WC for an industrial plant consists of the total amount of money invested in raw materials and supplies carried in stock, finished products in stock and semifinished products in the process of being manufactured, accounts receivable, cash kept on hand for monthly payment of operating expenses, such as salaries, wages, and raw-material purchases, accounts payable, and taxes payable.

The StC are frequently changes that have to be made before the plant can operate at maximum design conditions. These changes involve expenditures for materials and equipment and result in loss of income while the plant is shut down or is operating at only partial capacity (Peters and Timmerhaus, 1991).

4.1.2. Cost of manufacturing

The cost of manufacturing (COM_d) is related to the day-to day operation of the plant and can be divided into three categories (Turton *et al.*, 2008):

$$COM_d = DMC + FMC_d + GE \tag{4.3}$$

The direct cost of manufacturing (DMC) represents all the expenses that vary with the production rate. These can include:

- Raw materials consumed by the process;
- Utilities and consumables (all materials requiring continuous/frequent replacement);
- Effluent disposal and treatment;
- Packaging and shipping;
- Operating labour and supervision;
- Labour overheads;
- Licence fees and royalties.

It is worth noticing that, in the case of anaerobic digestion from OFMSW, the raw material represents a revenue and not a cost, since the facility is getting paid to dispose it.

The fixed manufacturing costs (FMC_d) are independent from changes in the production rate and they include:

- Maintenance;
- Local taxes and insurance;
- Rent of land/buildings;
- Plant overhead costs;
- Capital charges.

Lastly, general expenses (GE) comprise management, sales, R&D and financing functions. Usually they do not vary with production changes.

4.1.3. Literature data elaboration

The total capital costs and the cost of manufacturing were estimated for the process described chapter 2 by referring to literature data. To better compare the costs found in literature, these need to be adjusted for inflation, according to equation 4.4.

$$TCI_{t_1} = TCI_{t_0} \cdot \left(\frac{I_{t_1}}{I_{t_0}}\right) \tag{4.4}$$

In this equation I is the cost index, t_0 is the reference year in which the literature data is available, while t_1 is the year in which the cost needs to be estimated. The Chemical Engineering Plant Cost Index (CEPCI) is the cost index of choice.

Moreover, literature data found for different plant sizes were interpolated using an exponential relation between the plant cost and its characteristic size using a capacity scale factor n. For the anaerobic digestion plant (which comprehends the cogeneration section) the characteristic size is the electrical power installed P, while for the raceway reactor it is the surface area S.

$$TCI_A = TCI_0 \cdot \left(\frac{Size_A}{Size_0}\right)^n \tag{4.5}$$

The subscript 0 in equation 4.5 indicates a reference plant for which characteristic size and cost are known. A linear relation between size and cost can be obtained (equation 4.6).

$$\log_{10}\frac{TCI_A}{TCI_0} = n \cdot \log_{10}\frac{Size_A}{Size_0} \tag{4.6}$$

By plotting the $\log_{10}(Cost_A/Cost_0)$ versus $\log_{10}(Size_A/Size_0)$ this equation corresponds to a straight line with intercept at the point (0,0). The value of n was regressed by fitting the experimental data.

Once the value of n is known for both the digester and the raceway, it is possible to estimate the total capital cost for each unit by using equation 4.5. It should be specified that, given the small size of the plant under analysis in this study, an extrapolation of the capital costs is necessary.

To estimate the cost of manufacturing it is assumed they are directly proportional to the total capital cost.

$$COM_d = k \cdot TCI \tag{4.7}$$

k is the parameter representing the slope of the line, which was also regressed from a number of literature data. Once this parameter is known it is possible to calculate the COM_d for both the digester and the raceway, respectively, using equation 4.7 and the previously calculated values of TCI.

4.1.4. Cumulated cash flow diagram process profitability indexes

The profitability analysis is performed by evaluating for both the configurations (with and without the raceway reactor) the net present value over the capital investment, NPV/TCI, the internal rate of return, IRR, and the discounted payback period, DPBP. These indexes are based on the cumulative cash flow diagram for each configuration.

This diagram is obtained by reporting the cash flow for each year discounting it to year 0 using an interest rate i defined a priori (assumed equal to 10%). The cash flow CF for each year is calculated as:

$$CF = (R - COM_d - d) \cdot (1 - t) + d \tag{4.8}$$

In which R is the revenues of the process, d is the depreciation of the capital investment and t is the taxation rate. For simplicity, the depreciation is considered to be linear and applicable for 10 years on the entire capital investment. In the cumulated cash flow diagram the entirety of the capital is invested in the first year. It is also assumed a taxation rate of 43% since its close to the value of the income tax in Italy (Bradbury and Harding, 2019).

To discount the CF back to year 0 the following equation is applied:

$$CF_0 = \frac{CF_n}{(1+i)^n} \tag{4.9}$$

In this equation n is the year in which the cash flow is referred while CF_0 is the cash flow discounted back to year 0. The cumulative cash flow CCF for each year is then obtained by summing up all the previous cash flows.

$$CCF_n = \sum_{1}^{n} CF_n \tag{4.10}$$

The NPV is the cumulative cash position at the end of the project life, with all cash flows discounted back to time zero. This index is always larger for bigger plants so for a better comparison the ratio between the NPC and the TCI is evaluated instead.

The IRR is the interest rate at which all the cash flows must be discounted in order for the net present value of the project to be equal to zero. Thus, it is a measure of the maximum interest rate that the project could pay and still break even by the end of the project life.

The DPBP is the time required, after start-up, to recover the FCI and the StC, with all cash flows discounted back to time zero.

4.2. Literature data

Parameters n and k are found using literature data. The total capital investment has been updated using equation 4.4 to the latest value of the CEPCI available (equal to 603,1 for 2018).

4.2.1. Anaerobic digestion

Table 4.1 summarized the literature data used to determine the TCI and $(COM)_d$ for the anaerobic digestion process. All the data refers to anaerobic digestion plants built in Italy between 1991 and 2013.

This dataset contains data from AD plants that use agricultural waste as feed. Differently from plant that treat OFMSW these tend to have a lower capital costs (since the raw material is easier to handle) but lower revenues.

Table 4.1: *literature data for anaerobic digestion. The values of TCI are updated to account for inflation*

kW	TCI (€)	COM_d (€/y)	Reference	Source
850	3.443.662	-	(Primante, 2009)	Sorghum, corn, scraps
100	633.009,7	-	(Primante, 2009)	Waste water
108	554.681	39.342,7	(Fouepi, 2010)	Waste water and manures
972	3.790.320	283.053,43	(Fouepi, 2010)	Waste water, biomass
25	111.800,6	1.384,96	(Reichhalter *et al.*, 2011)	bovine slurry
100	1.110.128	40.515	(Reichhalter *et al.*, 2011)	bovine slurry
325	1.933.068	192.619,26	(Reichhalter *et al.*, 2011)	bovine slurry
750	5.456.243	362.836,28	(Reichhalter *et al.*, 2011)	bovine slurry
88	850.484,8	32.384	(Marchesi *et al.*, 2013)	bovine slurry
267	2.475.949	100.802,65	(Marchesi *et al.*, 2013)	bovine slurry
500	1.572.211	875.00	(Marchesi *et al.*, 2013)	chopped corn
540	2.166.456	142.560	(Marchesi *et al.*, 2013)	corn, triticale, powdered sorghum, stable meadow grass, sorghum with added slurry and bovine manure
540	2.166.456	144.493,2	(Marchesi *et al.*, 2013)	corn, triticale, powdered sorghum, stable meadow grass, sorghum with added slurry and bovine manure
540	2.166.456	140.243,4	(Marchesi *et al.*, 2013)	corn, triticale, powdered sorghum, stable meadow grass, sorghum with added slurry and bovine manure
540	2.166.456	153.252	(Marchesi *et al.*, 2013)	corn, triticale, powdered sorghum, stable meadow grass, sorghum with added slurry and bovine manure
540	2.166.456	153.252	(Marchesi *et al.*, 2013)	corn, triticale, powdered sorghum, stable meadow grass, sorghum with added slurry and bovine manure

4.2.2.Raceway reactor

Table 4.2 summarized the literature data used to determine the TCI and COM_d for the biomass production process, involving a raceway reactor.

Table 4.2: *literature data for anaerobic digestion. The values of TCI are updated to account for inflation*

m²	TCI (€)	COM_d (€/y)	Reference
48750000	1.018.809.860	94.916.666,67	(Rogers *et al.*, 2014)
29097000	163.990.540	30.731.481,48	(Richardson, Johnson and Outlaw, 2013)
100000000	727.768.720,1	-	(Tapie and Bernard, 1988)
8000000	44.147.659,83	-	(Tapie and Bernard, 1988)
5300000	121.575.152,8	-	(Tapie and Bernard, 1988)
83000	8.631.274,46	-	(Tapie and Bernard, 1988)
200000	10.312.054,33	-	(Tapie and Bernard, 1988)
50000	6.123.697,23	-	(Tapie and Bernard, 1988)
100000	4.863.539,15	-	(Tapie and Bernard, 1988)
40000	4.233.090,86	-	(Tapie and Bernard, 1988)
340000	47.186.731,17	-	(Tapie and Bernard, 1988)
4	20.000	-	Private communication
173810000	2.953.015.337	191.541.149,2	(Banerjee and Ramaswamy, 2017)
60230000	943.666.014	117.932.360,5	(Banerjee and Ramaswamy, 2017)
50690000	801.968.510,4	112.391.914	(Banerjee and Ramaswamy, 2017)
54970000	988.930.494,4	128.221.761,1	(Banerjee and Ramaswamy, 2017)
8093720	52.712.561,92	3.090.740,74	(Benemann *et al.*, 1982)
258999040	1.431.846.756	85.333.333,33	(Benemann *et al.*, 1982)
64749,76	9.930.733,66	635.555,56	(Benemann *et al.*, 1982)
202343	7.750.382,76	543.981,48	(Benemann *et al.*, 1982)
64749,76	4.489.744,44	719.555,56	(Benemann *et al.*, 1982)
1011715	7.558.312,69	2.881.944,44	(Benemann *et al.*, 1982)

In this case the data related to the cost of manufacturing is not always available. When possible, from the cost of the nutrients necessary to produce the biomass is removed, since in this particular situation the nutrients are freely available. From this data it is possible to derivate an average of the percentage of COM_d which can be related to nutrients (equal to 14,5%). From the data by (Banerjee and Ramaswamy, 2017) it is not possible to ascertain how much the nutrients affect the COM_d so the 14,5% of it is removed. Another limitation of this dataset is that the majority of the entries are related to surface areas above 10.000 m^2, while the process studied in this thesis implies a raceway reactor of 100 m^2.

4.3. Linear regression results

For the anaerobic digestion plant figure 4.3 shows the data related to table 4.1, the regression results and a reference value of $n = 2/3$ (Consulente-energia, 2019). This last value of the scale factor is valid from an installed power of 100 kW to 1 MW. (Consulente-energia, 2019) uses a reference value for TCI_0 of 4 million € for a plant producing 1 MW of electrical power. The same reference is used to apply equation 4.6.

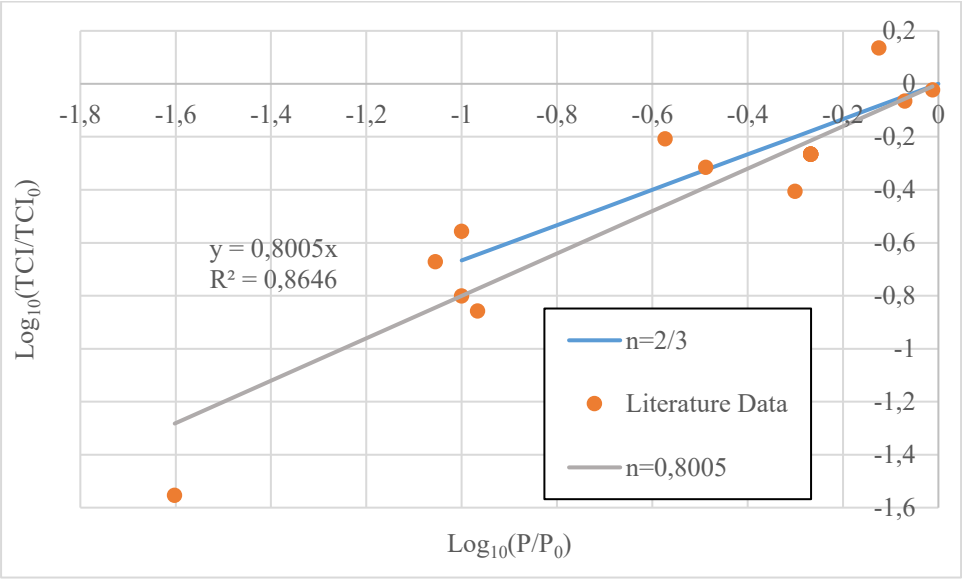

Figure 4.1: *logarithmic plot of the anaerobic digestion plant literature data (orange dot), literature value of n=2/3 (blue line) and resulting n=0,8005 (grey line). The reference values of cost and power are 4000000 € for a 1 MWe plant*

The resulting value of the scale factor n is 0,8005, with a $R^2 = 0{,}8646$. Given this n, the corresponding value of TCI for an AD plant with installed 15 kWe in cogeneration is 138.653,3 €. This value is affected by some uncertainty due to the dataset limitations. Using the same dataset, it is possible to obtain figure 4.2, and use equation 4.7 to obtain a regression line. The coefficient k obtained with this process is equal to 0,0668 1/y with a value of R^2 of 0,9113. Once the value of TCI is known for an installed power of 15 kWe, it is possible to use equation 4.7 to calculate the corresponding COM_d, which is equal to 9.262,04 €/y. The same procedure can be applied to the raceway actor using the literature data from table 4.2.

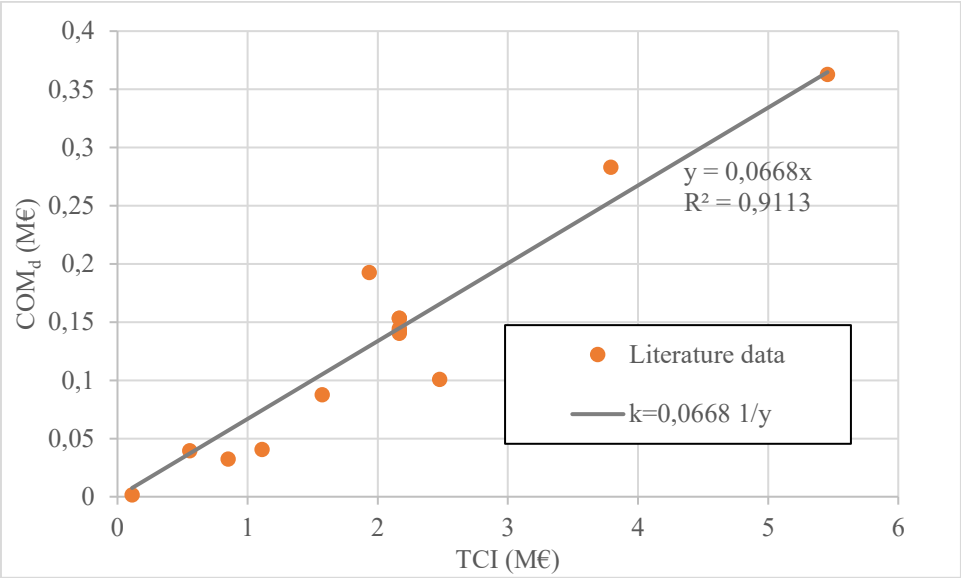

Figure 4.2: *plot of the literature data for anaerobic digestion plant (orange dot) and resulting k=0,0668 (grey line).*

Figure 4.3 and figure 4.4 shows the result of the linear regression. To apply equation 4.6 the data from (Rogers *et al.*, 2014) is used as a reference value.

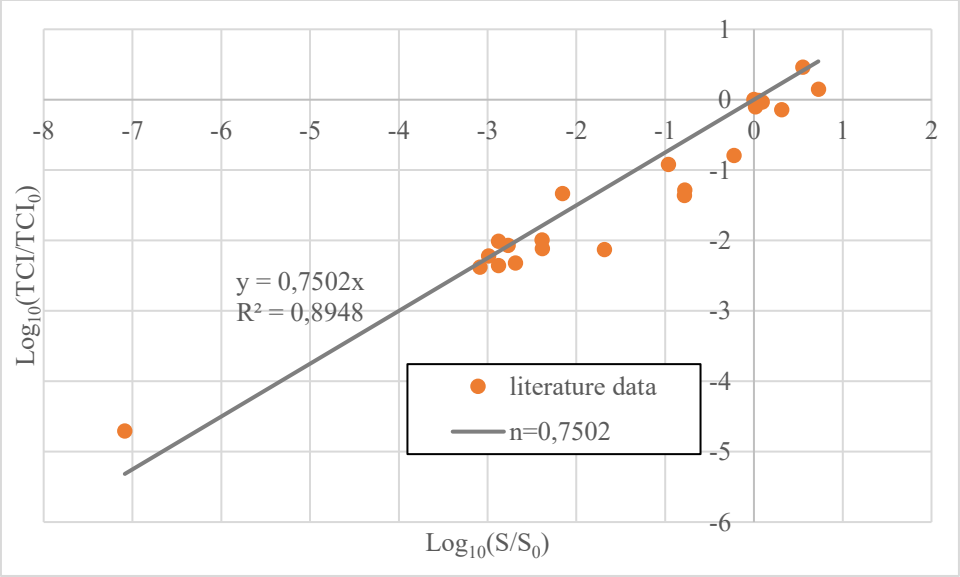

Figure 4.3: *logarithmic plot of the raceway reactor literature data (orange dot) and resulting n=0,7502 (grey line). The reference values of cost and surface are 1,02 Mld € for 48,75 km²*

The resulting scale factor n for a microalgae production plant is equal to 0,7502 with an R^2 of 0,8948. Applying equation 4.6 with this scale factor, the value of the TCI for a raceway reactor of 100 m^2 is equal to 55.222 €.

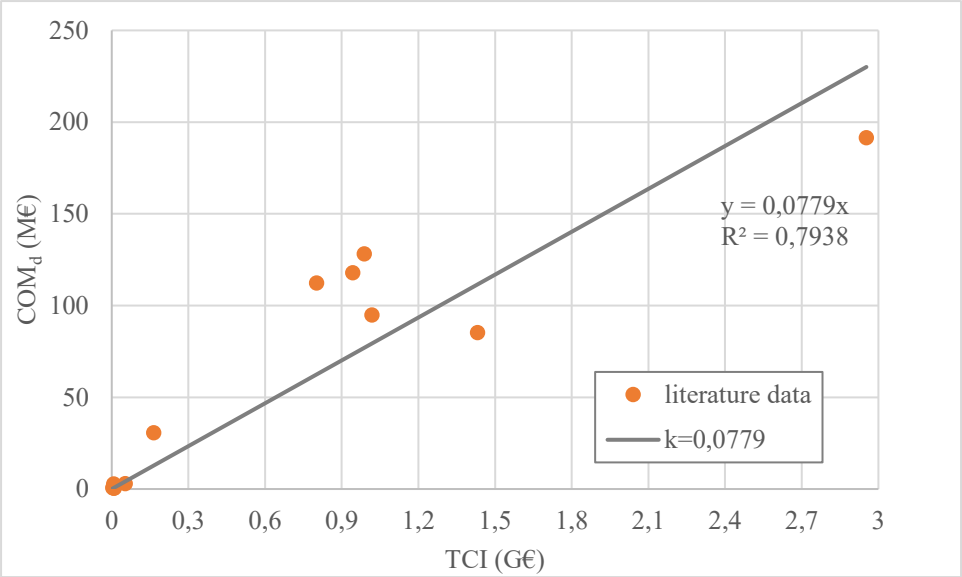

Figure 4.4: *plot of the literature data for a raceway reactor (orange dot) and resulting k=0,0779 (grey line).*

Using the same process as the anaerobic digestion plant, a value for coefficient k is obtained and it is equal to 0,0779 1/y with a value of R^2 of 0,7938. The uncertainty in this value might be caused by the fact the cost of manufacturing depend on the final use of the biomass. Using this value of k and equation 4.7 the resulting COM_d is 4301,79 €/y. Since the raceway reactor is only active for five months each year the actual value of COM_d is 1792,4 €/yr.

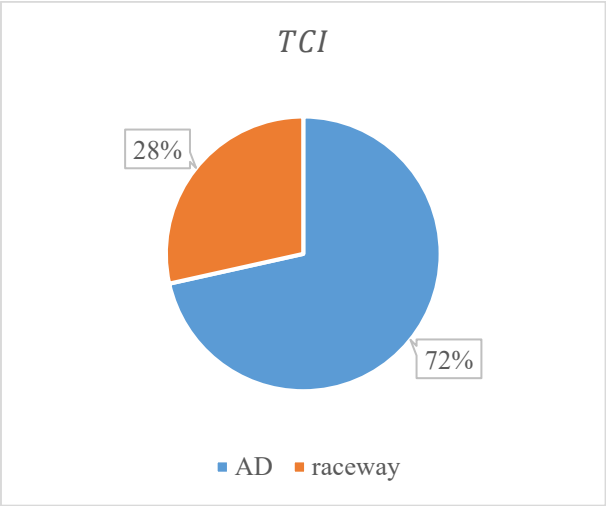

Figure 4.5: *effect of each component of the integrated process on the total capital investment.*

Figure 4.5 shows the effect that the raceway reactor has on the total capital investment. In the integrated process the raceway reactor is 28% of the overall TCI. On the other hand figure 4.6 shows the effect on the COM_d.

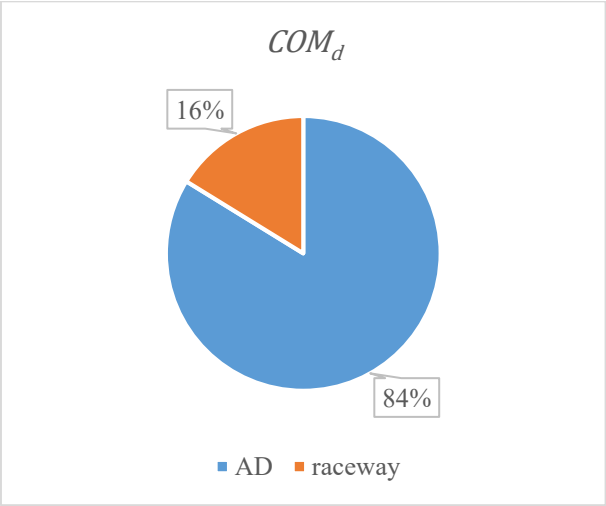

Figure 4.6: *effect of each component of the integrated process on the cost of manufacturing.*

The raceway reactor only affects the 16% of the overall COM_d, which means that while the raceway reactor implies a larger capital investment the cost of manufacturing are more sustainable over time.

4.4. Results of the profitability analysis

With the results obtained in the previous paragraph a profitability analysis is performed for the studied anaerobic digestion process and for the microalgae-integrated process. The required values of the revenues of both processes are determined using the simulation results. The three main sources of revenue are: the transfer fee related to the amount of OFMSW treated, the sale of electricity and the sale of microalgae. Providing OFMSW as a feed to the system is not a cost: in Italy the plants that treat OFMSW receive 80€/ton and assuming a cost for transport of 10€/ton the overall revenue of 70 €/ton. Since the plant is able to treat 1 ton/day of OFMSW the revenue related to it are equal to 70 €/day. In Italy is possible to take advantage of incentives to sell electricity from renewable resources at a more advantageous price. For electricity derived from biogas produced from anaerobic digestion of OFMSW the selling price is 0,233 €/MWh for 20 years (Ministero dello sviluppo Economico and Ministero dell'ambiente e della tutela del territorio e del mare, 2016). From table 3.6 the amount of electrical power produced is 12,47 MW. Taking into account maintenance, the stream factor for the AD process is 340 days/year which corresponds to 8160 hr/yr. This means that the revenues due to the OFMSW are 23.800 €/yr while selling electricity results in an annual revenue of 23.709 €/yr, On the other hand, the selling price of microalgae highly depends on their final use. Since in the EU microalgae produced from liquid digestate are still considered a waste, the success of this kind of production is linked to an update of the regulatory framework. For this reason a sensitivity analysis is conducted by varying the price per kilogram of biomass produced. An average of the biomass mass flowrate from table 3.9 is considered for revenue calculations. The resulting biomass flowrate is 0,057 kg/hr. Since the raceway reactor is active only for 5 months each year the stream factor is 3400 hr/yr.

Table 4.3: *relevant economic information for the profitability analysis*

	TCI k€	COM_d k€/yr	years	salvage value k€	Depreciation k€/yr	taxation rate %	Revenues k€/yr	Interest %
AD only	138,7	9,262	20	0	13,87	43	47,51	10
Integrated process	193,9	11,05	20	0	19,39	43	varies	10

Table 4.3 shows the main information required to compile the cumulated cash flow diagram for the AD process alone and the integrated process.

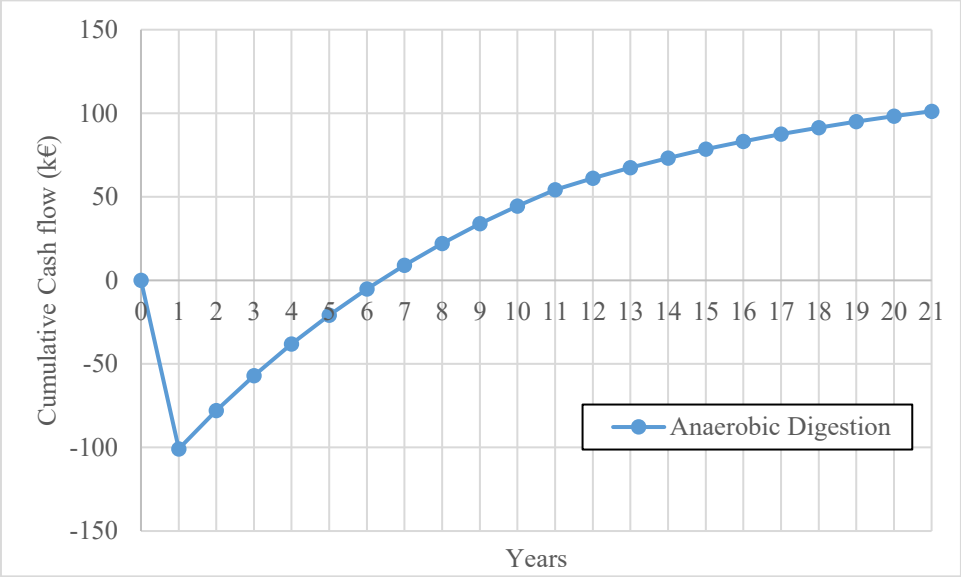

Figure 4.7: *cumulative cash flow diagram for the anaerobic digestion process*

The cumulative cash flow diagram of the anaerobic digestion process alone is show in figure 4.7. From this diagram it is possible to determine the value of the NPV/TCI and the DPBP. In this case the NPV is still positive and close to 100.000 € as shown in figure 4.7. On the other hand, the NPV/TCI is close to 0,73 which means that the NPV after 20 years is lower than the initial investment. In general the DPBP of large scale AD plants treating OFMSW is around 2-3 years. This small scale digester as a DPBP of 6,36 years. This is caused by the fact that for smaller scale the TCI has a larger impact on the profitability, increasing the DPBP. Looking at the IRR for this process, the value is 24,16%. Small-scale AD processes are a relatively novel technology, but with an expanding market due to the increase interest biogas production from waste. In this context this might be considered a moderate risk investment, so an IRR close to 25% is advisable.

To improve the economic performance of the process, the anaerobic digestion process is integrated with microalgae production.

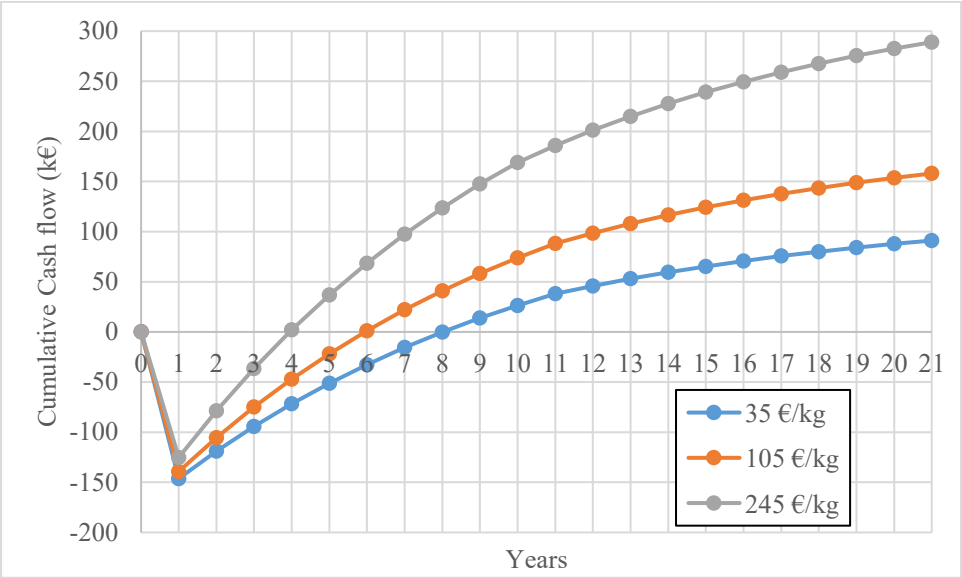

Figure 4.8: *cumulative cash flow diagram for the integrated process at increasing microalgae sale price*

The cumulative cash flow diagram is reported for different microalgae sale price in figure 4.8. In particular, the algal biomass selling price corresponding to a DPBP close to 4, 6 and 8 days, respectively, is calculated. The plot shows that increasing the microalgae sale price improves the overall economic viability of the integrated process. The resulting profitability indexes are summarized in table 4.4.

Table 4.4: *main profitability indexes at different microalgae sale price*

Alga sale price	**€/kg**	**35**	**105**	**245**
NPV/TCI	-	0,4698	0,8151	1,491
DPBP	years	8,020	5,951	3,950
IRR	%	19,14	25,83	40,51

With a sale price of 35 €/kg the main indexes do not improve with respect to the process involving only anaerobic digestion. In particular the ratio NPV/TCI is equal to 0,4698. This is caused by the fact that, with respect to the process involving only AD, the increase in total capital investment is reflected in a decrease of the NPV. The process is limited by the fact that the raceway reactor is functioning only for a limited amount of months per year, making it harder to compensate the higher investment with a higher revenue. This leads to an increase of the DPBP. A performance similar to the previous plant configuration is achieved with a microalgae

sale price of 105 €/kg. In this case the revenue related to microalgae production is roughly 1/3 of the overall revenue, with the remaining 2/3 split between OFMSW feeding and electricity production. In this case there is a slighter improvement in all the performance indexes with respect to the process involving only AD. A further improvement in the performance is obtained by further increasing the microalgae sale price, to 245 €/kg. This price increase makes microalgae production account for 50% of the total revenue. In this condition the NPV/TCI becomes higher than the plant configuration involving only AD while and the process has a DPBP around 4 years. The IRR also improves to 40,5% which is the suggested value for high-risk investments. However, these last two cases (105€/kg and 245 €/kg) imply unrealistic microalgae sale prices, which means that a better economic performance can be achieved only by reducing process costs or increased productivity. Instead a microalgae price of 35 €/kg can be considered realistic depending on the end use of the product. Even in this case, cost reduction or productivity increase is desirable since the economic indexes do not improve with respect to the non-integrated process. It should be noted that, by properly controlling the temperature in the raceway the microalgae production could be extended to more months, thus improving the results of the cost-benefit analysis.

Conclusions

The aim of this thesis was to carry out a techno-economic analysis of an anaerobic digestion process of the organic fraction of municipal solid waste integrated with cultivation of microalgae. The economic analysis was used to verify the profitability of a small-scale anaerobic digestion process and evaluated the effect that microalgae cultivation has on its economic viability. The overall plant mass balances were evaluated using the Aspen Plus process simulator. The liquid digestate from the anaerobic digestion process and the off-gases from the cogeneration system are used to provide nutrients for the growth of the microalgal biomass. The Aspen Plus simulation takes into account a small-scale anaerobic digestion plant producing 180 Nm^3 of biogas each day by treating 1 ton of OFMSW. This biogas goes through a 15 kWe cogeneration section. From the simulation results 179 Nm^3 of biogas produce 12,47 kWe and 27,08 kWt, instead of the declared 15 kWe and 20 kWt. Consequently the cogeneration outlet stream is enriched in CO_2 with respect to the biogas. This is then mixed with the liquid digestate in order to provide the biomass with the necessary nutrients. In order to simulate the photobioreactor the kinetic model was implemented using a Fortran subroutine. The required parameters are mainly found in the literature, excluding the absorption coefficient of the liquid digestate, which was measured/calibrated for two values of dilution ratio: 1:5 and 1:10. In the first case the parameter was found by fitting the kinetic model to previous experimental data using a Matlab script. In the second case, it was measured experimentally. The resulting values of the coefficient are 315 1/m and 126 1/m. The reason why these values do not follow the Lambert-Beer law is likely linked to the limitation of the model which does not consider scattering. Then the process performance of a 100 m^2 raceway reactor was evaluated at different digestate dilution ratio and different reactor liquid level. In this context, the most favourable operating variables are a dilution ratio of 1:10 and a liquid level of 5 cm. These operating variables were applied in the months of May, July and September which corresponds to different environmental conditions of surface light intensity and temperature. Increasing the liquid digestate temperature to 30°C was deemed necessary for sufficient biomass growth. With this temperature increase the higher concentration of biomass is mostly correlated

with the light intensity available in each month, leading to a better performance in the month of July. From these simulations it was possible to obtain an average biomass production rate, which is necessary to calculate a yearly revenue. In order to conduct the profitability analysis, total capital investment and cost of manufacturing were estimated using literature data. For a plant involving only anaerobic digestion and cogeneration the resulting costs were 138.653 € and 9.262 €/y respectively. For an integrated process the total capital investment was 193.875 € and the cost of manufacturing was 11.054 €/y. The raceway reactor required for microalgae cultivation account for 28% of the total capital costs and 16% of the cost of manufacturing.

The profitability indexes calculated by means of the economic analysis show that a plant involving only anaerobic digestion is economically sustainable even at a smaller scale. In particular the process has a DPBP of 6,36 years which is reasonable considering the low amount of organic fraction of municipal solid waste treated. The process also presents an IRR of 24,16% and a NPV/TCI of 0,73. Since the regulatory framework regarding the sale of microalgae produced from liquid digestate is not developed yet, the integrated process profitability was evaluated at different values of biomass sale price. In the case of a sale price of 35 €/kg, the addition of the raceway reactor does not improve the economic sustainability of the process, leading to worse values of the profitability indexes. A better performance is obtained with a sale price of 105 €/kg and 245 €/kg. In particular in the case of 105 €/kg the profitability indexes are similar to the ones obtained for the process involving only anaerobic digestion.

In summary, it was shown that integrating an anaerobic digestion process with microalgae production is not economically viable unless there is a sensible reduction in costs or the possibility to produce biomass for a larger portion of the year.

Appendix A

Fortran subroutine and compiling procedure

```
C$ #2 BY: PATNAIK DATE: 14-NOV-1998 INCLUDE COMMONS FOR RADFRAC/RATEFRAC
C$ #1 BY: ANAVI DATE:  1-JUL-1994 NEW FOR USER MODELS
C
C     User Kinetics Subroutine for RCSTR
C     (USER type Reactions)
C
      SUBROUTINE gasaria   (SOUT, NSUBS,  IDXSUB, ITYPE,  NINT,
     2                      INT, NREAL,  REAL,   IDS,    NPO,
     3                      NBOPST,  NIWORK, IWORK,  NWORK,  WORK,
     4                      NC,  NR, STOIC,  RATES,  FLUXM,
     5                      FLUXS,   XCURR,  NTCAT,  RATCAT, NTSSAT,
     6                      RATSSA,  KCALL,  KFAIL,  KFLASH, NCOMP,
     7                      IDX, Y,  X,  X1, X2,
     8                      NRALL,   RATALL, NUSERV, USERV,  NINTR,
     9                      INTR,    NREALR, REALR,  NIWR,   IWR,
     *                      NWR, WR, NRL,    RATEL,  NRV,
     1                      RATEV)
C
      IMPLICIT NONE
C
C     DECLARE VARIABLES USED IN DIMENSIONING
C
      INTEGER NSUBS,  NINT,   NPO,    NIWORK, NWORK,
```

```
     +      NC, NR, NTCAT,  NTSSAT, NCOMP,
     +      NRALL,  NUSERV, NINTR,  NREALR, NIWR,
     +      NWR
C
cinclude "ppexec_user.cmn"
c     EQUIVALENCE (RMISS, USER_RUMISS)
c     EQUIVALENCE (IMISS, USER_IUMISS)
#INCLUDE "dms_ncomp.cmn"
C
C.....RCSTR...
#include "rcst_rcstri.cmn"
#include "rxn_rcstrr.cmn"
EQUIVALENCE (VOL, RCSTRR_VOLRC) ! RCSTR reactor volume
C
C.....RPLUG...
#include "rplg_rplugi.cmn"
Cinclude "rplg_rplugr.cmn"
C     EQUIVALENCE (XLEN, RPLUGR_UXLONG)
C     EQUIVALENCE (DIAM, RPLUGR_UDIAM)
C
C.....RBATCH...
#include "rbtc_rbati.cmn"
#include "rbtc_rbatr.cmn"
C
C.....PRES-RELIEF...
#include "prsr_presri.cmn"
#include "rbtc_presrr.cmn"
C
C.....RADFRAC/RATEFRAC
#include "rxn_disti.cmn"
#include "rxn_distr.cmn"
```

```
C
C.....REACTOR (OR PRES-RELIEF VESSEL OR STAGE) PROPERTIES...
#include "rxn_rprops.cmn"
      EQUIVALENCE (TEMP, RPROPS_UTEMP)    ! Reactor/stage temperature (K)
      EQUIVALENCE (PRES, RPROPS_UPRES)    ! Reactor/stage pressure (N/m^2)
      EQUIVALENCE (VFRAC, RPROPS_UVFRAC)   ! Molar vapor fraction in the
reactor/stage
      EQUIVALENCE (BETA, RPROPS_UBETA)    ! Liquid 1/Total liquid molar ratio in the
reactor/stage
      EQUIVALENCE (VVAP, RPROPS_UVVAP)    ! Volume occupied by the vapor phase in
the reactor (m^3)
      EQUIVALENCE (VLIQ, RPROPS_UVLIQ)    ! Volume occupied by the liquid phase in
the reactor (m^3)
      EQUIVALENCE (VLIQS, RPROPS_UVLIQS)  ! Volume occupied by the liquid and solid
phases in the reactor (m3)

#include "shs_stwork.cmn"

C.....THE PLEX
#include "dms_plex.cmn"
      REAL*8 B(1)              ! Real Plex area
      EQUIVALENCE (B(1),IB(1))
      INTEGER DMS_IFCMNC           ! Determines DMS_PLEX offsets for component data
areas
C
C     INITIALIZE RATES
C
C     DECLARE ARGUMENTS
C
      INTEGER IDXSUB(NSUBS),  ITYPE(NSUBS),   INT(NINT),
     +        IDS(2), NBOPST(6,NPO),  IWORK(NIWORK),
```

```
     +       IDX(NCOMP_NCC), INTR(NINTR),    IWR(NIWR),
     +       NREAL,  KCALL,  KFAIL,  KFLASH, NRL,
     +       NRV,    I
      REAL*8 SOUT(1), WORK(NWORK),
     +       STOIC(NC,NSUBS,NR),  RATES(1),
     +       FLUXM(1),    FLUXS(1),   RATCAT(NTCAT),
     +       RATSSA(NTSSAT),  Y(NCOMP_NCC),
     +       X(NCOMP_NCC),    X1(NCOMP_NCC),  X2(NCOMP_NCC)
      REAL*8 RATALL(NRALL),   USERV(NUSERV),
     +       REALR(NREALR),   WR(NWR),    RATEL(1),
     +       RATEV(1),    XCURR,  VOL

C     DECLARE LOCAL VARIABLES
C
      INTEGER IMISS
      REAL*8 REAL(NREAL), RMISS,  XLEN,   DIAM,   TEMP,
     +       PRES,    VFRAC,  BETA,   VVAP,   VLIQ,
     +       VLIQS,   LMW,
     +       ntotC,   nliq,   vdotliq,    tauliq,
     +       pm(NCOMP_NCC),   m(NCOMP_NC), c(NCOMP_NC),
     +       mumax,   T,  Tmin,   Topt,   Tmax,   fT,
     +       kNH4,  fNH4, kPO4, fPO4, kCO2, fCO2,
     +       I0,  kalga,  h,  kd, Iav,    kl, ki, fIav,
     +       Rd,  mue,    Ri, Rtot,   kapp,   ni(NCOMP_NC),
     +       Iavtest, fIavtest, kapptest

! Component ID
! 1               CO2
! 2               CH4
! 3               WATER
! 4               AMMON-01
```

```
! 5              NH4+
! 6              OH-
! 7              H3PO4
! 8              H3O+
! 9              H2PO4-
! 10              HPO4--
! 11              PO4---
! 12              O2
! 13              N2
! 14              NO
! 15              H2S
! 16              S--
! 17          SO2
! 18  NH2COO-
! 19  HS-
! 20  HCO3-
! 21  HSO3-
! 22  CO3--
! 23 NCOMP_NCC  SO3--
! 24 NCOMP_NCC+9+1    ALGA
! 25 NCOMP_NCC+9+2    FORSU
! 26 NCOMP_NCC+9+3  FANGO

C
C     BEGIN EXECUTABLE CODE
C

! restitution of the molar flow rate conventional components kmol/s given as output by Aspen
      ntotC = SOUT(NCOMP_NCC+1)

! total molar flow rate in liquid phase kmol/s
```

```
nliq = ntotC*(1-vfrac)

! volumetric flow rate liquid phase computed [m^3/s] stwork_v1=molar volume mixture given by Aspen
    vdotliq = nliq*(STWORK_VL)

! computation of the residence time [sec]
tauliq = VLIQ/vdotliq

! restitution of the molecular weight of the mixture
    LMW = DMS_IFCMNC('MW')       ! offset of molecular weights in the plex

    pm = B(LMW+1:LMW+NCOMP_NCC)

!pmmix = SOUT(NCOMP_NCC+9)  ! molecular weight outgoing mixture conventional components

! computation of the mass flow rate [kg/s] of the conventional components in liquid phase
    m = nliq*X*PM

! mass flow rate of microalgae and OFMSW [kg/s] in liquid phase
m(NCOMP_NCC+1) = SOUT(NCOMP_NCC+9+1)
    m(NCOMP_NCC+2) = SOUT(NCOMP_NCC+9+2)
!     IF (m(ncomp_ncc+1) .EQ. 0) m(ncomp_ncc+1) = 0.015/3600
! computation of microalgae and nutrients concentration [kh/m^3]
    c = m/vdotliq
! computation of the reaction rate [kg/m^3 s]
    mumax = 2.63/(3600*24)  ! s^-1

    ! temperature related factor
    T=TEMP-273.15   ! °C
```

```
Tmin = 11.7 ! °C
Topt = 31.2 ! °C
Tmax = 43.65    ! °C
fT = ((T-Tmax)*(T-Tmin)**2)/
&     ((Topt-Tmin)*((Topt-Tmin)*(T-Topt)-
&     (Topt-Tmax)*(Topt+Tmin-2*T)))

! substrate related factors
kNH4 = 0.014*(pm(5)/14.0067) ! kg/m^3
fNH4 = c(5)/(kNH4+c(5))
kPO4 = (1.8/1000)*((m(9)+m(10))/(nliq*(X(9)+X(10)))/30.9738) ! kg/m^3
fPO4 = (c(9)+c(10))/(kPO4+(c(9)+c(10)))
kCO2 = (1.3/1000)*(pm(1)/12.0107) ! kg/m^3
fCO2 = c(1)/(kCO2+c(1))

! light related factor
I0 = 593    ! mumol/m2/s: July= 593, May= 509, September=360
kalga = 0.08*1000    ! m2/kg
h = 0.05   ! m: 0.05 or 0.75
kd = 315 ! 1/m: 1:5=315, 1:10=126
Iav = I0*(1-exp(-(kalga*c(NCOMP_NCC+1)+kd)*h))/
& ((kalga*c(NCOMP_NCC+1)+kd)*h)
kl = 125    ! mumol/m2/s
ki = 1570   ! mumol/m2/s
fIav = Iav/(kl+Iav+(Iav**2)/ki)

! direct reaction rate
Rd = mumax*c(NCOMP_NCC+1)*fT*fNH4*fPO4*fCO2*fIav

mue = 0.2166/(3600*24) ! s^-1
```

```
      ! inverse reaction rate
      Ri = mue*c(NCOMP_NCC+1)

      Rtot = Rd-Ri
      kapp = (mumax*fT*fNH4*fPO4*fCO2*fIav-mue)*(3600*24)

! stoichiometry coefficients of the biomass production reaction
      ni = (/-0.2849355,  ! CO2
     &       0,           ! CH4
     &      -0.227993,    ! H20
     &       0,           ! NH3
     &      -0.0386091,   ! NH4+
     &       0,           ! OH-
     &       0,           ! H3PO4
     &       0.0385377,   ! H3O+
     &      -0.0000238,   ! H2PO4-
     &      -0.0000238,   ! HPO4--
     &       0,           ! PO4---
     &       0.2889946,   ! O2
     &       0,           ! N2
     &       0,           ! NO
     &       0,           ! H2S
     &       0,           ! S--
     &       0,           ! SO2
     &       0,           ! NH2COO-
     &       0,           ! HS-
     &       0,           ! HCO3-
     &       0,           ! HSO3-
     &       0,           ! CO3--
     &       0,           ! SO3--
     &       1,           ! MICROALGAE
```

```
    &       0,          ! OFMSW
    &       0 /)        ! MUD

      RATES(1:NCOMP_NCC)     =     (ni(1:NCOMP_NCC)/7.367652566)*Rtot*VLIQ     !
conventional components (kmol/s)
      RATES(NCOMP_NCC+1) = ni(NCOMP_NCC+1)*Rtot*VLIQ       ! biomass (kg/s)
      RATES(NCOMP_NCC+2) = ni(NCOMP_NCC+2)*Rtot*VLIQ       ! OFMSW (kg/s)
c write results in a .TXT file
     open(1,FILE='cstrgasair.dat')

write (1, *) tauliq/86400, "Time in d"
write (1, *) VLIQ, "Volume occupied by the liquid in m3"
     write (1, *) VLIQ/h, "Reactor's surface"
     write (1, *) VLIQS, "volume occupied by liquid+solid in m3"
     write (1, *) VVAP, "volume occupied by gas in m3"
     write (1, *) pm, "molecular weight mixture"
     write (1, *) RATES(NCOMP_NCC+1)*86400, "reaction rate g/L d"
     write (1, *) nliq, "molar flow rate in liquid phase kmol/s"
     write (1, *) m(5)*3600, "mass flow rates kg/h"
     do i=1,NCOMP_NC
     write(1,*) "component concentration ", i, ": ", c(i)
     end do
     write (1, *) fT, fNH4, fPO4, fCO2, fIav, "Kinetics factors"
     write (1, *) Iav, "Average luminous intensity"
     write (1, *) (kalga*c(NCOMP_NCC+1)+kd)*h
     do i=1,NCOMP_NCC
     write(1,*) "Molar fraction component ", i, ": ", X(i)
     end do
     write (1, *) STWORK_VL
close(1,STATUS='keep')
```

```
RETURN
END
```

The subroutine can be complied using the Customize Aspen Plus program.
In order to be able to compile the program, the window must be referring to the same position (directory) in which the gasaria.f file is present. To do so, if the directory “nameofthedirectory”, which contains the Fortran file gasaria.f, is placed into the local disk (C:), the command is: cd C:\nameofthedirectory.
The Fortran source gasaria.f, written in Visual Studio 2013, must be compiled by the Fortran compiler using the aspcomp procedure, type: aspcomp gasaria.f

Appendix B

Matlab script

```
clc
clear all
close all

%% Experimental data
theta_exp = [9 6.5 5.5];    % d, experimental residence time
Texp = [24.3 25.6 25];      % °C, experimental temperature
Cexp = [1.920 1.020 0.680]; % g/L, experimental microalgae concentration
Rexp = Cexp ./ theta_exp;   % g/L/d, experimental volumetric productivity

% Temperature factor
Tmin = 11.7;    % °C
Topt = 31.2;    % °C
Tmax = 43.65;   % °C
fT = ((Texp - Tmax) .* (Texp - Tmin).^2) ./...
    ((Topt - Tmin) .* ((Topt - Tmin) .* ...
    (Texp - Topt) - (Topt - Tmax) .* (Topt + Tmin - 2 * Texp)));

%% Reactor parameters
L = 0.04;       % m, PBR thickness
VR = 0.002;     % m3, reactor volume
I0 = 559;       % umol m-2 s-1, incident light

% simulation extent
thetaV = 20:-0.02:1;    % d, simulated residence times array
TV = 25;                % °C, simulated temperatures array
```

```
Q0V = VR ./ thetaV;     % m3/d, feeding flow rates array
                    % Note: constant density is assumed

%% Initialization
Xi = [0.50832; 0.01107667; 0];  % g/L: N, P, incoming microalgae
kmax = 2.63;    % 1/days, maximum specific growth rate
kN = 0.014;     % kg/m^3, nitrogen factor
kP = 0.0018;    % kg/m^3, potassium factor
kl = 125;       % umol/(m^2*s), light saturation coefficient
ki = 1570;      % umol/(m^2*s), light inhibition coefficient
ka = 80;        % m^2/kg, microalgae light absorption coefficient
kd = 288;       % 1/m, digestate light absorption coefficient
mueV = 0.20;    % 1/days, cell death rate
k = [kmax kN kP ka kl ki mueV];
p0 = kd;
[p,fval] = fminsearch(@ER, p0, [],...
        Cexp, theta_exp, Rexp, TV, I0, L, Xi, thetaV, k);
disp(sprintf('Final S:   %8.3f  Optimal params: %7.3g %7.3g', fval, p));
disp(p)

%% evaluation of the mass balance over time
function err_p = ER(p, Cexp, theta_exp, Rexp, TV, I0, L, Xi, thetaV, k)
   % kg/m^3, matrix of output microalgae concentrations
   NV = zeros(1, length(thetaV));              % g/L, output nitrogen N
   PV = zeros(1, length(thetaV));              % g/L, output phosporous P
   XuV = zeros(1, length(thetaV));             % g/L, output microalgae
   XV = zeros(length(Xi), length(thetaV));     % g/L: output matrix
   guess = [0.51; 0.012; 3];

   %% Loop to evaluate different residence times
   for i = 1:1:length(thetaV)
```

```
    % Resolution of CSTR material balance
    options = optimoptions('lsqnonlin',...
            'MaxFunctionEvaluations', 1000000000,...
            'MaxIterations', 1000000000,...
            'OptimalityTolerance', 1e-10);
    XV(:, i) = lsqnonlin(@BM, guess, [0; 0; 0], [0.6; 0.015; 10],...
             options, TV, I0, p, L, Xi, thetaV(i), k);
    guess = XV(:, i);
    NV(1, i) = XV(1, i);
    PV(1, i) = XV(2, i);
    XuV(1, i) = XV(3, i);
end

Px_vol = XuV ./ thetaV;   % volumetric productivity
err_p = norm((Px_vol(thetaV == 9 | thetaV == 6.5 | thetaV == 5.5)...
    - Rexp) ./ Rexp);

%% Plots
subplot(2, 1, 1)
plot(thetaV, Px_vol, theta_exp, Rexp, 'o');
set(gca,'FontName','Times New Roman'), axis tight
xlabel('Hydraulic residence time (d)', 'FontName', 'Times New Roman');
ylabel('C_a_l_g_a/\tau_C_S_T_R (g m^{-3} d^{-1})',...
    'FontName', 'Times New Roman');
legend({num2str(p);  'Exp. Data'}, ...
    'Location', 'southeast', 'FontName', 'Times New Roman');

subplot(2, 1, 2)
plot(thetaV, XuV, theta_exp, Cexp, 'o');
set(gca, 'FontName', 'Times New Roman'), axis tight
xlabel('Hydraulic residence time (d)', 'FontName', 'Times New Roman');
```

```
    ylabel('C_a_l_g_a (g L^{-1})', 'FontName', 'Times New Roman');
    legend({num2str(p); 'Exp. Data'}, ...
        'Location', 'southeast', 'FontName', 'Times New Roman');

    drawnow
    disp(p)
end

%% CSTR material balance
function err_MB = BM(X, T, I0, p, L, Xi, theta, k)
    %% Reaction parameters
    ni = [-0.0734; -0.0002; 1];

    % temperature factor
    Tmin = 11.7;    % °C
    Topt = 31.2;% °C
    Tmax = 43.65;% °C
    fT = ((T - Tmax) * (T - Tmin)^2) /...
        ((Topt - Tmin) * ((Topt - Tmin) * (T - Topt) - ...
        (Topt - Tmax) * (Topt + Tmin - 2 * T)));

    % light factor
    Iav = I0 * (1 - exp(-k(4) * X(3) * L - p(1) * L)) ...
         / (k(4) * X(3) * L + p(1) * L);
    fIav = Iav / (k(5) + Iav + Iav^2 / k(6));

    % substrate factors
    fN = X(1) / (k(2) + X(1));
    fP = X(2) / (k(3) + X(2));

    % reaction rate
```

```
    rate = X(3) * k(1) * fT * fIav * fN * fP * 0.92 - k(7) * X(3);
    rX = ni * rate;
    err_MB = (X - Xi) / theta - rX;
end
```

Appendix C

Stream tables

Table C.1: *general stream information related to the anaerobic digestion and cogeneration section*

	T	P	Mass Vapor Fraction	Mass Liquid Fraction	Mass Solid Fraction	Mass Flows	Volume Flow (MIXED)	Mole Flows (MIXED)
UOM	C	bar	-	-	-	kg/hr	l/min	kmol/hr
Anaerobic Digestion								
BIOGAS	50	1,01325	1	0	0	8,5082	146,4318	0,332341
DIGIN	24	1,01325	0	0,87260	0,12740	79,141	1,151529	3,821715
DIGOUT	50	1,01325	0,10751	0,85250	0,03999	79,141	147,5661	4,058264
FLASHOUT	50	1,01325	0	0,95519	0,04481	70,633	1,134295	3,725923
LIQ-REC	24	1,01325	0	0,98469	0,01531	41,342	0,677825	2,248058
LIQOUT	24	1,01325	0	0,98469	0,01531	20,669	0,338887	1,123944
LIQUID	24	1,01325	0	0,98469	0,01531	62,008	1,016661	3,371832
SOL-LIQ	24	1,01325	0	0,95519	0,04481	70,633	1,123382	3,725781
SOLIDOUT	24	1,01325	0	0,74314	0,25686	8,6249	0,106721	0,353949
WETFORSU	24	1,01325	0	0,75	0,25	37,799	0,473714	1,573638
Cogeneration								
AIR	24	1,01325	1	0	0	160,37	2287,747	5,558534
COMBOUT	1100	13	1	0	0	168,87	864,2868	5,89097
COMPROUT	388	13	1	0	0	168,87	416,7028	5,890875
COOLED1	257	1,01325	1	0	0	168,87	4271,535	5,89097
COOLED2	40	1,01325	1	0	0	168,87	2520,679	5,89097
TURBOUT	564	1,01325	1	0	0	168,87	6744,106	5,89097
VAP-SUBS	40	1,01325	1	0	0	22,372	333,9278	0,780408
VENT1	40	1,01325	1	0	0	146,50	2186,751	5,110561

Table C.2: *component mass flowrate for the anaerobic digestion section*

	UOM	BIOGAS	DIGIN	DIGOUT	FLASHOUT	LIQ-REC
CO_2	kg/hr	4,867788	0,008541	4,886773	0,018985	0,00768
CH_4	kg/hr	2,890985	0,000341	2,891551	0,000566	0,000341
H_2O	kg/hr	0,734979	68,63921	67,51098	66,776	40,28955
NH_3	kg/hr	0,010449	0,028383	0,058753	0,048303	0,027689
NH_4^+	kg/hr	0	0,088604	0,144919	0,144919	0,089124
OH^-	kg/hr	0	5,86E-07	2,00E-06	2,00E-06	3,82E-07
H_3PO_4	kg/hr	0	2,16E-09	1,12E-08	1,12E-08	1,61E-09
H_3O^+	kg/hr	0	3,96E-08	7,37E-08	7,37E-08	2,35E-08
$H_2PO_4^-$	kg/hr	0	0,001173	0,002594	0,002594	0,000988
HPO_4^{2-}	kg/hr	0	0,006142	0,009536	0,009536	0,006325
PO_4^{3-}	kg/hr	0	4,32E-07	7,87E-07	7,87E-07	6,08E-07
H_2S	kg/hr	0,004009	0,001212	0,005696	0,001687	0,001106
S^{2-}	kg/hr	0	4,75E-10	5,72E-09	5,72E-09	5,96E-10
NH_2COO^-	kg/hr	0	0,001069	0,003739	0,003739	0,001788
HS^-	kg/hr	0	0,006122	0,010459	0,010459	0,006226
HCO_3^-	kg/hr	0	0,276613	0,449745	0,449745	0,276821
CO_3^{2-}	kg/hr	0	0,001073	0,001778	0,001778	0,001324
FORSU	kg/hr	0	10,0197	2,849088	2,849088	0,569861
FANGO	kg/hr	0	0,063149	0,315721	0,315721	0,063149

Table C.2 (continued): *component mass flowrate for the anaerobic digestion section*

	UOM	LIQOUT	LIQUID	SOL-LIQ	SOLIDOUT	WETFORSU
CO_2	kg/hr	0,00384	0,011519	0,012728	0,001209	0
CH_4	kg/hr	0,000171	0,000512	0,000566	5,38E-05	0
H_2O	kg/hr	20,14325	60,42975	66,77321	6,343455	28,34952
NH_3	kg/hr	0,013843	0,04153	0,04589	0,00436	0
NH_4^+	kg/hr	0,044558	0,133675	0,147708	0,014032	0
OH^-	kg/hr	1,91E-07	5,74E-07	6,34E-07	6,02E-08	4,65E-08
H_3PO_4	kg/hr	8,06E-10	2,42E-09	2,67E-09	2,54E-10	0
H_3O^+	kg/hr	1,18E-08	3,53E-08	3,90E-08	3,71E-09	5,20E-08
$H_2PO_4^-$	kg/hr	0,000494	0,001482	0,001637	0,000156	0
HPO_4^{2-}	kg/hr	0,003162	0,009487	0,010483	0,000996	0
PO_4^{3-}	kg/hr	3,04E-07	9,12E-07	1,01E-06	9,57E-08	0
H_2S	kg/hr	0,000553	0,001658	0,001833	0,000174	0
S^{2-}	kg/hr	2,98E-10	8,93E-10	9,87E-10	9,38E-11	0
NH_2COO^-	kg/hr	0,000894	0,002682	0,002964	0,000282	0
HS^-	kg/hr	0,003113	0,009338	0,010318	0,00098	0
HCO_3^-	kg/hr	0,1384	0,415199	0,458784	0,043584	0
CO_3^{2-}	kg/hr	0,000662	0,001986	0,002195	0,000208	0
FORSU	kg/hr	0,284909	0,854726	2,849088	1,994362	9,449841
FANGO	kg/hr	0,031572	0,094716	0,315721	0,221005	0

Table C.3: *component mass flowrates for the cogeneration section in different months of the year*

	CO_2	CH_4	H_2O	NH_3	O_2	N_2	NO	H_2S	SO_2
UOM	kg/hr	kg/hr	kg/hr	kg/hr	kg/hr	kg/hr	kg/hr	kg/hr	kg/hr
May									
AIR	0	0	0	0	36,6308	120,6391	0	0	0
COMBOUT	12,7981	0	7,2463	0	25,0684	120,6391	0,0184	0	0,0075
COMPROUT	4,8676	2,8909	0,7349	0,0104	36,6308	120,6391	0	0,0040	0
COOLED1	12,7981	0	7,2463	0	25,0684	120,6391	0,0184	0	0,0075
COOLED2	12,7981	0	7,2463	0	25,0684	120,6391	0,0184	0	0,0075
TURBOUT	12,7981	0	7,2463	0	25,0684	120,6391	0,0184	0	0,0075
VAP-SUBS	10,4234	0	5,9017	0	20,4170	98,2547	0,0150	0	0,0061
VENT1	2,3747	0	1,3445	0	4,6514	22,3844	0,0034	0	0,0014
July									
AIR	0	0	0	0	37,3520	123,0140	0	0	0
COMBOUT	12,7986	0	7,2466	0	25,7891	123,0140	0,0184	0	0,0075
COMPROUT	4,8678	2,8910	0,7350	0,0104	37,3520	123,0140	0	0,0040	0
COOLED1	12,7986	0	7,2466	0	25,7891	123,0140	0,0184	0	0,0075
COOLED2	12,7986	0	7,2466	0	25,7891	123,0140	0,0184	0	0,0075
TURBOUT	12,7986	0	7,2466	0	25,7891	123,0140	0,0184	0	0,0075
VAP-SUBS	1,6955	0	0,9600	0	3,4164	16,2963	0,0024	0	0,0010
VENT1	11,1031	0	6,2866	0	22,3727	106,7177	0,0160	0	0,0065
September									
AIR	0	0	0	0	36,8351	121,3118	0	0	0
COMBOUT	12,7986	0	7,2466	0	25,2722	121,3118	0,0184	0	0,0075
COMPROUT	4,8678	2,8910	0,7350	0,0104	36,8351	121,3118	0	0,0040	0
COOLED1	12,7986	0	7,2466	0	25,2722	121,3118	0,0184	0	0,0075
COOLED2	12,7986	0	7,2466	0	25,2722	121,3118	0,0184	0	0,0075
TURBOUT	12,7986	0	7,2466	0	25,2722	121,3118	0,0184	0	0,0075
VAP-SUBS	8,1847	0	4,6342	0	16,1615	77,5786	0,0118	0	0,0048
VENT1	4,6139	0	2,6124	0	9,1107	43,7332	0,0066	0	0,0027

Table C.4: *stream table for the biomass production section in the month of May*

	UOM	DILALGA	LIQ-SUBS	LIQFEED	LIQWASTE
Total Stream					
Temperature	C	30	17,00135	17,00011	17,00011
Pressure	bar	1,01325	1,01325	1,01325	1,01325
Mass Vapor Fraction		0	0	0	0
Mass Liquid Fraction		0,99847	0,998442	0,984688	0,984688
Mass Solid Fraction		0,00153	0,001558	0,015312	0,015312
Mass Flows	kg/hr	134,4502	132,069	13,43459	7,234012
Component Mass Flows					
CO_2	kg/hr	0,00906	0,003555	0,002571	0,001384
CH_4	kg/hr	4,13E-09	0,000111	0,000111	5,97E-05
H_2O	kg/hr	134,0904	131,7273	13,0926	7,04986
NH_3	kg/hr	0,004502	0,009757	0,009095	0,004897
NH_4^+	kg/hr	0,031778	0,028317	0,028889	0,015556
OH^-	kg/hr	5,44E-07	5,56E-07	7,68E-08	4,14E-08
H_3PO_4	kg/hr	6,86E-09	1,1E-09	4,45E-10	2,4E-10
H_3O^+	kg/hr	1,99E-07	6,75E-08	7,02E-09	3,78E-09
$H_2PO_4^-$	kg/hr	0,00103	0,000542	0,000314	0,000169
HPO_4^{2-}	kg/hr	0,001354	0,001837	0,002062	0,00111
PO_4^{3-}	kg/hr	2,04E-08	5,82E-08	1,81E-07	9,75E-08
O_2	kg/hr	0,000706	0	0	0
N_2	kg/hr	0,001753	0	0	0
NO	kg/hr	7,89E-07	0	0	0
H_2S	kg/hr	0,000172	0,000548	0,000418	0,000225
S^{2-}	kg/hr	1,06E-11	4,77E-11	1E-10	5,4E-11
SO_2	kg/hr	1,61E-08	0	0	0
NH_2COO^-	kg/hr	3,35E-05	4,99E-05	0,00048	0,000258
HS^-	kg/hr	0,00032	0,00184	0,001966	0,001059
HCO_3^-	kg/hr	0,09556	0,089265	0,089995	0,048459
HSO_3^-	kg/hr	0,003925	0	0	0
CO_3^{2-}	kg/hr	0,000101	0,000198	0,000391	0,00021
SO_3^{2-}	kg/hr	0,003795	0	0	0
ALGA	kg/hr	3,48E-07	0	0	0
FORSU	kg/hr	0,185183	0,185183	0,185183	0,099714
FANGO	kg/hr	0,020521	0,020521	0,020521	0,01105
MIXED Substream					
Volume Flow	l/min	2,246087	2,199349	0,219935	0,118426
Mole Flows	kmol/hr	7,447168	7,31577	0,730536	0,393366

Table C.4 (continued): *stream table for the biomass production section in the month of May*

	UOM	REACOUT	REACTIN	VENT2	WATER2
Total Stream					
Temperature	C	30	29,99963	30	17
Pressure	bar	1,01325	1,01325	1,01325	1,01325
Mass Vapor Fraction		0,496605	0,496605	1	0
Mass Liquid Fraction		0,502625	0,502625	0	1
Mass Solid Fraction		0,00077	0,00077	0	0
Mass Flows	kg/hr	267,087	267,087	132,6368	118,6344
Component Mass Flows					
CO_2	kg/hr	10,4225	10,4225	10,41344	0
CH_4	kg/hr	0,000111	0,000111	0,000111	0
H_2O	kg/hr	137,6255	137,6255	3,535093	118,6344
NH_3	kg/hr	0,006494	0,006494	0,001992	0
NH_4^+	kg/hr	0,031778	0,031778	0	0
OH^-	kg/hr	5,44E-07	5,44E-07	0	1,47E-07
H_3PO_4	kg/hr	6,86E-09	6,86E-09	0	0
H_3O^+	kg/hr	1,99E-07	1,99E-07	0	1,65E-07
$H_2PO_4^-$	kg/hr	0,00103	0,00103	0	0
HPO_4^{2-}	kg/hr	0,001354	0,001354	0	0
PO_4^{3-}	kg/hr	2,04E-08	2,04E-08	0	0
O_2	kg/hr	20,41701	20,41701	20,41631	0
N_2	kg/hr	98,25466	98,25466	98,25291	0
NO	kg/hr	0,014994	0,014994	0,014993	0
H_2S	kg/hr	0,002115	0,002115	0,001943	0
S^{2-}	kg/hr	1,06E-11	1,06E-11	0	0
SO_2	kg/hr	5,88E-08	5,88E-08	4,27E-08	0
NH_2COO^-	kg/hr	3,35E-05	3,35E-05	0	0
HS^-	kg/hr	0,00032	0,00032	0	0
HCO_3^-	kg/hr	0,09556	0,095561	0	0
HSO_3^-	kg/hr	0,003925	0,003925	0	0
CO_3^{2-}	kg/hr	0,000101	0,000101	0	0
SO_3^{2-}	kg/hr	0,003795	0,003795	0	0
ALGA	kg/hr	3,48E-07	0	0	0
FORSU	kg/hr	0,185183	0,185183	0	0
FANGO	kg/hr	0,020521	0,020521	0	0
MIXED Substream					
Volume Flow	l/min	1899,023	1899,019	1896,777	1,979418
Mole Flows	kmol/hr	12,02607	12,02607	4,578902	6,585211

Table C.5: *stream table for the biomass production section in the month of July*

	UOM	DILALGA	LIQ-SUBS	LIQFEED	LIQWASTE
Total Stream					
Temperature	C	30	24,00079	24,00001	24,00001
Pressure	bar	1,01325	1,01325	1,01325	1,01325
Mass Vapor Fraction		0	0	0	0
Mass Liquid Fraction		0,996803	0,998442	0,984688	0,984688
Mass Solid Fraction		0,003197	0,001558	0,015312	0,015312
Mass Flows	kg/hr	46,11883	45,71923	4,65062	16,0188
Component Mass Flows					
CO_2	kg/hr	0,002829	0,001195	0,000864	0,002976
CH_4	kg/hr	2,95E-09	3,84E-05	3,84E-05	0,000132
H_2O	kg/hr	45,94274	45,60092	4,532232	15,61102
NH_3	kg/hr	0,000471	0,003349	0,003115	0,010729
NH_4^+	kg/hr	0,005573	0,009832	0,010026	0,034533
OH^-	kg/hr	1,04E-07	3,12E-07	4,3E-08	1,48E-07
H_3PO_4	kg/hr	5,51E-09	4,48E-10	1,81E-10	6,25E-10
H_3O^+	kg/hr	1,14E-07	2,52E-08	2,65E-09	9,12E-09
$H_2PO_4^-$	kg/hr	0,000461	0,000191	0,000111	0,000383
HPO_4^{2-}	kg/hr	0,000318	0,000633	0,000712	0,002451
PO_4^{3-}	kg/hr	2,37E-09	2,18E-08	6,84E-08	2,36E-07
O_2	kg/hr	0,000251	0	0	0
N_2	kg/hr	0,0006	0	0	0
NO	kg/hr	2,65E-07	0	0	0
H_2S	kg/hr	0,000112	0,000164	0,000124	0,000428
S^{2-}	kg/hr	2,02E-12	3,21E-11	6,7E-11	2,31E-10
SO_2	kg/hr	6,15E-09	0	0	0
NH_2COO^-	kg/hr	1,78E-06	2,11E-05	0,000201	0,000693
HS^-	kg/hr	0,000116	0,000662	0,0007	0,002412
HCO_3^-	kg/hr	0,016651	0,030939	0,03114	0,10726
HSO_3^-	kg/hr	0,000835	0	0	0
CO_3^{2-}	kg/hr	9,19E-06	7,51E-05	0,000149	0,000513
SO_3^{2-}	kg/hr	0,000423	0	0	0
ALGA	kg/hr	0,076226	0	0	0
FORSU	kg/hr	0,064104	0,064104	0,064104	0,220804
FANGO	kg/hr	0,007104	0,007104	0,007104	0,024468
MIXED Substream					
Volume Flow	l/min	0,769378	0,762495	0,07625	0,262637
Mole Flows	kmol/hr	2,550944	2,532549	0,252887	0,871056

Table C.5 (continued): *stream table for the biomass production section in the month of July*

	UOM	REACOUT	REACTIN	VENT2	WATER2
Total Stream					
Temperature	C	30	29,99981	30	24
Pressure	bar	1,01325	1,01325	1,01325	1,01325
Mass Vapor Fraction		0,322687	0,322986	1	0
Mass Liquid Fraction		0,675148	0,675968	0	1
Mass Solid Fraction		0,002165	0,001046	0	0
Mass Flows	kg/hr	68,09088	68,09088	21,97205	41,06861
Component Mass Flows					
CO_2	kg/hr	1,57732	1,69378	1,574491	0
CH_4	kg/hr	3,84E-05	3,84E-05	3,84E-05	0
H_2O	kg/hr	46,52956	46,55944	0,586812	41,06861
NH_3	kg/hr	0,000572	0,002095	0,000101	0
NH_4^+	kg/hr	0,005573	0,011162	0	0
OH^-	kg/hr	1,04E-07	2,04E-07	0	6,74E-08
H_3PO_4	kg/hr	5,51E-09	2,06E-09	0	0
H_3O^+	kg/hr	1,14E-07	6,24E-08	0	7,54E-08
$H_2PO_4^-$	kg/hr	0,000461	0,000339	0	0
HPO_4^{2-}	kg/hr	0,000318	0,000486	0	0
PO_4^{3-}	kg/hr	2,37E-09	8,04E-09	0	0
O_2	kg/hr	3,512091	3,416417	3,511841	0
N_2	kg/hr	16,29632	16,29632	16,29572	0
NO	kg/hr	0,002439	0,002439	0,002439	0
H_2S	kg/hr	0,000726	0,000639	0,000614	0
S^{2-}	kg/hr	2,02E-12	7,26E-12	0	0
SO_2	kg/hr	1,4E-08	5,23E-09	7,88E-09	0
NH_2COO^-	kg/hr	1,78E-06	1,37E-05	0	0
HS^-	kg/hr	0,000116	0,000201	0	0
HCO_3^-	kg/hr	0,016651	0,035017	0	0
HSO_3^-	kg/hr	0,000835	0,00061	0	0
CO_3^{2-}	kg/hr	9,19E-06	4,03E-05	0	0
SO_3^{2-}	kg/hr	0,000423	0,000645	0	0
ALGA	kg/hr	0,076226	0	0	0
FORSU	kg/hr	0,064104	0,064104	0	0
FANGO	kg/hr	0,007104	0,007104	0	0
MIXED Substream					
Volume Flow	l/min	315,563	315,4119	314,7936	0,686247
Mole Flows	kmol/hr	3,310859	3,312875	0,759915	2,279654

Table C.6: *stream table for the biomass production section in the month of September*

	UOM	DILALGA	LIQ-SUBS	LIQFEED	LIQWASTE
Total Stream					
Temperature	C	30	19,00117	19,00001	19,00001
Pressure	bar	1,01325	1,01325	1,01325	1,01325
Mass Vapor Fraction		0	0	0	0
Mass Liquid Fraction		0,998466	0,998442	0,984688	0,984688
Mass Solid Fraction		0,001534	0,001558	0,015312	0,015312
Mass Flows	kg/hr	123,7721	121,9155	12,40165	8,267769
Component Mass Flows					
CO_2	kg/hr	0,008291	0,003229	0,002334	0,001556
CH_4	kg/hr	4,44E-09	0,000102	0,000102	6,83E-05
H_2O	kg/hr	123,4394	121,6	12,08594	8,057296
NH_3	kg/hr	0,004274	0,008972	0,008359	0,005573
NH_4^+	kg/hr	0,029439	0,026176	0,026698	0,017799
OH^-	kg/hr	5,13E-07	5,95E-07	8,22E-08	5,48E-08
H_3PO_4	kg/hr	6,09E-09	1,05E-09	4,25E-10	2,83E-10
H_3O^+	kg/hr	1,78E-07	6,33E-08	6,61E-09	4,4E-09
$H_2PO_4^-$	kg/hr	0,000937	0,0005	0,00029	0,000193
HPO_4^{2-}	kg/hr	0,001263	0,001696	0,001904	0,001269
PO_4^{3-}	kg/hr	1,96E-08	5,54E-08	1,73E-07	1,15E-07
O_2	kg/hr	0,000651	0	0	0
N_2	kg/hr	0,001614	0	0	0
NO	kg/hr	7,22E-07	0	0	0
H_2S	kg/hr	0,000178	0,000482	0,000367	0,000245
S^{2-}	kg/hr	1,15E-11	5,39E-11	1,13E-10	7,53E-11
SO_2	kg/hr	1,22E-08	0	0	0
NH_2COO^-	kg/hr	3,24E-05	4,92E-05	0,000472	0,000314
HS^-	kg/hr	0,00034	0,001721	0,001833	0,001222
HCO_3^-	kg/hr	0,08964	0,082464	0,083087	0,055391
HSO_3^-		0,003044	0	0	0
CO_3^{2-}	kg/hr	9,68E-05	0,000189	0,000374	0,000249
SO_3^{2-}	kg/hr	0,003018	0	0	0
ALGA	kg/hr	2,27E-07	0	0	0
FORSU	kg/hr	0,170945	0,170945	0,170945	0,113964
FANGO	kg/hr	0,018943	0,018943	0,018943	0,012629
MIXED Substream					
Volume Flow	l/min	6,855663	6,75333	0,674367	0,449578
Mole Flows	kmol/hr	2,067678	2,031012	0,203101	0,135401

Table C.6 (continued): *stream table for the biomass production section in the month of September*

	UOM	REACOUT	REACTIN	VENT2	WATER2
Total Stream					
Temperature	C	30	29,99959	30	19
Pressure	bar	1,01325	1,01325	1,01325	1,01325
Mass Vapor Fraction		0,458306	0,458306	1	0
Mass Liquid Fraction		0,540863	0,540863	0	1
Mass Solid Fraction		0,000831	0,000831	0	0
Mass Flows	kg/hr	228,491	228,491	104,7189	109,5139
Component Mass Flows					
CO_2	kg/hr	8,182785	8,182785	8,174493	0
CH_4	kg/hr	0,000102	0,000102	0,000102	0
H_2O	kg/hr	126,2307	126,2307	2,791328	109,5139
NH_3	kg/hr	0,005897	0,005896	0,001622	0
NH_4^+	kg/hr	0,029439	0,029439	0	0
OH^-	kg/hr	5,13E-07	5,13E-07	0	1,48E-07
H_3PO_4	kg/hr	6,09E-09	6,09E-09	0	0
H_3O^+	kg/hr	1,78E-07	1,78E-07	0	1,65E-07
$H_2PO_4^-$	kg/hr	0,000937	0,000937	0	0
HPO_4^{2-}	kg/hr	0,001263	0,001263	0	0
PO_4^{3-}	kg/hr	1,96E-08	1,96E-08	0	0
O_2	kg/hr	16,16152	16,16152	16,16087	0
N_2	kg/hr	77,57856	77,57856	77,57694	0
NO	kg/hr	0,011773	0,011773	0,011773	0
H_2S	kg/hr	0,001906	0,001906	0,001728	0
S^{2-}	kg/hr	1,15E-11	1,15E-11	0	0
SO_2	kg/hr	3,99E-08	3,99E-08	2,77E-08	0
NH_2COO^-	kg/hr	3,24E-05	3,24E-05	0	0
HS^-	kg/hr	0,00034	0,00034	0	0
HCO_3^-	kg/hr	0,08964	0,08964	0	0
HSO_3^-	kg/hr	0,003044	0,003044	0	0
CO_3^{2-}	kg/hr	9,68E-05	9,68E-05	0	0
SO_3^{2-}	kg/hr	0,003018	0,003018	0	0
ALGA	kg/hr	2,27E-07	0	0	0
FORSU	kg/hr	0,170945	0,170945	0	0
FANGO	kg/hr	0,018943	0,018943	0	0
MIXED Substream					
Volume Flow	l/min	10,47121	10,47121	3,615547	6,078943
Mole Flows	kmol/hr	1499,783	1499,78	1497,716	1,827915

References

Aishvarya, V. *et al.* (2015) 'Microalgae: Cultivation and Application', in Sukla, Lala Behari et al. (eds). Cham: Springer International Publishing (Soil Biology), pp. 289–311. doi: 10.1007/978-3-319-19018-1_15.

Angelidaki, I. and Batstone, D. J. (2010) 'Anaerobic Digestion: Process', in *Solid Waste Technology & Management*. Chichester, UK: John Wiley & Sons, Ltd, pp. 583–600. doi: 10.1002/9780470666883.ch37.

Aspen Technology Inc (2000) 'Aspen Plus User Guide version 10.2', *Aspen Plus User Guide*.

Banerjee, S. and Ramaswamy, S. (2017) 'Dynamic process model and economic analysis of microalgae cultivation in open raceway ponds', *Algal Research*. Elsevier, 26(August), pp. 330–340. doi: 10.1016/j.algal.2017.08.011.

Benemann, J. R. *et al.* (1982) 'Final technical report: microalgae as a source of liquid fuels', pp. 1–16. Available at: http://www.nrel.gov/docs/legosti/old/1808.pdf#page=5.

Bradbury, D. and Harding, M. (2019) 'Revenue Statistics 2019 - Canada'.

Campuzano, R. and González-Martínez, S. (2016) 'Characteristics of the organic fraction of municipal solid waste and methane production: A review', *Waste Management*. doi: 10.1016/j.wasman.2016.05.016.

CEN/TC 408 (2016) *Natural gas and biomethane for use in transport and biomethane for injection in the natural gas network - Part 1: Specifications for biomethane for injection in the natural gas network.*

Cesaro, A. and Belgiorno, V. (2013) 'Sonolysis and ozonation as pretreatment for anaerobic digestion of solid organic waste', *Ultrasonics Sonochemistry*. Elsevier B.V., 20(3), pp. 931–936. doi: 10.1016/j.ultsonch.2012.10.017.

Cesaro, A., Belgiorno, V. and Naddeo, V. (2010) 'Comparative technology assessment of anaerobic digestion of organic fraction of MSW', *WIT Transactions on Ecology and the Environment*, 142, pp. 355–366. doi: 10.2495/SW100331.

Chen, L. *et al.* (2008) 'Ultrasound-assisted hydrolysis and acidogenesis of solid organic wastes in a rotational drum fermentation system', *Bioresource Technology*, 99(17), pp. 8337–8343. doi: 10.1016/j.biortech.2008.02.043.

CIB (2018) ‘Il futuro della mobilità’, *CIBinforma*.

Collos, Y. and Harrison, P. J. (2014) ‘Acclimation and toxicity of high ammonium concentrations to unicellular algae’, *Marine Pollution Bulletin*. Elsevier Ltd, 80(1–2), pp. 8–23. doi: 10.1016/j.marpolbul.2014.01.006.

Consulente-energia (2019) ‘COSTO DI UN IMPIANTO A BIOGAS DA 100 KW A 1 MW’. Available at: http://www.consulente-energia.com/ah-costo-impianto-a-biogas-da-100kw-quale-e-il-prezzo-di-acquisto-di-impianto-a-biogas-da-100kw-a-1mw-di-potenza-costi-di-gestione-sistema-a-biogas-da-100-kw.html.

Cruz, Y. R. *et al.* (2018) ‘Cultivation Systems of Microalgae for the Production of Biofuels’, *Biofuels - State of Development*. doi: 10.5772/intechopen.74957.

Cucchiella, F. and D’Adamo, I. (2016) ‘Technical and economic analysis of biomethane: A focus on the role of subsidies’, *Energy Conversion and Management*. Elsevier Ltd, 119, pp. 338–351. doi: 10.1016/j.enconman.2016.04.058.

Deublein, D. and Steinhauser, A. (2008) *Biogas from Waste and Renewable Resources*.

Dewil, R. *et al.* (2007) ‘Peroxidation enhances the biogas production in the anaerobic digestion of biosolids’, *Journal of Hazardous Materials*, 146(3), pp. 577–581. doi: 10.1016/j.jhazmat.2007.04.059.

Duan, N. *et al.* (2018) ‘Performance evaluation of mesophilic anaerobic digestion of chicken manure with algal digestate’, *Energies*, 11(7), pp. 1–11. doi: 10.3390/en11071829.

Eisted, R. and Christensen, T. H. (2011) ‘Characterization of household waste in Greenland’, *Waste Management*. doi: 10.1016/j.wasman.2011.02.018.

EU (2008) *2020 climate & energy package*. Available at: https://ec.europa.eu/clima/policies/strategies/2020_en.

European Biogas Association (2018) *EBA Statistical Report 2018*, *Annual Report*. doi: 10.1139/e11-014.

European Commission (1997) ‘Communication from the Commission: Energy for the Future: Renewable Sources of Energy–White Paper for a Community Strategy and Action Plan’, *Com (97) 599*, (97), p. 53. Available at: http://scholar.google.com/scholar?hl=en&btnG=Search&q=intitle:Communication+from+the+Commission+ENERGY+FOR+THE+FUTURE+:+RENEWABLE+SOURCES+OF+ENERGY+White+Paper+for+a+Community+Strategy+and+Action+Plan#0.

European Commission (2009) 'Directive 2009/28/EC of the European Parliament and of the Council of 23 April 2009 on the promotion of the use of energy from renewable sources and amending and subsequently repealing Directives 2001/77/EC and 2003/30/EC', *Official Journal of the European Union*, L140(16), pp. 16–62. doi: 10.3000/17252555.L_2009.140.eng.

European Commission (2018) 'EU and the Paris Climate Agreement: Taking stock of progress at Katowice COP -COM/2018/716 final - Climate action progress report', (525), p. 23. Available at: https://eur-lex.europa.eu/legal-content/EN/TXT/DOC/?uri=CELEX:52018DC0716&from=EN.

European Commission and Hub, E. science (2016) *Photovoltaic Geographical Information System*. Available at: https://re.jrc.ec.europa.eu/pvg_tools/en/tools.html#MR.

European Council (2014) 'Outcome of the October 2014 European Council', (October). Available at: http://ec.europa.eu/clima/policies/2030/docs/2030_euco_conclusions_en.pdf.

European Union (2018a) 'DIRECTIVE (EU) 2018/ 2002 on Energy Efficiency', 2018(December), pp. 210–230. Available at: https://eur-lex.europa.eu/legal-content/EN/TXT/PDF/?uri=CELEX:32018L2002&from=EN.

European Union (2018b) 'Directive (EU) 2018/2001 of the European Parliament and of the Council on the promotion of the use of energy from renewable sources', *Official Journal of the European Union*, 2018(L 328), pp. 82–209. Available at: https://eur-lex.europa.eu/legal-content/EN/TXT/PDF/?uri=CELEX:32018L2001&from=EN.

Fdez.-Güelfo, L. A. *et al.* (2011) 'The effect of different pretreatments on biomethanation kinetics of industrial Organic Fraction of Municipal Solid Wastes (OFMSW)', *Chemical Engineering Journal*, 171(2), pp. 411–417. doi: 10.1016/j.cej.2011.03.095.

Fouepi, P. (2010) 'Analisi di fattibilità economica di un impianto a biogas con la teoria delle opzioni reali', *Università degli studi di Padova*, p. 89.

Greenwell, H. C. *et al.* (2010) 'Placing microalgae on the biofuels priority list: A review of the technological challenges', *Journal of the Royal Society Interface*, 7(46), pp. 703–726. doi: 10.1098/rsif.2009.0322.

Grobbelaar, J. U. (2013) *Handbook of Microalgal Culture*, *Handbook of Microalgal Culture*. Edited by A. Richmond and Q. Hu. Oxford, UK: John Wiley & Sons, Ltd. doi: 10.1002/9781118567166.

Hagos, K. *et al.* (2017) 'Anaerobic co-digestion process for biogas production: Progress,

challenges and perspectives', *Renewable and Sustainable Energy Reviews*. Elsevier Ltd, 76(November 2016), pp. 1485–1496. doi: 10.1016/j.rser.2016.11.184.

Hansen, T. L. *et al.* (2007) 'Effects of pre-treatment technologies on quantity and quality of source-sorted municipal organic waste for biogas recovery', *Waste Management*. doi: 10.1016/j.wasman.2006.02.014.

Heaven, S. *et al.* (2010) 'SEVENTH FRAMEWORK PROGRAMME THEME ENERGY.2009.3.2.2 Biowaste as feedstock for 2nd generation', pp. 1–54.

Hena, S., Fatimah, S. and Tabassum, S. (2015) 'Cultivation of algae consortium in a dairy farm wastewater for biodiesel production', *Water Resources and Industry*. Elsevier, 10, pp. 1–14. doi: 10.1016/j.wri.2015.02.002.

Hilkiah Igoni, A. *et al.* (2008) 'Designs of anaerobic digesters for producing biogas from municipal solid-waste', *Applied Energy*, 85(6), pp. 430–438. doi: 10.1016/j.apenergy.2007.07.013.

Jankowska, E., Sahu, A. K. and Oleskowicz-Popiel, P. (2017) 'Biogas from microalgae: Review on microalgae's cultivation, harvesting and pretreatment for anaerobic digestion', *Renewable and Sustainable Energy Reviews*. Elsevier Ltd, 75(October 2015), pp. 692–709. doi: 10.1016/j.rser.2016.11.045.

Jansen, C. (1986) 'Anaerobic Digestion: Technology', in *Solid Waste Technology & Management*, pp. 601–617. doi: 10.1002/9780470666883.ch38.

Jeon, E.-J. *et al.* (2007) 'Methane Generation Potential and Biodegradability of Msw Components', *Proceedings Sardinia*, (October 2007), pp. 1–5.

Kangle, K. M. *et al.* (2012) 'Recent Trends in Anaerobic Codigestion : A Review', *Universal journal of environmental research and technology*, 2(4), pp. 210–219.

De Laclos, H. F., Desbois, S. and Saint-Joly, C. (1997) 'Anaerobic digestion of municipal solid organic waste: Valorga full-scale plant in Tilburg, the Netherlands', *Water Science and Technology*, 36(6–7), pp. 457–462. doi: 10.1016/S0273-1223(97)00555-6.

Lavens, P. and Sorgeloos, P. (1996) *Manual on the production and use of live food for aquaculture*, *Fao Fisheries Technical Paper*. doi: 10.1017/CBO9781107415324.004.

Li, H. *et al.* (2012) 'Optimized alkaline pretreatment of sludge before anaerobic digestion', *Bioresource Technology*. Elsevier Ltd, 123, pp. 189–194. doi: 10.1016/j.biortech.2012.08.017.

Lissens, G. *et al.* (2001) 'Solid waste digestors: Process performance and practice for municipal

solid waste digestion', *Water Science and Technology*, 44(8), pp. 91–102. doi: 10.2166/wst.2001.0473.

Logan, M. and Visvanathan, C. (2019) 'Management strategies for anaerobic digestate of organic fraction of municipal solid waste: Current status and future prospects', *Waste Management and Research*, 37(1_suppl), pp. 27–39. doi: 10.1177/0734242X18816793.

López Torres, M. and Espinosa Lloréns, M. del C. (2008) 'Effect of alkaline pretreatment on anaerobic digestion of solid wastes', *Waste Management*, 28(11), pp. 2229–2234. doi: 10.1016/j.wasman.2007.10.006.

Lynn, A. K. and Bonfield, W. (2005) 'A novel method for the simultaneous, titrant-free control of pH and calcium phosphate mass yield', *Accounts of Chemical Research*, 38(3), pp. 202–207. doi: 10.1021/ar040234d.

Madigan, M. *et al.* (2008) *Brock Biology of Microorganisms*.

Maier, R. M. (2009) 'Bacterial Growth', in *Environmental Microbiology*. Elsevier, pp. 37–54. doi: 10.1016/B978-0-12-370519-8.00003-1.

Małgorzata, C.-R. (1999) 'Effect of Anaerobic Sludge Composition', *Sustainable Municipal Sludge and Solid Waste Handling*, pp. 69–76.

Marchesi, P. *et al.* (2013) 'Incentivi per la produzione di energia elettrica da fonti rinnovabili, 2010-2012'. doi: 10.1787/9789264188754-table31-it.

Markou, G., Vandamme, D. and Muylaert, K. (2014) 'Microalgal and cyanobacterial cultivation: The supply of nutrients', *Water Research*. Elsevier Ltd, 65, pp. 186–202. doi: 10.1016/j.watres.2014.07.025.

Mata, T. M., Martins, A. A. and Caetano, N. S. (2010) 'Microalgae for biodiesel production and other applications: A review', *Renewable and Sustainable Energy Reviews*, 14(1), pp. 217–232. doi: 10.1016/j.rser.2009.07.020.

Metha, A. (2012) *Ultraviolet-Visible (UV-Vis) Spectroscopy – Limitations and Deviations of Beer-Lambert Law*. Available at: https://pharmaxchange.info/2012/05/ultraviolet-visible-uv-vis-spectroscopy-–-limitations-and-deviations-of-beer-lambert-law/.

Ministero dello sviluppo Economico, I. (2010) *Piano di azione nazionale per le energie rinnovabili dell ' Italia*.

Ministero dello sviluppo Economico, I. and Ministero dell'ambiente e della tutela del territorio e del mare, I. (2016) 'DECRETO 4 luglio 2019 Incentivazione dell'energia elettrica prodotta

dagli impianti eolici on shore, solari fotovoltaici, idroelettrici e a gas residuati dei processi di depurazione.', pp. 1–26.

Ministero dello sviluppo Economico, I., Ministero dell'ambiente e della tutela del territorio e del mare, I. and Ministro delle politiche agricole alimentari e forestali, I. (2018) 'Promozione dell'uso del biometano e degli altri biocarbu- ranti avanzati nel settore dei trasporti', pp. 12–32.

MØller, J., Christensen, T. H. and Jansen, J. la C. (2010) 'Anaerobic Digestion: Mass Balances and Products', in *Solid Waste Technology & Management*, pp. 618–627. doi: 10.1002/9780470666883.ch39.

Munisamy, P. *et al.* (2017) 'Biological aspects of anaerobic digestion and its kinetics: An overview', *Journal of Microbiology, Biotechnology and Food Sciences*, 6(4), pp. 1090–1097. doi: 10.15414/jmbfs.2017.6.4.1090-1097.

Muñoz, R. *et al.* (2015) 'A review on the state-of-the-art of physical/chemical and biological technologies for biogas upgrading', *Reviews in Environmental Science and Biotechnology*, 14(4), pp. 727–759. doi: 10.1007/s11157-015-9379-1.

Musolino, V. (2016) 'Anaerobic Digestion for Nutrient Recycling in Industrial Microalgae Cultivation ':

Niesner, J., Jecha, D. and Stehlík, P. (2013) 'Biogas upgrading technologies: State of art review in european region', *Chemical Engineering Transactions*, 35, pp. 517–522. doi: 10.3303/CET1335086.

Olaizola, M. (2003) 'Commercial development of microalgal biotechnology: From the test tube to the marketplace', *Biomolecular Engineering*, 20(4–6), pp. 459–466. doi: 10.1016/S1389-0344(03)00076-5.

Ortega, V. (2019) *APPLICATION OF MICROALGAE-BACTERIA CONSORTIUM IN WASTEWATER TREATMENT : DEVELOPMENT OF AN INTEGRATED MODEL IN AQUASIM*.

Peng, W. and Pivato, A. (2019) 'Sustainable Management of Digestate from the Organic Fraction of Municipal Solid Waste and Food Waste Under the Concepts of Back to Earth Alternatives and Circular Economy', *Waste and Biomass Valorization*. Springer Netherlands, 10(2), pp. 465–481. doi: 10.1007/s12649-017-0071-2.

Peters, M. and Timmerhaus, K. (1991) *Plant design and economics for chemical engineers*, *Seminars for nurse managers*. Routledge. Available at:

https://www.taylorfrancis.com/books/9780429696381.

Primante, A. (2009) 'Digestione Anaerobica: valutazione costi/benefici, analisi tecnica di alcuni casi studio e prospettive di sviluppo'.

Rabii, A. *et al.* (2019) 'A review on anaerobic co-digestion with a focus on the microbial populations and the effect of multi-stage digester configuration', *Energies*, 12(6). doi: 10.3390/en12061106.

Rao, M. S. and Singh, S. P. (2004) 'Bioenergy conversion studies of organic fraction of MSW: Kinetic studies and gas yield-organic loading relationships for process optimisation', *Bioresource Technology*. doi: 10.1016/j.biortech.2004.02.013.

Ras, M., Steyer, J. P. and Bernard, O. (2013) 'Temperature effect on microalgae: A crucial factor for outdoor production', *Reviews in Environmental Science and Biotechnology*, 12(2), pp. 153–164. doi: 10.1007/s11157-013-9310-6.

Reichhalter, H. *et al.* (2011) 'Analisi energetica , ambientale ed economica di impianti a biogas in Provincia di Bolzano - Relazione conclusiva -', pp. 1–106.

Renesto, A. (2019) *An integrated process for microalgal biomass production from anaerobic digestion of OFMSW : experimental study and process simulation*.

Richardson, J. W., Johnson, M. D. and Outlaw, J. L. (2013) 'Economic Comparison of Open Pond Raceways to Photo Bio-Reactors for Profitable Production of Algae for Transportation Fuels in the Southwest'.

Riva, G. (2009) 'La filiera del biogas', *ASSAM - Agenzia Servizi Settore Agroalimentare delle Marche Trasferimento*.

Rogers, J. N. *et al.* (2014) 'A critical analysis of paddlewheel-driven raceway ponds for algal biofuel production at commercial scales', *Algal Research*. The Authors, 4(1), pp. 76–88. doi: 10.1016/j.algal.2013.11.007.

Sforza, E. *et al.* (2019) 'Respirometry as a tool to quantify kinetic parameters of microalgal mixotrophic growth', *Bioprocess and Biosystems Engineering*. Springer Berlin Heidelberg, 42(5), pp. 839–851. doi: 10.1007/s00449-019-02087-9.

Smith, P. H. and Mah, R. A. (1966) 'Kinetics of acetate metabolism during sludge digestion.', *Applied microbiology*, 14(3), pp. 368–371.

Spolaore, P. *et al.* (2006) 'Commercial applications of microalgae', *Journal of Bioscience and Bioengineering*, 101(2), pp. 87–96. doi: 10.1263/jbb.101.87.

Stamatelatou, K., Antonopoulou, G. and Michailides, P. (2014) *Biomethane and biohydrogen production via anaerobic digestion/fermentation*, *Advances in Biorefineries: Biomass and Waste Supply Chain Exploitation*. doi: 10.1533/9780857097385.2.476.

Tam, N. F. Y. and Wong, Y. S. (1996) 'Effect of ammonia concentrations on growth of Chlorella vulgaris and nitrogen removal from media', *Bioresource Technology*, 57(1), pp. 45–50. doi: 10.1016/0960-8524(96)00045-4.

Tapie, P. and Bernard, A. (1988) 'Microalgae production: Technical and economic evaluations', *Biotechnology and Bioengineering*, 32(7), pp. 873–885. doi: 10.1002/bit.260320705.

Turton, R. *et al.* (2008) *Analysis, Synthesis, and Design of Chemical Processes*.

Vandevivere, P., De Baere, L. and Verstraete, W. (2003) 'Types of anaerobic digester for solid wastes', *Biomethanization of the organic fraction of municipal solid wastes*, (January 2002), pp. 111–140.

Wilken, D. *et al.* (2017) 'Biogas to Biomethane', *Unido*. Available at: https://www.biogas-to-biomethane.com/Download/BTB.pdf.

Xia, A. and Murphy, J. D. (2016) 'Microalgal Cultivation in Treating Liquid Digestate from Biogas Systems', *Trends in Biotechnology*. Elsevier Ltd, 34(4), pp. 264–275. doi: 10.1016/j.tibtech.2015.12.010.

Yadvika *et al.* (2004) 'Enhancement of biogas production from solid substrates using different techniques - A review', *Bioresource Technology*, 95(1), pp. 1–10. doi: 10.1016/j.biortech.2004.02.010.

Zinder, S. (1993) *Methanogenesis*.

Zou, H. *et al.* (2019) 'Methane production from food waste via mesophilic anaerobic digestion with ethanol pre-fermentation: Methanogenic pathway and microbial community analyses', *Bioresource Technology*. Elsevier, 297(November 2019), p. 122450. doi: 10.1016/j.biortech.2019.122450.

Zuliani, L. *et al.* (2016) 'Microalgae cultivation on anaerobic digestate of municipalwastewater, sewage sludge and agro-waste', *International Journal of Molecular Sciences*, 17(10). doi: 10.3390/ijms17101692.

Ringraziamenti

Innanzitutto vorrei ringraziare il Professor Bertucco, di cui ho apprezzato le conoscenze e la professionalità dimostratomi durante la stesura di questo elaborato. Inoltre ringrazio l'Ingegner Elena Barbera, per la disponibilità dimostrata nella supervisione del lavoro di simulazione e per il supporto intellettuale.

Ringrazio anche i miei colleghi universitari che mi hanno sostenuto in questo periodo, la cui piacevole compagnia ha alleviato le fatiche giornaliere. Un grazie va ai miei amici e alla mia ragazza per i momenti felici passati insieme e le gioie condivise.

Un ringraziamento speciale va alla mia famiglia che mi ha supportato nella mia carriera scolastica, in particolare durante il periodo universitario.